

Fall 2013

# Modeling long-term carbon accumulation of tropical peat swamp forest ecosystems

Sofyan Kurnianto

*University of New Hampshire, Durham*

Follow this and additional works at: <https://scholars.unh.edu/thesis>

---

## Recommended Citation

Kurnianto, Sofyan, "Modeling long-term carbon accumulation of tropical peat swamp forest ecosystems" (2013). *Master's Theses and Capstones*. 822.

<https://scholars.unh.edu/thesis/822>

This Thesis is brought to you for free and open access by the Student Scholarship at University of New Hampshire Scholars' Repository. It has been accepted for inclusion in Master's Theses and Capstones by an authorized administrator of University of New Hampshire Scholars' Repository. For more information, please contact [nicole.hentz@unh.edu](mailto:nicole.hentz@unh.edu).

MODELING LONG-TERM CARBON ACCUMULATION OF TROPICAL PEAT  
SWAMP FOREST ECOSYSTEMS

BY

SOFYAN KURNIANTO

Bachelor of Science, Bogor Agricultural University, 2004

THESIS

Submitted to the University of New Hampshire

in Partial Fulfillment of

the Requirements for the Degree of

Master of Science

in

Earth Sciences

September, 2013

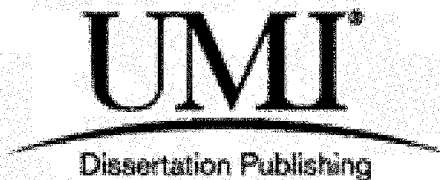
UMI Number: 1524453

All rights reserved

INFORMATION TO ALL USERS

The quality of this reproduction is dependent upon the quality of the copy submitted.

In the unlikely event that the author did not send a complete manuscript and there are missing pages, these will be noted. Also, if material had to be removed, a note will indicate the deletion.



UMI 1524453

Published by ProQuest LLC 2013. Copyright in the Dissertation held by the Author.

Microform Edition © ProQuest LLC.

All rights reserved. This work is protected against unauthorized copying under Title 17, United States Code.



ProQuest LLC  
789 East Eisenhower Parkway  
P.O. Box 1346  
Ann Arbor, MI 48106-1346

This thesis has been examined and approved.

---

Thesis Director, Dr. Steve Frolking,  
Research Professor,  
Biogeochemical Modeling

---

Dr. Ruth Varner,  
Research Associate Professor,  
Biogeochemistry

---

Dr. J. Boone Kauffman,  
Research Professor, Ecosystem Ecology  
Oregon State University

---

Dr. Matthew W. Warren  
Research Ecologist,  
Northern Research Station,  
USDA Forest service

---

Date

*For my family, and the red-white*

## ACKNOWLEDGEMENTS

Alhamdulillahirabbil'alamin. All praises belongs to Allah, Lord of all the worlds.

I would like to express the deepest gratitude to my advisor, Steve Frolking, for his guidance and introducing me to the world of research especially modeling. His insightful comments in writing process teach me how to write in scientific paper in a better way. I would like to thank my committee members: Ruth Varner, Boone Kauffman, and Matthew Warren for providing me great suggestions to improve my thesis. My sincere thank also to my supervisor in CIFOR who always encourage me to continue my study in graduate school. I thank to Julie Talbot for all the discussions, supports, and introduce me to Matlab and HPM.

I also would like to thank my family, friends and colleagues. I wish to thank my parents for always giving me their prayer and supports; thank my lovely wife, Nur Febrianti, and my son, Azzam N. Kurnianto, for letting me away from you both, your love and always giving me spirits to finish my study. My big thank to my graduate fellows who support and help me since first time I came at UNH: Adan Hernandez, Katie Jennings, Susana Alvarado, and Chris Dorich. For all Indonesian community in New England especially to Bapak and Ibu Gampang, Bang Ujang, Pak Edi 'Pesilat', Bang Mawardi and Bang Acing for keeping me to feel as if I am still at my home. For all my brothers in VTComm, Om Tum Agung,

Pak Beva, Cak Andri, Yai Eko, Koh VV, Bang Bom, Abah Seno, Amud, Tatang, Risqi, Pak Dhe Widayat, Kang Rips, Febry, Kong Alwi, om Wawan, and Wippa who always cheer me up; our brotherhood is limitless.

This project was funded by US Forest Service and I got the tuition waiver from College of Engineering and Physical Sciences of UNH. The travel expenses for doing the field research in Kalimantan and Sumatra, Indonesia were covered by CIFOR and USFS.

## TABLE OF CONTENTS

|                       |      |
|-----------------------|------|
| DEDICATION.....       | iii  |
| ACKNOWLEDGEMENT ..... | iv   |
| LIST OF TABLES .....  | viii |
| LIST OF FIGURES ..... | ix   |
| ABSTRACT.....         | xii  |

| CHAPTER  | PAGE |
|--|------|
| I. INTRODUCTION .....  | 1    |
| II. METHODS.....   | 8    |
| 2.1. Holocene Peat Model (HPM) .....                               | 8    |
| 2.2. HPM for tropical peat swamp forest ecosystems (HPMTrop) ..... | 10   |
| 2.2.1. Overview of Modification from HPM.....                      | 10   |
| 2.2.2. HPMTrop structure and equations .....                       | 11   |
| 2.3. Water table reconstruction.....                               | 17   |
| 2.3.1. Water table empirical model.....                            | 17   |
| 2.3.2. Generating rainfall data since late Pleistocene.....        | 18   |
| 2.4. Model evaluation.....   | 20   |
| 2.5. Sensitivity analysis.....                                     | 21   |
| 2.6. A land cover change scenario .....                            | 21   |



|  |    |
|--|----|
| 2.7. Field surveys.....  | 22 |
| 2.7.1. Study area.....   | 22 |
| 2.7.2. Peat core sampling and analysis .....                             | 23 |
| III. RESULTS .....   | 25 |
| 3.1. Rainfall data generation since late Pleistocene .....               | 25 |
| 3.2. HPMTrop results .....   | 27 |
| 3.3. Sensitivity analysis.....   | 32 |
| 3.4. Land cover change scenario.....                                     | 36 |
| 3.5. Measured peat carbon stocks.....                                    | 36 |
| IV. DISCUSSION .....   | 39 |
| 4.1. Carbon accumulation rates in tropical PSF during the Holocene ..... | 39 |
| 4.2. Carbon stocks in tropical PSF .....                                 | 44 |
| 4.3. The impact of land cover change on PSF carbon dynamics.....         | 45 |
| 4.4. Model uncertainty .....   | 48 |
| V. CONCLUSIONS .....   | 53 |
| LIST OF REFERENCES .....   | 82 |
| APPENDIX.....  | 90 |

## LIST OF TABLES

Table 1. List of parameters used in HPMTrop.

Table 2. ENSO probabilities used for different intervals in Holocene simulations.

Table 3. Sensitivity analysis for the coastal peatland scenario. Peat carbon mass remaining for each tree component, total peat carbon, peat depth, total NPP through the 5000 year simulation, and the ratio of peat mass at the end simulation to total NPP were chosen as the model responses. Base run values are the model output simulated using the default parameters shown in Table 1. Parameters were adjusted  $\pm 25\%$ .

Table 4. Summary of measured carbon density in this study and previously published literature.

Table 5. Reported area and depth of peat burning, and simulated total carbon loss caused by the fires in Indonesia estimated using coastal peatlands scenario.

## LIST OF FIGURES

Figure 1. A schematic of some of the links among variables and processes in HPM.

Figure 2. Flowchart of HPMTrop calculations.

Figure 3. Measured peat water table in Sebangau peat swamp forests, Kalimantan Indonesia from 1993-2006 (modified from Wösten, Ritzema, & Rieley, 2010).

Figure 4. Quadratic relationship between measured monthly water table and gross primary production (GPP) in Sebangau, Kalimantan (modified from Hirano et. al 2012). Positive values in monthly water table (X-axis) shows the position of water table is below the peat surface.

Figure 5. Scatterplot of estimated monthly water deficit (Equation 15) and measured monthly mean water table (see Figure 3); line is linear fit.

Figure 6. Annual rainfall classification based on the Southern Oscillation index from 1900-2010 (McKeon, et. al., 2004). The Y-axis shows the rainfall classes: 1. La Niña, 2. Normal, 3. El Niño.

Figure 7. The stalagmite  $\delta^{18}\text{O}$  record sampled from Gunung Buda, northern Borneo since late Pleistocene (modified from Partin et al., 2007). More negative values can be interpreted as wetter conditions. Note that time on x-axis is time since start of record, so 0 = 15,000 years BP and 15,000 is present day. Line is polynomial fit (Equation 16).

Figure 8. The dendrogram of the two-way cluster analysis using the monthly rainfall data classified as the El Niño years. Four clusters of years were extracted from this analysis (P1, P2, P3, and P4). The X-axis and Y-axis represent month and year, respectively, with the rainfall depth shown for each month.

Figure 9. Same as Figure 7 with the rainfall data from normal years. Clusters are P5-P8.

Figure 10. Same as Figure 7 with the rainfall data from La Niña years. Clusters are P9-P12.

- Figure 11. Mean monthly rainfall depth of each group derived by the cluster analysis (see Figures 7-9) for El Niño (top), normal (middle), and La Niña (bottom). Values in the legends represent the probability for every rainfall group within the broad El Niño, normal, and La Niña classes.
- Figure 12. Mean monthly water deficit of each rainfall group (P1-P12, see Figure 10) for: El Niño (top), normal (middle), and La Niña (bottom).
- Figure 13. Mean monthly water table of each water deficit group (WD1-WD12; see Figures 10-11) for: El Niño (top), normal (middle), and La Niña (bottom).
- Figure 14. (*top*) Estimated annual rainfall over 15,000 years. Estimated mean annual water table for inland (*middle*) and coastal peatland (*bottom*) calculated as a distance from peat surface to the water level. The black line represents the 25-year moving average. Note that monthly water table is much more variable, and goes much deeper than the annual values (see Figure 10).
- Figure 15. (*top*) Simulated annual NPP calculated as the total of litter fall, wood productivity and root mortality, and as a function of water table. (*middle*) Simulated annual decomposition rate. (*bottom*) Simulated rate of change peat mass remaining; a positive value corresponds to net carbon gain in the peat, a negative value to net carbon loss. The black line represents the 25-year moving average. This simulation was generated for coastal peatlands.
- Figure 16. (*top*) Simulated annual NPP calculated as the total of litter fall, wood productivity and root mortality, and as a function of water table. (*middle*) Simulated annual decomposition rate. (*bottom*) Simulated rate of change peat mass remaining; a positive value corresponds to net carbon gain in the peat, a negative value to net carbon loss. The black line represents the 25-year moving average. This simulation was generated for inland peatlands.
- Figure 17. Time series of simulated accumulation of peat mass for coastal (blue) and inland (red) peatlands.
- Figure 18. The simulated apparent peat accumulation rate ( $\text{mm y}^{-1}$ ) (top) and carbon accumulation rate (bottom) for coastal and inland peatlands.

- Figure 19. Relationship of peat age to depth at the end of the simulations for the coastal (black) and inland (green) peatlands, overlaid with measured age-depth profiles of coastal (blue) and inland (red) peatlands from Southeast Asia. Measured peat depth-age profiles were obtained from Dommain et al. (2011).
- Figure 20. Simulated peat mass accumulation for coastal peatlands over 5,000 years and inland peatland over 13,000 years, with conversion to oil palm and periodic burning in the last 100 years of the simulation.
- Figure 21 Simulated age-depth relationship for coastal and inland peatlands with the forest conversion to oil palm plantation scenario.
- Figure 22. Measured depth of peat profiles (red bars) and stored carbon per unit area (blue bars) for sites in Tanjung Puting National Park, Kalimantan, Indonesia (TPG1-TGP3) and Berbak National Park, Sumatra, Indonesia (BBK1-BBK3). The bars and error lines represent the average and standard error from six plots sampled within each site.
- Figure 23. (*top*) Plot of the principal component scores of the first two components in different sites. (*bottom*) Plot of the individual loading score generated by bulk density (BD,  $\rho$  in the text), carbon content (C) along the peat profiles, peat depth (PD) and C-stocks. Numbers following the bulk density and carbon content represents the standardized depth, 1: 0 – 0.1 m, 2: 0.1 – 0.2 m, 3: 0.2 – 0.3 m, 4: 0.3 – 0.4 m, 5: 0.4 - 0.5 m, 6: 0.5 – 0.6 m, 7: 0.6 – 0.7 m, 8: 0.7-0.8 m, 9: 0.8 – 0.9 m, 10: 0.9 -1.0 m.
- Figure 24. Bulk density (*top*), and carbon concentration (*bottom*) along the peat profile (standardized depth) sampled from three sites in Tanjung Puting National Park (TPG, red) and three sites in Berbak National Park (BBK, blue), Indonesia. The standardized depth in a profile was calculated as the ratio between sampling depths and the maximum depth of that profile.

## ABSTRACT

### MODELING LONG-TERM CARBON ACCUMULATION OF TROPICAL PEAT SWAMP FOREST ECOSYSTEMS

by

Sofyan Kurnianto

University of New Hampshire, September, 2013

Peatlands play an important role in the global climate system and carbon cycle; their large carbon stocks could be released to the atmosphere due to climate change or disturbance, resulting in increased climate forcing. I modified the Holocene Peat Model (HPM), a process-based model coupling water and carbon balance for simulating carbon dynamic over millennia, to be applicable for tropical peatlands.

HPMTrop outputs are generally consistent with the field observations from Indonesia. The simulated long-term carbon accumulation rate for coastal and inland peatlands were 0.63 and 0.26 Mg C ha<sup>-1</sup> y<sup>-1</sup>, and the resulting peat carbon stocks at the end of the simulations were 3,150 Mg C ha<sup>-1</sup> and 3,270 Mg C ha<sup>-1</sup>, respectively. The simulated carbon loss for the coastal scenario caused by forest conversion to oil palm plantation with periodic burning was 1,500 Mg C ha<sup>-1</sup> y<sup>-1</sup> over 100 years, which is equivalent to ~3,000 years of peat accumulation.

## I. INTRODUCTION

Peatlands play an important role in both the global climate system and carbon cycle. Worldwide, peatlands cover an area of 4 to 4.4 million km<sup>2</sup> and store about 600 Gt C (Yu et al., 2010; Page et al., 2011). About 90% of peatland area is located in Northern boreal and subarctic regions. Furthermore, Yu et al. (2011) reported that global peatland carbon sequestration ranged from 16 to 88 Gt C per millennia, due to peat carbon accumulation during the Holocene. However, disturbances occurring in these ecosystems can release large amounts of carbon to atmosphere, contributing to changes in global climate (Frolking, et al., 2011).

Tropical peatlands cover approximately 441,000 km<sup>2</sup> or ~10% of global peatland area. Southeast Asia contains about 60% of the tropical peat area, and Indonesia contains the largest area, about 207,000 km<sup>2</sup>, followed by Malaysia with an area of 26,000 km<sup>2</sup> (Page et al., 2010). The high productivity and litter production from tropical forest ecosystems and low decomposition rates due to soil saturation leads to organic matter accumulation as peat (Chimner and Ewel, 2004). In addition, flat topography and high rainfall also favor tropical peat development (Page et al., 2010). The volume of tropical peat was reported as  $1,758 \times 10^9$  m<sup>3</sup> (Page et al., 2011) or 22% of the northern peat volume (Gorham, 1991). Tropical peatlands store a large amount of carbon, about 88.6 Gt C overall; Southeast Asia has the highest proportion (77%) (Page et al., 2011) with

the carbon accumulation rate during the Holocene is estimated to average  $13 \text{ g C m}^2 \text{ y}^{-1}$  (Yu et al., 2010). Hence, tropical peatlands are significant carbon sinks since Holocene and influencing the global carbon budget.

Some tropical peatlands are characterized by a domed shape, permanent water saturation, and anoxic conditions (Jaenicke et al., 2008; Dommain et al., 2010). These ecosystems are mostly situated in lowland areas with elevation less than 50 m a.s.l and classified in two main types based on the distance from the coast: coastal peatlands and inland peatlands which are >150 km from the coast (Rieley et al., 2008). In addition, the vegetation of tropical peatlands in Southeast Asia is predominantly lowland evergreen forests, often called peat swamp forests (PSF; Phillips, 1998; Page et al., 1999).

The accumulation process of tropical peatlands began at some sites in the late Pleistocene, and the youngest peatlands initiated about 2,000 calendar years before present (hereafter kBP) (Rieley et al., 2008; Yu et al., 2010). Coastal peatland development in Southeast Asia initiated 4 – 7 kBP (Dommain et al., 2011). This is much younger than inland peatland initiation, where peat accumulation began as early as 20 to 30 kBP (Anshari et al., 2001, 2004; Page et al., 2004). However, the rate of peat accumulation in coastal peatlands has been faster than for inland peatlands, averaging  $1.8$  and  $0.5 \text{ mm y}^{-1}$ , respectively due to a weaker influence of both decreased rainfall and higher ENSO intensity (Dommain et al., 2011). Additionally, Rieley et al. (2008) reported peat



accumulation rates in tropical peat swamp ecosystems, especially in Southeast Asia region, to vary between 0 – 3 mm y<sup>-1</sup>, with a median value of 1.3 mm y<sup>-1</sup>.

Recently, tropical PSFs have been heavily impacted by the increase of deforestation and land conversion. In a 10-year period (2000-2010), the upland deforestation rate in Southeast Asia was 1% y<sup>-1</sup>, while deforestation of PSF was 2.2% y<sup>-1</sup> (Miettinen et al., 2011). Most of the PSF deforestation occurred in Indonesia's Sumatra and Borneo Islands (Miettinen and Liew, 2010a; Miettinen et al., 2011). By 2010, about 36% of peatlands in Sumatra, Borneo, and peninsular Malaysia that were covered by forest, while about 77% had forest cover in 1990 (Miettinen et al., 2012).

A vast amount of carbon dioxide (CO<sub>2</sub>) emissions are produced as a result of deforestation of PSF, not only from the loss of aboveground biomass (Miettinen and Liew, 2010b) but also from the lowering of the water table level (Hooijer et al., 2010) as well as from fire and peat combustion (Page et al., 2002; Heil et al., 2006). Wösten et al. (1997) reported that there is a positive relationship between CO<sub>2</sub> emissions and water level draw-down.

Peat oxidation generated by the disturbances will release the stored carbon in the peat as CO<sub>2</sub>. Following PSF conversion to oil palm plantation, carbon release to the atmosphere is about 16.2 Mg C ha<sup>-1</sup> y<sup>-1</sup>, mostly as CO<sub>2</sub>; this includes emissions from peat burning, change in aboveground biomass, and peat oxidation (Murdiyarso et al., 2010). PSF conversion generally also leads to a decline in or ceasing of peat accumulation (Murdiyarso et al., 2010). Moreover,

Koh et al. (2011) estimated a carbon loss of about 4.6 Tg C  $y^{-1}$  from peat oxidation and plus about 140 Tg C from aboveground biomass removal due to conversion of ~880,000 ha of forest to oil palm plantation by 2010. Miettinen, et al. (2012), however, produced a much higher estimation of plantation area – 3.1 Mha of peatlands had been converted to industrial plantations in Sumatra, Borneo and peninsular Malaysia by 2010 and ~69% of the total plantation area (2.1 Mha) was oil palm.

Land cover changes from pristine PSF to agriculture, including plantations, followed by canal development for lowering water table, generate peat subsidence. Subsidence consists of three components: consolidation, oxidation and shrinkage. Consolidation, or physical collapse of the peat, dominates the early stage of the subsidence process, with a higher subsidence rate until the water table depth reaches 50 cm below the peat surface; after this point, the subsidence rate is relatively constant, and is dominated by oxidation and shrinkage components (Couwenberg et al., 2009).

Ecosystem modeling is one tool that can be utilized to represent and understand dynamical process in tropical peatlands and, in turn, can be used as a tool for assessing the impact of climate change and land-use pressure on peatlands. Although no models have been developed for tropical peat swamp forest systems, some ecosystem models that have relevant processes for estimating peat accumulation or greenhouse gas fluxes had been summarized by

Farmer et al. (2011), and are briefly described below with some additional description of the HPM model.

The McGill Wetland Model (MWM) is a process-based model that simulates gross primary production (GPP), net ecosystem production (NEP), and ecosystem respiration (ER) at hourly time steps (St-Hilaire et al., 2010). These outputs are simulated based on four carbon pools including two living material pools: mosses and other vascular plants, with four plant functional types (PFTs), i.e., mosses, sedges, shrubs, and conifer trees, and two non-living matter pools, i.e., litter and peat. An 8-year eddy-covariance measurement dataset of net CO<sub>2</sub> flux from Mer Bleue peatland (Ontario, Canada) had been used to evaluate this model.

PEATBOG is a new process-based biogeochemical model that couples carbon and nitrogen cycles (Wu and Blodau, 2013). It consists of four sub-models: an environment sub-model for simulating peat water table; vegetation sub-model for simulating both carbon and nitrogen flows among three PFTs, i.e. mosses, graminoids, and shrubs; a soil organic matter (SOM) sub-model for simulating decomposition and peat accumulation, as well as an interlink between vegetation and a dissolved carbon and nitrogen sub-model. Similar to MWM, the pool system was also implemented, and the vegetation sub-model has four pools: structural and substrate pools for both roots and shoots; SOM has four pools: labile and recalcitrant for both carbon and nitrogen. These sub-models are calculated in a daily time step, and the model outputs are GPP, ER, NEE, CH<sub>4</sub>

flux, N<sub>2</sub>O flux, dissolved organic carbon (DOC), dissolved organic nitrogen (DON), and dissolved inorganic nitrogen (DIN). The model output was tested and showed an agreement with the measured dataset from the Mer Bleue peatland.

MILLENNIA is one dimensional and process based model for estimating peat accumulation in the Holocene (Heinemeyer et al., 2010) developed based on the Peat Decomposition Model (PDM, Frohking et al., 2001). It couples carbon and water balances, and requires as input long-term climate data and vegetation characteristics. Mean annual precipitation (MAP) and mean annual temperature (MAT) are used to calculate evapotranspiration, which then affects NPP and water table depth. Total NPP is partitioned into eight PFTs: trees, shrubs, herbs, mosses, other bryophytes, grasses, rushes, and sedges, and is assumed to be equal to the litter input. For estimating the decomposition rates, litter is divided into three pools, i.e., soluble, holocellulose, and lignin, and the mass remaining was added as annual cohorts. Then, peat mass is converted to peat depth using peat bulk density estimated as a function of peat water table. The outputs of the model are NPP, water table depth, peat mass increments, peat accumulation, and peat depth during the Holocene. The simulated carbon accumulation and peat age was consistent with the measured data from peatlands in the United Kingdom.

A combination of CLIMBER2-LPJ (Lund-Potsdam-Jena), a model for peat accumulation and decomposition, with the model for determining the wetland area (TOPMODEL) had been used for simulating peat accumulation north of

40°N over millennia at regional scale (Kleinen et al., 2012). CLIMBER2-LPJ had been used for simulating the CO<sub>2</sub> emission, terrestrial biomass, litter and soil carbon stocks throughout the Holocene (Kleinen et al., 2010). LPJ-Why, another version of LPJ, has been also developed for simulating the net ecosystem production (NEP), net ecosystem production (NPP), heterotroph respiration (HR), and soil carbon stocks for northern peatlands, which consists of two PFTs: flood-tolerant C<sub>3</sub> graminoids and sphagnum (Wania et al., 2009a, 2009b).

Holocene Peat model (HPM) is one dimensional and annual time steps model that couples carbon and water balance components for simulating carbon accumulation throughout Holocene in northern Peatlands (Frolking et al. 2010). This model had been compared against the dataset from Mer Bleue, Canada. A brief description of HPM is provided in Chapter 2.1.

It is important to note that all of the peat models described above have been developed for northern peatlands and would require some modifications to simulate carbon dynamics in tropical peatlands. Since most tropical peatlands are covered by forests and have negligible moss/bryophyte vegetation cover, exchanging non-vascular PFTs such as mosses to vascular PFTs such as trees is one of important step to implement those models in the tropics. The goal of my research was to modify the Holocene Peat Model (Frolking et al. 2010), developed for northern peatlands, to be applicable to a tropical setting.

## II. METHODS

### 2.1. Holocene Peat Model (HPM)

HPM is a one-dimensional, annual time step model for simulating carbon dynamics in northern peatlands, and has been successfully tested using a dataset from Mer Bleue peatland, near Ottawa, Canada (Frolking et al., 2010). This model integrates a peat decomposition model (Frolking et al., 2001) and a dynamic peat accumulation model that coupled carbon and water balances (Hilbert et al., 2000). HPM estimates characteristics of the vegetation and peat column such as litter production, litter decomposition, peat accumulation, hydrological properties of peat, and water table depth by coupling the carbon and water balance sub-models.

In the carbon balance sub-model, above- and below-ground Net Primary Production (NPP) of twelve plant functional types (PFTs), including sedges, mosses, grasses, and shrubs, are estimated by taking into account PFT characteristics such as relative maximum NPP, optimal peat depth and water table depth, sensitivity to non-optimal peat depth and water table, and above and belowground productivity partitioning. Peat depth was used as a proxy for nutrient status – either minerotrophic (shallow peat depth) or ombrotrophic (deep peat). HPM does not simulate vegetation biomass accumulation and growth and,

hence, assumes that annual vegetation litter input to the peat is the same as annual NPP.

The peat is represented by a vertical column of annual litter cohorts, with each cohort potentially containing litter from each PFT. A simple mass balance is used to calculate the rate of change of a peat cohort mass, with the vegetation litter (above-ground and root) as an input and decomposition as an output for each PFT. The decomposition rate is a function of water content in the peat cohort, which is determined by the relative position of the cohorts related to the water table.

The ratio between cohort mass remaining at a certain time with initial mass (total mass input), i.e., the degree of decomposition ( $m/m_0$ ), is utilized to estimate cohort bulk density. In HPM, peat density influences the calculation of cohort thickness and, eventually, affects the peat depth for the whole profile. Peat bulk density also plays an important role as a link between carbon balance and water balance equations (Figure 1).

In the water balance section, cohort bulk density affects the hydraulic conductivity of the peat cohort and, in turn, influences the unsaturated peat water content. This sets up a carbon-water feedback, as water content affects decomposition rate, and degree of decomposition (cohort mass remaining) affects the water content. In addition, the peat column water balance is also calculated as a simple box model, in which precipitation is an input and evapotranspiration and runoff are outputs. At each annual time step, by

simultaneously solving the water and carbon balances, HPM simulates vegetation NPP (litter production) for all PFTs, total peat height, peat cohort bulk densities and thicknesses for all cohorts in the accumulating peat column, and peat water content as well as peat water table.

## **2.2. HPM for tropical peat swamp forest ecosystems (HPMTrop)**

### **2.2.1. Overview of Modifications from HPM**

To apply HPM to tropical peatlands, we developed a new model, HPMTrop, that used the basic functionality of HPM, but with three fundamental changes – PFTs, time step, and water balance calculation – along with some new vegetation and peat parameter values. PFTs in HPM include mosses, sedges, herbs and shrubs. However, in tropical peatlands (peat swamp forest) the vegetation is dominated by trees while mosses are negligible (Anderson, 1963; Phillips, 1998). Hence, HPMTrop considers only tree NPP, but this is partitioned into three components: leaves, wood, and roots; this is described in more detail in section 2.2.2.1 below.

Typical climate in tropical regions includes warm temperatures year-round, with little seasonality, and seasonal rainfall partitioned into dry and rainy seasons. To capture the impact of the climate seasonality on tropical peat development, HPM was modified from an annual time step to a monthly time step, and monthly water table (WT) values are required for both decomposition and NPP calculations. Since tropical peat swamp forest water balance modeling



is not well-developed (Wösten et al., 2008), and since few data exist for run-on, run-off or water table depth in tropical peat swamp forests, HPMTrop does not calculate a monthly water balance, but instead uses an empirical relationship between WT and monthly water deficit to set the monthly WT for NPP and decomposition calculations; this is described in more detail in section 2.2.2.2 below.

Decomposition and peat mass balance calculations in HPMTrop followed HPM methodology more closely and this is described in more detail in sections 2.2.2.3 and 2.2.2.4 below.

#### 2.2.2. HPMTrop structure and equations

The script of HPMTrop was written in Matlab; the model consists of a main routine and several sub-routines: parameters required by the model, NPP calculation, root (belowground litter) input calculation, decomposition rate factor as a function of water table calculation, and bulk density profile estimation (the model code is listed in Appendix 1). HPMTrop simulates thousands of years of peat accumulation (or loss), and so requires a monthly water table depth reconstruction for the simulation period (see Section 2.3 below). For each month of the simulation, HPMTrop uses the monthly WT to calculate NPP (litter production), peat profile water content, decomposition, and peat depth. A flowchart outlining the calculation steps in HPMTrop is shown in Figure 2.

2.2.2.1. Monthly NPP. As in HPM (Frolking et al. 2010), trees biomass is not simulated as a dynamic variable in HPMtrop. Instead, monthly tree NPP is added as monthly litterfall to the peat, disaggregated into three components: leaves, wood, and roots. Leaf and wood litter is added to a surface litter layer, which accumulates for 12 months, and then becomes the surface peat cohort at the end of the year. Root litter is added to the peat profile each month, following the HPM algorithm for non-sedge vascular plants.

Using the eddy covariance technique, the measured PSF gross primary productivity (GPP) in Sebangau, Kalimantan (Indonesian Borneo) depicts a quadratic relationship with water table depth (Figure 3, Hirano et al., 2012). We assume constant carbon use efficiency (CUE), the ratio of NPP to GPP, which for the tropical forests is in a range of 0.3 – 0.5 (Amthor, 2000; Giardina et al., 2003; DeLucia et al., 2007). Hence, monthly NPP in HPMTrop was calculated with a multiplicative factor based on the quadratic relationship with water table depth (*WT*).

$$GPP_j = -2.9545WT_j^2 + 1.6803WT_j + 9.5782 \dots\dots\dots 1$$

$$f_j = GPP_j/9.8 \dots\dots\dots 2$$

hence

$$f_j = -0.3046WT^2 + 0.1732WT + 0.9874 \dots\dots\dots 3$$

and so

$$NPP_{j,k} = NPP_{o,j,k} \times f_j \dots\dots\dots 4$$

where  $GPP_j$  is the monthly GPP for month  $j$  based on Hirano et. al. (2012) (Figure 3),  $f_j$  is a monthly standardized GPP ( $9.8 \text{ g C m}^{-2} \text{ d}^{-1}$ , was the maximum monthly mean GPP),  $NPP_{j,k}$  is the adjusted monthly  $NPP$  for tree component  $k$ ,  $NPP_{o,j,k}$  is the monthly  $NPP$  based on the previously published literatures for each tree component calculated as annual  $NPP$  divided by twelve (Table 1), and  $WT_j$  is the water table depth (m, positive values down from the peat surface). This factor equals 1.0 when  $WT = 0.12 \text{ m}$ . The partitioning the total  $NPP$  to leaf, wood, and root was not affected by the water table.

2.2.2.2. Peat water content profile. The peat profile is divided in two zones based on the position of the water table: an unsaturated zone located above the water table, and a saturated zone below the water table. Above the water table, the degree of saturation of a peat cohort ( $W$ ) is determined by two factors, cohort bulk density and cohort distance from the water table:

$$W_l = W_{min} + (1 - W_{min})e^{-(z_{WT}-z_l)/z_l^*} \dots\dots\dots 5^*$$

$$z_l^* = W_{min} + (c_1 - W_{min}) \left( \frac{\rho_l - \rho_{min}}{c_2 + \rho_l - \rho_{min}} \right) \dots\dots\dots 6^*$$

where,  $W_{min}$  is the peat minimum water content,  $\rho_l$  is the cohort bulk density and  $\rho_{min}$  is minimum bulk density,  $z_{WT} - z_l$  is the distance of the cohort to the water table (above the water table  $z_{WT} > z_l$ ). Note: in this thesis, all equations that are not modified from HPM (other than possible differences in parameter values) have an asterisk on their equation number (e.g., 5\*).

2.2.2.3. Decomposition rate. Peat decomposition follows HPM, where each litter type decomposes independently in each annual peat cohort (and the surface litter layer). Decomposition rates,  $k$ , decline linearly from their initial value,  $k_0$ , as the cohort loses mass,  $k = k_0 \cdot m/m_0$ , and there is a water content rate multiplier for cohorts above the water table, and different rate multiplier for cohorts below the water table. Above the water table, the rate multiplier is

$$f_{j,1} = 1 - \frac{(W_j - W_{opt})^2}{4 \times c_3} \dots\dots\dots 7^*$$

$$c_3 = \frac{(W_{sat} - W_{opt})^2}{4(f_{max} - f_{sat})} \dots\dots\dots 8^*$$

where  $f_{j,1}$  is the multiplicative factor for the decomposition rate of the cohort above the water table,  $W_{opt}$  is optimum water content for the decomposition,  $W_{sat}$  is peat water content at saturated condition,  $f_{max}$  is maximum decomposition multiplier at  $W = W_{opt}$ .

Below the water table,  $W = 1.0$ , the multiplier is reduced exponentially with depth below the water table,  $\hat{z}_j$  and determined by an anoxia scale length parameter,  $c_4$ ; a shorter scale length value causes decomposition rates to decline more rapidly with depth below the water table towards a minimum and an decrease in overall peat column decomposition rates.  $c_4$  might be influenced by the inter- and especially by intra-annual variability of peat water table.

$$f_{j,2} = f_{min} + (f_{sat} - f_{min})e^{-\hat{z}_j/c_4} \dots\dots\dots 9^*$$

where  $f_{j,2}$  is the multiplicative factor for the decomposition rate in the saturated zone,  $f_{min}$  is minimum decomposition multiplier, and  $f_{sat}$  is decomposition multiplier at the water table.

The monthly decomposition rate for each tree litter component was the product of the ratio of cohort mass remaining to initial mass and the decomposition multiplier as shown as

$$k_{j,k} = k_{o,j,k} \left( \frac{m_{j,k}}{m_{o,j,k}} \right) f_n \dots\dots\dots 10^*$$

where  $k_{o,j,k}$  is the monthly decomposition rate for each PFT based on the previous literatures (Table 1),  $m_{o,j,k}$  is the initial mass,  $m_{j,k}$  is the mass remaining, and  $f_n$  is the scalar multiplier as a function of the cohort water content with range from 0.3 to 1 for the peat cohort above the water table ( $f_{j,1}$ , Equation 7) and from 0.001 to 0.3 for the peat cohort below the water table ( $f_{j,2}$ , Equation 9).

2.2.2.4. Monthly peat mass balance and peat depth. Finally, cohort mass remaining was calculated as the balance of the litter input and the decomposition rate

$$\frac{dM_i}{dt} = \frac{d\sum_{j,k} m_i}{dt} = \sum_{j,k} (AG_j + BG_j - k_{j,k} m_{j,k}) \dots\dots\dots 11^*$$

where  $M_i$  is the annual cohort mass remaining,  $AG_j$  is the monthly aboveground input as the total of the litter fall and wood productivity, and  $BG_j$  is the root input to the cohort. The root input profile was assumed to be uniform from the surface of the peat down to the maximum of 0.5 m or the water table depth.

The peat cohort bulk density was estimated as a non-linear function of the degree of the decomposition,  $M/M_o$ . Therefore, bulk density provides a feedback to decomposition by affecting cohort water content (Equation 6). The formula to calculate bulk density for each cohort,  $l$ , is

$$\rho_l = \rho_{min} + \Delta\rho \left( 1 - 0.5 \left( 1 + \operatorname{erf} \left( \frac{\mu_l c_5}{c_6 \sqrt{2}} \right) \right) \right) \dots\dots\dots 12^*$$

where  $\rho_l$  is bulk density of cohort  $l$ ,  $\rho_{min}$  is minimum bulk density,  $\mu_l$  is degree of the decomposition and calculated as ratio of cohort mass remaining to the total mass input,  $M_l/M_{l,o}$ ,  $c_5$  is a parameter for determining the curvature of the error function (erf), and  $c_6$  is the parameter at which  $\mu_l$  will set  $\rho_l$  at halfway between its maximum and minimum.

The thickness of the peat cohort was calculated as the ratio of the total peat mass remaining from each tree components to its bulk density. It can be shown as

$$h_l = \frac{M_l}{\rho_l} = \frac{\sum_l m}{\rho_l} \dots\dots\dots 13^*$$

where  $h_l$  is the cohort thickness. The accumulation of the thickness along the peat profile determines the peat depth,  $H$ .

### 2.3. Water table reconstruction

Since HPMTrop does not calculate a monthly peat water balance, long-term monthly water table depth was required drive the model. There are two main steps used to generate this data for HPMTrop: 1. the development of a simple empirical model that relates peat water table with rainfall, and 2. stochastic rainfall data generation over millennia based on the 20<sup>th</sup> century rainfall patterns and probabilities.

#### 2.3.1. Water table empirical model.

A simple linear regression between estimated peat water deficit and measured water table was employed to estimate the water table depth over the long-time period. Required data for this analysis were rainfall and measured peat water table. Figure 4 shows the water table depth measured in Sebangau peat swamp of forest in Kalimantan, Indonesia for about 14 years (Wösten et al. 2010); monthly water table values were manually read from this graph for each year. Global, gridded monthly rainfall for 1900-2010 (Matsuura and Willmott, 2009) was downloaded from the Earth System Atlas (<http://earthatlas.sr.unh.edu/maps/>; download date: March 20, 2013). The spatially averaged monthly rainfall data from nine grid cells centered on Sebangau (-2.8°S, 113.8°E) were utilized to estimate peat water deficit, as

$$D_j = \max (0, D_{j-1} + (100 - P_j)), \dots \dots \dots 14$$

where  $D_j$  is water deficit and  $P_j$  is rainfall in month  $j$ . This equation had been widely applied to calculate water deficit for tropical forests (Aragão et al., 2007; Frohking et al., 2011; Hutrya et al., 2005; Malhi et al., 2009).

Using the measured monthly water table and calculated deficit using Equation 14, about 65% of the variation in monthly measured water table could be explained by the water deficit using a simple linear regression (Figure 5). Thus, the monthly water table was estimated by

$$WT_j = 0.1984D_j \dots\dots\dots 15$$

where  $WT_j$  is the monthly water table (cm) and  $D_j$  is the monthly water deficit (mm), based on monthly precipitation and Equation 14.

### 2.3.2. Generating rainfall data since late Pleistocene

The 1900-2010 annual rainfall in Sebangau, Kalimantan was disaggregated into three classes based on the southern oscillation index (SOI): El-Niño, normal, and La-Niña (McKeon et. al., 2004), with about half of the years classified as normal years and the remaining divided to El-Niño and La-Niña (Figure 6).

A cluster analysis of the 1900-2010 rainfall was done for each class – El-Niño, normal, and La-Niña years – using Ward’s method for clustering the monthly data based on the dissimilarity matrix calculated using Euclidian distance; the cluster analysis used JMP pro 10 software to obtain 12 rainfall groups, four in each class. These were associated with particular monthly water table depth time series (Figure 4). A dendrogram graph showing the rainfall



grouping was scaled by using dissimilarity distance and the probability of each rainfall group was calculated as the ratio of the number of years within the group generated by cluster analysis to the number of years in its rainfall class.

Paleoclimate reconstruction has demonstrated that the intensity and frequency of El-Niño-Southern Oscillation (ENSO) in the Holocene was lower than in modern years (Conroy et al., 2008; Cobb et al., 2013). Furthermore, Sandweiss et al. (2001) reported that El Niño in the period between 5.8 and 3.2-2.8 kBP were less frequent than occurrences in present years. Based on this, a scenario for capturing the variability frequency of El-Niño since the Holocene was implemented in this study. I separated simulation years into three periods: before 6 kBP, 6 – 3 kBP, and after 3 kBP as shown in Table 2. The probability of the El-Niño in 3 kBP to present was assumed the same as the El Niño probability in 20<sup>th</sup> century: 30% El Niño, 50% normal, and 20% La Niña (Figure 6). Before 3 kBP, the El-Niño probability was lower than the modern values (Table 2).

Oxygen isotope content ( $\delta^{18}\text{O}$ ) from stalagmite samples can be used as an indicator of rainfall conditions in the tropics since it is negatively correlated with the precipitation amount (Wang et al., 2005; Partin et al., 2007; Griffiths et al., 2009). In this study, the pattern of rainfall data over the past 15,000 years was generated based on the  $\delta^{18}\text{O}$  taken from the cave stalagmites in northern Borneo since late Pleistocene (Figure 7, Partin et al., 2007) with the inter-annual variability of rainfall based on the monthly rainfall probability in 20<sup>th</sup> century.

Figure 7 shows that the stalagmite  $\delta^{18}\text{O}$  in the late Pleistocene, about 15,000 years ago, was heavier than modern values, indicating the drier conditions at that time. The wettest condition based on  $\delta^{18}\text{O}$  possibly occurred in the mid Holocene (3,000 – 5000 yrs ago). About 92% variation of  $\delta^{18}\text{O}$  can be explained by time in the third-order polynomial equation. The modern value of  $\delta^{18}\text{O}$  was used to calculate the multiplier factor for generating rainfall over the longer time period is shown as

$$P_{i,j} = P_{20,j} (3 \times 10^{-12} i^3 - 4 \times 10^{-8} i^2 - 4 \times 10^{-5} i - 7.5886) / -9.3 \dots\dots\dots 16$$

where  $P_i$  is the rainfall for year  $i$  and month  $j$ .  $P_{20,j}$  is the 20<sup>th</sup> century rainfall in month of  $j$ . Then, using this estimated rainfall, the long-term water table can be estimated using the equation 14 and 15.

#### **2.4. Model evaluation**

A simple model calibration between observed and modeled values was implemented in this study. Dommain et al. (2011) collected published radiocarbon data sampled from peat cores in South East Asia, particularly in Sumatra, Borneo and peninsular Malaysia. Based on the characteristics of peat development and their distance to the sea, they classified peat profiles as coastal (number of cores,  $N = 15$ ), inland peatlands ( $N = 11$ ) and Kutai peatlands ( $N = 4$ ). Using those data and some explanation about the differences among the peatlands types, in this study I simulated peat profiles for both coastal and inland types, excluding the Kutai peatlands, by (i) using different anoxia scale length

values (Table 1), (ii) adjusting the water table for coastal peatlands 25% closer to the peat surface, and (iii) different peat initiation times: 5 and 13 kBP for coastal and inland peatlands, respectively. In comparison between simulation and measurement, I tuned the anoxia scale length of coastal and inland peatlands. In addition, the total peat mass remaining at the end of simulation year were compared to total peat carbon stocks obtained from the field survey in PSF in Sumatra and Kalimantan, Indonesia. The detailed site descriptions, peat sampling procedure, and laboratory analysis are explained in Section 2.7

### **2.5. Sensitivity analysis**

A number of simulations using different parameter values were run to test the sensitivity of the HPMTrop model. In this sensitivity test, a systematic parameter alteration was implemented: changing by  $\pm 25\%$  the multiplier factor of rainfall, *NPP* parameters, or *k* parameters for each plant component, anoxia scale length, and the range of peat bulk density. The peat depth and peat mass at the end of the simulation were chosen as the model response in the sensitivity test.

### **2.6. A land-cover change scenario**

The impact of forest conversion to oil palm plantation on the carbon dynamics in tropical peatlands was also modeled in HPMTrop. Some assumptions used in this scenario are:

- The period of simulation for the land cover change is 100 years with a 25-year crop rotation.

- Drainage ditches were installed to lower the WT (Melling et al., 2005); this was simulated by lowering the monthly water table by 60 cm; the drainage ditches were 'maintained' so the lower water table persisted even as the peat surface lowered due to decomposition (net mass loss).
- At the beginning of each rotation, the site was burned; it was assumed that the upper 20 cm of peat and all aboveground biomass was lost due to combustion (Hergoualc'h and Verchot, 2011).
- During these rotations, the litter input to the peat came from oil palm litter fall and root production (Hergoualc'h and Verchot, 2011).

## **2.7. Field surveys**

### **2.7.1 Study area**

The Center for International Forestry Research (CIFOR), based in Bogor, Indonesia, in collaboration with USDA Forest Service, is running a project initially named Tropical Wetlands Initiative for Climate Adaptation and Mitigation (TWINCAM), and later renamed the Sustainable Wetlands Adaptation and Mitigation Program (SWAMP). The main objective of TWINCAM/SWAMP is to increase understanding of the role of peat swamp and mangrove forests in reducing emissions from deforestation and forest degradation and enhancing forest carbon stocks in developing countries (REDD+) (Murdiyarso et al., 2010). One of the activities of TWINCAM/SWAMP is quantifying the total carbon stocks and greenhouse gas emissions in tropical wetland forest ecosystems. In 2011,

TWINCAM researchers sampled over 50 forest stands (mangroves and peat swamp forests) in Indonesia for estimating the total carbon stock in Indonesian wetlands. In addition, a major campaign to measure greenhouse gas emissions in both pristine and disturbed peatlands was begun in 2012. In parallel with these ongoing efforts, field research for this study was established in Tanjung Puting National Park (TPG) and Berbak National Park (BBK). To strengthen the assessment of carbon cycle in the tropical peat swamp forest, peat cores were collected to determine total organic carbon pools as well as for radiocarbon dating analysis of peat cores.

TPG, located in Central Kalimantan Province of Indonesia, and BBK, Sumatra were chosen as field sites for peat coring. TPG is situated in the southern part of Indonesian Borneo and surrounded by the Java Sea in southern and western part of the area (-2°49'20" S and 115°50'25.8" E). It covers an area of about 400,000 ha and is predominantly occupied by peat swamp forest.

The transect method, modified from Kauffman and Donato (2012), was applied in the field survey for collecting the peat samples. Peat cores were collected at 50 m intervals along 250-m transects (6 plots per transect). A total of 3 transects were established in the pristine PSF of TPG and 3 transects in BBK. These field surveys were performed in conjunction with other TWINCAM research in this area and involved researchers from OSU, IPB, CIFOR, USFS, and the Orangutan Foundation International (OFI) and the park officers as a local partners.

### 2.7.2. Peat core sampling and analysis

A peat core was extracted from each plot, coring from the peat surface down to the peat/mineral substrate interface, using an Eijkelkamp soil auger. Since it was not logistically possible to transport the entire peat core from the field, the cores were subsampled in the field, with 5 cm of peat extracted at the middle of each segment from the peat core. The number of subsamples per core varied depending on the total peat depth. For example, for the peat depth of 250 cm, we take 5 cm subsamples in the middle of each segment: 0 – 30 cm; 30 – 50 cm; 50 – 70 cm; 70 – 90 cm; 90 – 110 cm ; 110 cm – 130 cm; 130 – 150 cm; 150 – 200 cm; and 200 – 250 cm.

After coring, peat samples were packed using the aluminum foil, put in the whirl pack and transported to the Soil Biotechnology Laboratory at Bogor Agricultural University (IPB), Java, Indonesia, for laboratory analysis to determine bulk density, carbon and nitrogen content. Peat sub-samples of known volume were dried to constant weight at 60°C, the sub sample dry weight and its pre-drying volume were used to calculate peat bulk density for each peat segment. The dried peat was then ground, homogenized and analyzed for carbon and nitrogen concentration using a LECO TruSpec induction furnace C analyzer (LECO Corporation, St. Joseph MI, USA). Radiocarbon analysis on a subset of the peat sub samples will be done by Michigan Technological University (sample prep) and Lawrence Livermore National Lab (radiocarbon dating); this dating will be done in collaboration with the USFS. Results of the radiocarbon dating of

samples from TPG and BBK are not presented in this thesis, as the analysis has not been completed.

Peat carbon stock for each site was calculated as the product of carbon concentration, bulk density and peat depth. To avoid the pseudoreplication, the analysis is summarized in each site instead of plot analysis. The carbon concentration and bulk density were presented along the peat profile from the surface until underlain mineral substrates were reached, shown as standardized depth, which is calculated as the depth where the subsamples taken divided by the peat depth. Principle components analysis was performed using JMP pro 10 software to obtained the pattern of carbon concentration and bulk density along the peat profiles, peat depth and total peat carbon among the sites.

### **III. RESULTS**

#### **3.1. Rainfall data generation since late Pleistocene**

Based on the cluster analysis of the 1900-2010 annual rainfall in each class – El Niño, normal, and La Niña – the years were aggregated into four groups, and a mean monthly precipitation was calculated for each of these 12 sets of years. Figures 8 – 10 shows the dendrogram resulting from the two-way cluster analysis in which the X-axis is clustered by the monthly rainfall and Y-axis is clustered by the rainfall inter-annual variability. The rainfall amount for each month, P, is also shown in Figure 11.

In the El Niño class, the rainfall clusters P1 and P2 were similar, as were P3 and P4. P2 and P4 had the minimum and maximum annual rainfall respectively, but occurred less frequently than P1 and P3 (Figure 8). About half the years in 1900 – 2010 were in the normal class, based on the SOI; the P8 cluster had the lowest rainfall and its pattern was closer to P7 than to P6 and P7. The dendrogram also shows that the pattern of P5 was very different with P8 in which both clusters only connected by using the inter-link of clusters P6 and P7 (Figure 9). In the La Niña class, only three years were aggregated into one cluster, P12, which had the least annual rainfall of the La Niña class; the other three clusters, P9 – P11, were relatively similar (Figure 10).



In terms of monthly precipitation, the La Niña clusters had the least seasonality (Figure 11) – monthly rainfall in May to October was still relatively high, at about 150 – 200 cm, but rainfall < 100 cm also occurred in those months with a probability of only 10%. In contrast, El Niño years had a distinct and relatively long dry season from May to October – most of the groups had 90% probability of rainfall less than 100 cm during one or more of those months. In normal years, the rainfall pattern was moderately seasonal, but the dry season was typically shorter and not as dry as in the El Niño years (Figure 11).

The water deficit in El Niño years, driven by less than 100 cm monthly rainfall in May to October, was higher than in normal and La Niña years (Figure 12). Water deficit in a range of 140 to 300 mm occurred in October and had a probability of about 90% and equivalent with the water table of 30 – 60 cm below the peat surface (Figure 13). In normal years, the water deficit still showed the seasonality, ranging from 0 to 110 cm and with a resulting water table up to 20 cm from the peat surface. La Niña years show less seasonality, with a probability of ~90% that the water table was nearly close to the peat surface; there was only a 10% probability that the water table deeper than a few cm, but it was always less than 20 cm.

Long-term rainfall since the late Pleistocene was estimated based on the rainfall cluster probabilities in the 20<sup>th</sup> century, changes in ENSO intensity over the millennia, and modified by the pattern of stalagmite  $\delta^{18}\text{O}$  sampled in northern Borneo, (Figure 14; top). Using a 25-year moving average, mean annual rainfall

in the late Pleistocene (15 kBP) was about 2,000 mm y<sup>-1</sup>. It gradually increased and reached the maximum value in the mid Holocene (5 – 4 kBP) of about 2,500 mm y<sup>-1</sup>. After 5 kBP, rainfall dropped the current condition of about 2,200 mm y<sup>-1</sup>. For the absolute rainfall, the maximum and minimum value is about 3,200 mm y<sup>-1</sup> around 4 kBP and 1,500 mm y<sup>-1</sup> in recent strong El Niño years, respectively.

The peat water table in inland peatlands estimated as a function of the monthly water deficit was always near the peat surface with the lowest annual water table of about 20 cm below the peat surface (Figure 14, middle, blue line). Mean water table in late Pleistocene fluctuated within 5 cm below the peat surface and it rose gradually following the increasing of annual rainfall. Around 6 kBP, the annual average water table was less than 2 cm below the peat surface and then dropped to about 5 cm in the recent past.

The monthly water table in coastal peatlands was calculated in the same way as for the inland peatland as a function of water deficit but set at only 75% as deep as the inland peatland values (Figure 14, bottom). In the last 5,000 years, the mean water table varied between 2 cm to 5 cm. The water table decreased gradually after 5,000 year and lowered to about 5 cm in the last 100 years.

### **3.2. HPMTrop Results**

Simulated NPP (or litter input), with a weak dependence on water table depth, was roughly constant over the long simulation period, with an annual mean of 9.6 Mg C ha<sup>-1</sup> y<sup>-1</sup> (Figure 15, top) for coastal peatlands. Almost half of the simulated litter production was composed of leaves, 35% as wood, and 15% as roots.

For the coastal peatlands scenario, simulated decomposition increased in the first 500 years of the simulation from 6 to about 8 Mg C ha<sup>-1</sup> y<sup>-1</sup> (Figure 15, middle), as peat accumulated. After this time, the decomposition rate increased very slowly with the inter-annual variability within a range of 8 to 10 Mg C ha<sup>-1</sup> y<sup>-1</sup> and at the end simulation the decomposition was about 9.5 Mg C ha<sup>-1</sup> y<sup>-1</sup>. Increasing decomposition rates over long-term period followed the gradual lowering water table trend in the past 5,000 years, with the mean annual rate of 8.9 Mg C ha<sup>-1</sup> y<sup>-1</sup>.

Net peat accumulation, or dC/dt, is the balance between NPP and the decomposition rate and is shown for the coastal peatlands in Figure 15 (bottom). Peat will accumulate if dC/dt is positive and, conversely, peat mass will be lost when dC/dT is negative. A decrease from about 2 to 1 Mg C ha<sup>-1</sup> y<sup>-1</sup> occurred in the first 500 year of simulation based on the 25-year moving average. From this year until the end of the simulation dC/dT is relatively constant with inter-annual variability ranging from 0 to 2 Mg C ha<sup>-1</sup> y<sup>-1</sup>. Figure 15 also shows that through the simulation, vegetation input is generally greater than the decomposition rate, as dC/dt is mostly greater than zero and peat slowly accumulates.

Similar to the coastal peatland, the long-term trend of simulated NPP in inland peatlands was relatively constant in a range of about 9.5 to 9.8 Mg C ha<sup>-1</sup> y<sup>-1</sup> with the mean annual of 9.7 Mg C ha<sup>-1</sup> y<sup>-1</sup> (Figure 16, top).

The mean annual simulated decomposition rate increased from about 5.3 to 9.8 Mg C ha<sup>-1</sup> y<sup>-1</sup> after about 1,000 years of simulation and subsequently was

relatively constant, in a range of 7.9 to 10.8 Mg C ha<sup>-1</sup> y<sup>-1</sup> (Figure 16, middle). The mean annual decomposition rate for over 13,000 years was about 9.3 Mg C ha<sup>-1</sup> y<sup>-1</sup>; the minimum value, 2.9 Mg C ha<sup>-1</sup> y<sup>-1</sup> occurred in the first century of the simulation, and the maximum value, 17.5 Mg C ha<sup>-1</sup> y<sup>-1</sup>, occurred in a very dry year around after 550 years of simulation (~12400 BP).

Due to relatively constant NPP and an increasing decomposition rate in the first 1,000 years of the simulation, the mean annual dC/dt of the inland peatlands decreased from 2.4 Mg C ha<sup>-1</sup> y<sup>-1</sup> in the initial years to about 0.2 Mg C ha<sup>-1</sup> y<sup>-1</sup> (Figure 16, bottom). For the remainder of the simulation, the mean annual dC/dT did not have a trend, and was within the range of -0.7 to 1.3 Mg C ha<sup>-1</sup> y<sup>-1</sup>. The mean long-term annual dC/dt was 0.3 Mg C ha<sup>-1</sup> y<sup>-1</sup> and maximum and minimum values were -7.9 and 5.2 Mg C ha<sup>-1</sup> y<sup>-1</sup>.

Although the simulated inland peatland started to accumulate carbon in the late Pleistocene, about 13 kBP, the carbon stored at the end of simulation was about the same as for the coastal, which initiated 8,000 years later (Figure 17). The peat carbon stocks at the end of simulation for both inland and coastal peatland were 3,270 Mg C ha<sup>-1</sup> and 3,150 Mg C ha<sup>-1</sup>, respectively. For inland peatland, the simulated peat mass increased to about 650 Mg C ha<sup>-1</sup> after 2,000 years and rose steadily to about 3,000 Mg C ha<sup>-1</sup> after about 10,000 years. In the last 3 millennia of simulation, the peat mass increased at slower rate, due to gradual drying of the climate, and reached about 3,300 Mg C ha<sup>-1</sup> at the end of simulation.

The peat carbon accumulation rate of the coastal peatland is much higher than in inland peatland due to the shallower water table and shorter anoxia scale length (Figure 17). It took only 2,000 years to accumulate about 1,700 Mg C ha<sup>-1</sup>. The peat mass continued to increase, though more slowly over time, and reached to 2,700 Mg C ha<sup>-1</sup> after 4,000 years and 3,100 Mg C ha<sup>-1</sup> at the end of simulation.

The apparent peat accumulation rate, which is different from  $dC/dt$ , and which can be compared to carbon accumulation in peat cores, was estimated by the peat cohort thickness at the end of simulation (as if the simulated peat was 'cored') and is shown in Figure 18. For coastal peatlands, in the mid-Holocene, the peat accumulation was in a range of 1.2 to 1.3 mm y<sup>-1</sup> and dropped quickly to about 1 mm y<sup>-1</sup> in 2500 year BP, then reached minimum rate of about 0.9 mm in 1600 year BP. In recent years, the peat accumulation increased to ~1.5 mm y<sup>-1</sup> due to these cohorts being less fully decomposed than the older and deeper cohorts. Overall, the long-term carbon accumulation rate in the coastal peatland, calculated as the average cohort thickness, year is 1.2 mm y<sup>-1</sup>.

Over 13,000 years of simulation, the inland peatlands had a lower peat accumulation rate compared to coastal peatland, ranging from 0.4 to 1.5 mm y<sup>-1</sup> (Figure 18). For the oldest and deepest peat, the apparent accumulation rate is about 0.4 mm y<sup>-1</sup> for about 2,000 years. It then increased gradually to about 0.5 mm y<sup>-1</sup> in 7000 year BP, and then slowly decreased after 7000 year BP and reached a minimum rate of about 0.4 mm y<sup>-1</sup> 3000 year BP. In the late Holocene,

the apparent peat accumulation rate increased rapidly to about  $1.5 \text{ mm y}^{-1}$ . The simulated long-term apparent peat accumulation rate in inland peatland is  $0.5 \text{ mm y}^{-1}$ .

The carbon accumulation rate, the product of accumulation rate and cohort bulk density, shows a greater variability in the coastal peatland, ranging from 0.5 to  $0.8 \text{ Mg C ha}^{-1} \text{ y}^{-1}$  (Figure 18, bottom). In the beginning of development, 5000 – 3500 year BP, the carbon accumulation was about  $0.6 \text{ Mg C ha}^{-1} \text{ y}^{-1}$  and, then, dropped to  $0.5 \text{ Mg C ha}^{-1} \text{ y}^{-1}$  in 2000 year BP. In the last century, the carbon accumulation increased to about  $0.8 \text{ Mg C ha}^{-1} \text{ y}^{-1}$ . Overall, the mean carbon accumulation year in coastal peatland was  $0.62 \text{ Mg C ha}^{-1} \text{ y}^{-1}$  over 5,000 years. The pattern of apparent carbon accumulation rate in the inland peatland simulation was slightly different than the coastal peatland. Overall the inland peatland had a slower rate of accumulation that varied between 0.19 to  $0.45 \text{ Mg C ha}^{-1} \text{ y}^{-1}$  and the mean long term carbon accumulation rate was  $0.26 \text{ Mg C ha}^{-1} \text{ y}^{-1}$ , about half that of the coastal peatland simulation. The apparent accumulation rate rose slowly from  $0.22 \text{ Mg C ha}^{-1} \text{ y}^{-1}$  13,000 years ago to  $0.28 \text{ Mg C ha}^{-1} \text{ y}^{-1}$  after 6500 years. For the period of 3000 – 1000 BP, the carbon accumulation rate was relatively consistent at about  $0.2 \text{ Mg C ha}^{-1} \text{ y}^{-1}$ . Again, the rise in the apparent carbon accumulation rate for the most recent, shallow peat is due to these cohorts being less fully decomposed than the older and deeper cohorts.

The variability of peat accumulation rate in inland peatlands over 13,000 years affects the pattern of simulated age-depth profile (Figure 19). In the

beginning of the development prior to 10 kBP, with the peat accumulation rate of about  $0.4 \text{ mm y}^{-1}$ , the peat depth varied from 5.0 to 6.1 m. A faster accumulation rate occurred after 10 kBP resulting in the peat depth of about 2 m in 4 kBP and then reach 0.5 m in 500 year BP. The high variability of the peat accumulation rate in coastal peatland did not lead to significant curvature in age-depth profile. Over 5000 years, the relatively linear relationship between peat age and depth was depicted with the maximum depth was about 5.8 m. However, the rate of long-term carbon accumulation was much more stable in the simulated inland peatland scenario than observed at many field sites (Figure 19). This may relate to the influence of regional sea-level variation during the Holocene of peatland water tables (Dommain et al. 2011), which is not included in these simulations.

### **3.3. Sensitivity analysis**

Sensitivity runs were done for the coastal peat swamp forest (Table 3). Increasing total tree productivity/litter production (leaves, wood, and roots) by 25%, while leaving the decomposition parameters ( $k_0$  values) unchanged, increased the peat carbon after 5000 years by about 80% ( $5,700 \text{ Mg C ha}^{-1}$ ) and, hence, increased the peat depth by about 80% to 10.7 m at the end of simulation. In addition, the fraction of peat carbon to the total NPP also increased by about 40% from 6.7% in the base run to 9.6%. Conversely, the decreasing of total tree productivity by 25% reduced the peat mass remaining by about 60%, and the peat depth by about 60%. The change of the total tree productivity ( $\pm 25\%$ ) is the same as a change of total NPP at the end simulation since HPMTrop did not

simulate NPP as function of the any peat characteristic but only as a quadratic function of water table.

For each component of plant productivity, alteration of NPP rates influenced the model output differently. The model was very sensitive to the change of the wood productivity; the peat carbon reduced by about 40% and increased by ~50% due to a 25% decrease and increase of the wood productivity, respectively. Increasing root productivity by 25%, however, only led to a small change to the peat mass remaining of about 10%. Despite having the largest magnitude change, increasing/decreasing leaf NPP by  $\pm 25\%$  had a much smaller impact on total peat accumulation (~15%) than changing wood NPP. Peat depth changes were similar to the changes in mass.

As the main factor of the decomposition component of the mass balance equation, the litter quality, represented by  $k_0$ , influences the model results strongly. Increasing the  $k_0$  for all three tree components by 25% would reduce the peat accumulation at the end simulation by ~45% due to the higher decomposition rate, and hence reduced the peat depth 45%. Total NPP was the same in all of these simulations since it was only influenced by the water table. Therefore, the fraction of the total NPP that remains as peat,  $C/NPP$ , reduced with an increase of  $k_0$ . Among three litter components, the model is very sensitive to the change of the  $k_0$  of wood; changing wood's  $k_0$  to  $0.017 \text{ month}^{-1}$  resulted in an increase ~45% of both peat carbon and peat.



The anoxia scale length,  $c_4$ , plays an important role in simulated peat accumulation by affecting the decomposition rate of peat cohorts located near to but below the water table. Increasing the anoxia length to 0.23 m (from a base value of 0.18 m) reduced the peat carbon, depth and the ratio of peat carbon by NPP about 30%, but did not influence to the total NPP during the simulation. Decreasing the value of anoxia scale length to 0.14 m led to an increase of about 45% in peat carbon, depth, and  $C/NPP$  after 5000 years.

Unlike NPP or  $k_0$ , which increase or decrease both peat carbon and peat depth, the minimum bulk density parameter,  $\rho_{\min}$ , has a much larger impact on peat depth than peat mass. Increasing  $\rho_{\min}$  to  $110 \text{ kg m}^{-3}$  from the base value of  $90 \text{ kg m}^{-3}$  and unchanged  $\Delta\rho$  of  $40 \text{ kg m}^{-3}$ , so the maximum  $\rho$  is  $150 \text{ kg m}^{-3}$ , resulted in a 31% decrease of peat mass and decreased the peat depth by about 43%. Conversely, reducing  $\rho_{\min}$  to  $70 \text{ kg m}^{-3}$  while retaining the value of  $\Delta\rho$  caused the peat carbon and peat depth increase by about 50% and 90%, respectively. Again, total NPP during the simulation was not influenced by changing of  $\rho_{\min}$ .

Changing  $\Delta\rho$  from  $40 \text{ kg m}^{-3}$  to  $50 \text{ kg m}^{-3}$  caused a small decrease ( $\sim 10\%$ ) in peat carbon and peat depth. On the other hand, reducing  $\Delta\rho$  to  $30 \text{ kg m}^{-3}$  resulted an increase of peat mass and depth by 5% and 10%, respectively. This is much smaller than the changes in both peat mass and peat depth generated by the alteration of  $\rho_{\min}$ . Similarly, the changing of  $c_5$  and  $c_6$ , parameters for controlling how bulk density increases with peat humification, had little impact on

the peat mass, peat depth, and *C/NPP* (simulation runs #24-27 in Table 3); in all cases the impact was <5%.

Sensitivity analyses of the multiplier of the rainfall pattern based on  $\delta^{18}\text{O}$  of cave stalagmites (equation 16) and the linear relationship for estimating water table (equation 15) were also performed. Increasing monthly rainfall by 25% generated an increase of peat mass remaining of ~15%, and also increased the peat depth by the same magnitude, due to unchanged bulk density parameters. Simulating a drier climate over 5,000 years by reducing the rainfall multiplier by 25% reduced the peat mass and peat depth of about 30%. Increasing the monthly water table depth by 25% resulted in a decrease of peat mass remaining and peat depth of ~13% at the end of the simulation. Setting the monthly water table in a constant value of 0.1 m over 5,000 years reduced the peat carbon by about 50%. Yet the mean annual WT was still the same (0.1 m), lowering monthly water table to 0.4 m for three months and 0 m for nine months reduced the peat carbon and peat depth by ~60%.

#### **3.4. Land cover change scenario**

Simulated peat mass for the coastal peatland accumulated to 3,150 Mg C ha<sup>-1</sup> in the last millennia of the simulation, and then decreased sharply to only 1,660 MgC ha<sup>-1</sup> in the 100 years following forest conversion (Figure 20). The carbon loss of 1,490 MgC ha<sup>-1</sup> over the period of 100 years generated by land cover change practices was equivalent to peat development over the previous 3,000

years. In addition, it would require an area of about 2,500 ha of pristine PSF to sequester the amount of carbon lost over 100 years in one ha area. A truncated peat age-depth profile also resulted from the scenario of forest conversion, with the surface peat dating to about 2400 BP (Figure 20). At the end simulation of 4x25-year rotation of oil palm plantation and burning, the peat depth was about 2.8 m, down ~3 m from the simulation run without forest conversion. Peat subsidence simulated from HPMTrop was only caused by peat oxidation and neglected the consolidation and compaction components.

For the inland peatland, accumulated peat mass reached about 3,300 Mg C ha<sup>-1</sup> before forest conversion and reduced to 2,200 MgC ha<sup>-1</sup> due to the the land cover change (Figure 20). The carbon loss resulted from that scenario was about 1,100 Mg C ha<sup>-1</sup> over 100 years (~1.1 Mg C ha<sup>-1</sup> y<sup>-1</sup>); it had required about 6,000 years to accumulate the final 1100 Mg C ha<sup>-1</sup>. The peat depth at the end simulation was 3.8 m, down about 2.3 m from the pristine scenario, again with a truncated peat age-depth profile (Figure 21). This carbon loss estimations are conservative values as I did not include the lost caused by the aboveground biomass.

### **3.5. Measured peat carbon stocks**

The field measurements indicate that PSF in both Tanjung Putting NP (TPG) and Berbak NP (BBK) stored a large amount of belowground C that varied between 1,000 Mg C ha<sup>-1</sup> in TPG3 to 3,100 Mg C ha<sup>-1</sup> in BBK2 (Figure 22) taken

from the cores with depth ranging from 2.1 m to 6.3 m. Based on the distance from the coastline, all sites in both NPs would be classified as coastal peatlands. On average, TPG stored  $1,100 \pm 160$  (mean  $\pm$  SD) Mg C ha<sup>-1</sup> with the carbon concentration of  $45.6 \pm 5.9\%$  and bulk density of  $113.8 \pm 37.3$  kg m<sup>-3</sup>. BBK sites contained  $2,470 \pm 626$  Mg C ha<sup>-1</sup> with the carbon concentration of  $51.0 \pm 5.7\%$  and bulk density of  $107.1 \pm 30.6$  kg m<sup>-3</sup>.

Using the information of the carbon content and bulk density along the profile represented by the standardized depth, the depth of the samples taken from the core divided by the peat depth, actual peat depth and carbon stocks, a principal components analysis was performed. The first two axes explained about 78% of the data variation; the first axis (PC1) explained the most variation, 58% (Figure 23). By plotting of scores values in both PC1 and PC2, it shows that sites in BBK were separated from TPG along the PC1, which was highly associated with carbon content along the profiles and negatively correlated with bulk density in the middle of the cores. Additionally, PC2, which can explain 18.9% of the variation, is mostly correlated with the bulk density close to mineral layer (p7, p8, p9, and p10) and carbon content (C7 and C8). One of sites in BBK, BBK3 was positively associated with the PC2, which means this site may have lower carbon concentration but higher bulk density. Based on that carbon content, bulk density, peat depth and carbon stock, sites in BBK were significantly different with TPG ( $p = 0.024$ ).

The profiles of C-content (%C) in the peat columns of BBK were relatively higher than TPG (Figure 24, top). The peat carbon content in BBK and TPG varied between 45 – 55% and 40 – 50% along the profiles, with the relatively similar value in the middle of the cores. Bulk density at BBK was higher near the surface, 100 – 130 kg m<sup>-3</sup>, and then reduced to about 90 kg m<sup>-3</sup> for the remainder of the profiles (Figure 24, bottom). In contrast, peat bulk density in TPG increased in the lower 20% of the peat profile, close to the underlying clay layer; %C also declined in the lower 20% of the TPG core data.

## **IV. DISCUSSION**

### **4.1. Carbon accumulation rates in tropical PSF during the Holocene**

Tropical peatland forests play an important role in the global climate system by absorbing carbon from atmosphere and storing it for long periods as organic matter in surface peat deposits. Some tropical peatlands started to accumulate carbon as peat in the late Pleistocene (Yu et al., 2010; Dommain et al., 2011), but they were initiated predominantly in the mid Holocene, around 4 – 7 kBP (Yu et al., 2010). Peatlands in the Sebangau catchment in Central Kalimantan, which can be classified as inland peatlands, initiated up to about 20 kBP (Page et al., 2004a), and some other inland peatlands in Palangkaraya, Kalimantan began accumulating about 10 kBP (Neuzil, 1997). However, some younger peatlands that began to form around 2,000 to 8,000 years ago are also found in the coastal area of Riau, Sumatra (Neuzil, 1997). For simulating carbon accumulation in coastal and inland peatlands using HPMTrop, the length of simulation of 5,000 and 13,000 years were chosen for coastal and inland peatlands, respectively.

There were two dominating regional changes during the late Pleistocene and Holocene that would have influenced regional hydrology – changes in sea level and changes in precipitation. Globally, sea level rose abruptly by about 60 m in the early Holocene from the period ~12 to 7 kyr; sea level at about 7 kBP was similar to modern sea level (Smith et al., 2011). In the Sunda Shelf of Southeast

Asia, sea level was 64 m below present mean sea level (i.e., -64 m) in 13 kBP and increased to -50 m in 11 kBP (Hanebuth et al., 2000). Then, in the period between 11 to 6 kBP a higher rate of sea level rise occurred, and sea level rose from -50 m to mean sea level (MSL) at the present (~0 m) (Sathiamurthy and Voris, 2006). Sea level continued to increase, but at a lower rate, and reached to about +5 m around 5 kBP, and then decreased gradually to modern MSL (Steinke et al., 2003). The abrupt increase in sea level in the early Holocene led to inundation of the Sunda Shelf, which had been exposed during the last glaciation (Smith et al., 2011) and, hence, increased the regional evaporating area as a source of moisture. This, coupled with an increase in sea surface temperature (SST) in the western equatorial Pacific (Rosenthal, 2003), may have increased convective forcing, resulting higher rainfall in Southeast Asia.

During the Holocene, Southeast Asia rainfall varied greatly, influenced by multiple factors: northern summer insolation, mean position of Inter-Tropical Convergence Zone (ITCZ), sea surface temperature, and sea level rise. Rainfall reconstruction based on  $\delta^{18}\text{O}$  speleothems sampled from cave stalagmite's calcite in northern Borneo (Partin et al., 2007) and Liang Luar, Flores, Indonesia (Griffiths et al., 2009) demonstrated that annual rainfall in the mid-Holocene was higher than both the late Pleistocene/early Holocene and the present. However, the two paleo-reconstructions show different patterns: stalagmite  $\delta^{18}\text{O}$  from northern Borneo indicate a precipitation maximum occurred ~ 4 kBP; while at Liang Luar it was ~7 kBP. In addition, El-Niño began to intensify after about 6

kBP (Sandweiss et al., 2001; Conroy et al., 2008; Cobb et al., 2013), which probably caused a decrease of rainfall, at least in some years, in the Indonesian region (Aldrian and Dwi Susanto, 2003). In this study, I only considered the rainfall regime and neglected the sea-level history after the last glaciation that probably also affected peatland hydrology and influenced peat accumulation (Yu et al., 2010, Dommain et al. 2011).

In the late Pleistocene to early Holocene, 13 – 10 kBP, inland peatlands were in the early phase of their development, possibly caused by sea level rise in the Sunda Shelf associated with the last deglaciation (Steinke et al., 2003; Dommain et al., 2011), while coastal peatlands had not yet begun to form. HPMTrop simulated an initial peat accumulation rate for inland peatlands of about 0.4 mm y<sup>-1</sup>. Somewhat higher peat accumulation rates of about 0.6 and 0.8 mm y<sup>-1</sup> were recorded from cores collected in the Sebangau catchment, Kalimantan, dated from 13 to 10 kBP, and the Palangkaraya peatland dated 9 kBP respectively (Neuzil, 1997; Page et al., 2004). In addition, the simulated carbon accumulation rate in this period varied from 0.22 to 0.25 Mg C ha<sup>-1</sup> y<sup>-1</sup>. This is in the range of C-accumulation rates recorded from a core sampled in the Sebangau catchment of about 0.18 to 0.33 Mg C ha<sup>-1</sup> y<sup>-1</sup> (Page et al., 2004), but lower than rates from a core from Palangkaraya, Kalimantan, which ranged from 0.5 to 0.7 Mg C ha<sup>-1</sup> y<sup>-1</sup> (Neuzil, 1997).

Around 8 to 7 kBP, both peat and carbon accumulation rates were higher than the rates in the late Pleistocene. Simulated peat accumulation rates for the inland



peatland scenario were about  $0.5 \text{ mm y}^{-1}$ , equivalent to a carbon accumulation rate of  $0.27 \text{ Mg C ha}^{-1} \text{ y}^{-1}$ . These simulation results were in line with the accumulation rate measured from a peat core sampled in Sebangau catchment, Kalimantan in a range of  $0.4$  to  $0.9 \text{ mm y}^{-1}$  ( $0.2$  to  $0.5 \text{ Mg C ha}^{-1} \text{ y}^{-1}$ ). These simulated rates, however, are lower than observed values from Palangkaraya peatlands of  $1.2 \text{ mm y}^{-1}$  (Neuzil, 1997).

Favorable environmental conditions that generated higher accumulation probably existed 8 to 7 kBP. The abrupt rise of sea level after last glaciation generated flooding in Sunda Shelf and in 7 kBP the sea level was the same as present MSL. A rising sea level would decrease the overall landscape gradient to the sea, particularly for low-relief coastal regions; this could impede overall landscape drainage and lead to rising water tables in peatlands (Dommain et al., 2011). The combination of sea level rise (Sathiamurthy and Voris, 2006), and higher rainfall or reduced frequency of dry years (Partin et al., 2007; Griffiths et al., 2009) associated with a lower frequency of El-Niño (Conroy et al., 2008) possibly caused the lowlands to become more inundated by water, and this condition would reduce decomposition rates (Chimner and Ewel, 2005) and lead to a higher accumulation rate.

From 6 to 5 kBP, the mean peat accumulation rate in Sebangau was  $0.23 \text{ mm y}^{-1}$ ; combining this value with peat bulk density and carbon content produced the average of carbon accumulation rate of  $0.1 \text{ Mg C ha}^{-1} \text{ y}^{-1}$  (Page et al., 2004). Based on peat cores sampled from an inland peatland in Kalimantan, peat

accumulation rates reduced from  $\sim 0.8 \text{ mm y}^{-1}$  circa 8 kBP to about  $0.5 \text{ mm y}^{-1}$  in 5 kBP (Dommain et al., 2011). Simulated rates were similar, with a peat accumulation rate of  $0.46 \text{ mm y}^{-1}$  in 5 kBP, which is equivalent to carbon accumulation of  $0.25 \text{ Mg C ha}^{-1} \text{ y}^{-1}$ .

In coastal Sumatra and Kalimantan, however, peat initiation began at higher accumulation rates in the period after 7 kBP. A core taken from Bengkalis Island, near Sumatra shows that the onset of peatland development in this area was 5.8 kBP, with an initial accumulation rate of about  $2.5 \text{ mm y}^{-1}$  and carbon accumulation of about  $5.7 \text{ Mg C ha}^{-1} \text{ y}^{-1}$  (Neuzil, 1997). Dommain et al., (2011) also reported that the accumulation rate of the initial development of coastal peatlands in Sumatra, peninsular Malaysia, and Borneo was about  $1.7 \text{ mm y}^{-1}$  at 6 to 5 k year BP. HPMTrop simulated rates for the coastal peatland scenario were lower, however, with about  $1.2 \text{ mm y}^{-1}$  of peat accumulation in the early stage of development ( $\sim 5 \text{ kBP}$ )

After 5 kBP, sea level gradually decreased from 5 m above present MSL to the present MSL (Steinke et al., 2003). In this period, the Sunda Shelf was flooded due to sea level rise after deglaciation, and the islands of Sumatra, and Borneo, as well as peninsular Malaysia, were similar to present (Sathiamurthy and Voris, 2006). Decreasing rainfall in the western part of Indonesia was probably associated with the weakening of both the East Asian summer monsoon (Wang et al., 2005) and the Australian-Indonesian summer monsoon (Griffiths et al., 2009) as well as more frequent El-Niño (Cobb et al., 2013). More

stabilized sea level, combined with decreasing rainfall, led to a decline in the water table and enhanced decomposition, and thus a lower peat accumulation rate. From ~5 kBP onward, a declining peat accumulation rate in both coastal and inland peatland was simulated in HMP-Trop. Peat accumulation rate reduced to 1 mm y<sup>-1</sup> (0.54 Mg C ha y<sup>-1</sup>) and 0.36 mm y<sup>-1</sup> (0.2 Mg C ha<sup>-1</sup> y<sup>-1</sup>) in coastal and inland peatlands, respectively. The same decreasing pattern of accumulation rate also measured from peat cores taken in Southeast Asia: ~1.5 mm yr<sup>-1</sup> and ~0.3 mm year (Dommain et al., 2011).

#### **4.2. Carbon Stocks in tropical PSF**

Soil organic carbon was the largest component of the total carbon stock in tropical PSF, accounting for 1,000 to 3,000 Mg C ha<sup>-1</sup>, based on field sampling in BBK and TPG (Figure 22); both sites would be classified as coastal peatlands. These values were measured from sites where the peat depth varied between 2.1 to 6.3 m (Figure 22). The simulated carbon stock at the end of the HPM-Trop simulations – 3,100 and 3,300 Mg C ha<sup>-1</sup> for coastal and inland peatland, respectively (Figure 17), with peat depth of ~6 m (Figure 19) – were similar to the high end of observed values. A larger peat depth of ~12 m, however, has been measured in inland peatlands in Sentarum National Park, Kalimantan, which results a higher carbon stock of about 7,900 Mg C ha<sup>-1</sup> (Warren et al., 2012). The peat depth measured in TPG and BBK are comparable with the Amazonian peatlands, with a maximum value of 6 m (Lähteenoja et al., 2009), and those in the northern boreal and subarctic peatlands – average boreal and sub-arctic peat

depths are about 2.3 – 2.5 m, with some areas reaching up to 6 m (Gorham, 1991; Beilman et al., 2008).

One of the main characteristics of peatlands is a high concentration of organic carbon contained within the soil. We measured a mean organic carbon content that varied from 40% to 55%, and was relatively constant along the peat profiles. This result is comparable with the measured carbon concentration sampled in Kalimantan and Sumatra: 31 – 61% (Warren et al., 2012); 44 – 57% (Shimada et al., 2001); 53% (Anshari et al., 2010); 58.1 – 60.3% (Dommain et al., 2011). Carbon concentration (%OC) measured from TPG and BBK are also consistent with values from tropical peatlands in the Amazon (Lähteenoja and Page, 2011), and northern peatlands (Malmer and Holm, 1984; Gorham, 1991).

The peat bulk density in both BBK and TPG ranged between 90 – 160 kg m<sup>-3</sup> with the average of 106 kg m<sup>-3</sup>. This range is higher when compare to the coastal peatland in central Kalimantan, which averaged of 84.1 ± 11.5 kg m<sup>-3</sup>; lower than Kalimantan floodplain peatlands (141 ± 35.1 kg m<sup>-3</sup>) and Kalimantan terrace peatlands (124 ± 31.3 kg m<sup>-3</sup>); and comparable with peat bulk density for others types of Kalimantan peatlands: 117 ± 27.5 kg m<sup>-3</sup> for riverine, 98.4 kg m<sup>-3</sup> for basin type, and 94.9 ± 25.2 kg m<sup>-3</sup> for marginal (Shimada et al., 2001). Samples taken from Sebangau and Sentarum peatlands of Kalimantan in which both sites classified as inland peatlands gave a higher values of 122 ± 52 and 131 ± 43 kg m<sup>-3</sup>, respectively (Warren et al., 2012). In all cases, however, measured bulk density ranges area large and overlapping.

By combining %OC and bulk density, the estimated mean C-densities were  $53.2 \pm 13.2$  and  $50.6 \pm 13.2$  kg C m<sup>-3</sup> (mean  $\pm$  SD) for BBK and TPG respectively. These are similar to the C-density measured in coastal peatland in Central Kalimantan with an average of  $48.7 \pm 6.3$  kg C m<sup>-3</sup> (Shimada et al., 2001). Incorporating our results with other studies, the carbon density in Indonesian peatlands is  $62.3 \pm 14.6$  kg C m<sup>-3</sup> (Table 4). Assuming an average peat depth in Indonesia of 5.5 m (Page et al., 2011) and a PSF extent in Indonesia excluding Papua of 4,210,400 ha (Miettinen et al., 2012), the total peat carbon stock in the western part of Indonesia is about 11 – 18 Pg C. Measurements in Amazonian peatlands, however, yielded a lower mean C-density of 37 kg C m<sup>-3</sup> due to lower peat bulk density, when compared to Indonesian peatlands (Lähteenoja and Page, 2011).

#### **4.3. The impact of land cover change on PSF carbon dynamics**

Tropical PSFs are now experiencing strong land use pressure, including conversion to agriculture or plantation forestry (Miettinen et al., 2012), which usually includes canal development for lowering the water table (Hooijer et al., 2010) and peat fires (Page et al., 2002; Saharjo and Munoz, 2005); both drainage and fires release peat carbon to atmosphere. The amount of carbon loss caused by forest conversion to an oil palm plantation was simulated using HPMTrop. In a coastal peatland, the simulation of a 100-year conversion with periodic peat burning reduced the peat carbon by about 1,500 Mg C ha<sup>-1</sup> or ~15

Mg C ha<sup>-1</sup> y<sup>-1</sup> carbon emission due to both peat oxidation and fires. This amount of annual carbon loss is equivalent to about 30 years of peat accumulation. A carbon release from peat of about 11 Mg C ha<sup>-1</sup> y<sup>-1</sup> was estimated for the same land cover change scenario in an inland peatland. A similar rate of carbon loss of about 10.8 Mg C ha<sup>-1</sup> y<sup>-1</sup> was estimated using a flux change method proposed by IPCC (Hergoualc'h and Verchot, 2011). Using the linear relationship of water table and carbon emission, (Hooijer et al., 2010) reported that carbon emission in the drained peatlands are within the range of 1.6 to 27.3 Mg C ha<sup>-1</sup> y<sup>-1</sup>. Based on field measurements using the closed chamber method, soil respiration in oil palm plantation was 15 Mg C ha<sup>-1</sup> y<sup>-1</sup> (Melling et al., 2005); this value, however, is total soil respiration, which both includes the autotrophic (root respiration) and heterotrophic (peat decomposition) respiration, and so cannot be directly compared to peat loss.

Based on analysis of MODIS satellite imagery, the area of peatlands that had already been converted to oil palm plantation by early 2010 in lowland Peninsular Malaysia, Borneo, and Sumatra was about ~880,000 ha (Koh et al., 2011). Using the simulated carbon loss of 15 Mg C ha<sup>-1</sup> y<sup>-1</sup> as an emission factor due to the conversion and peat fires, the amount of carbon potentially released to the atmosphere by oil palm expansion is 13.2 Tg C y<sup>-1</sup>. Carbon loss of 7.9 Tg C y<sup>-1</sup> was produced by the forest conversion to oil palm without burning. This model-based estimate is higher than the annual carbon loss estimated by Koh et al., (2011) of about 4.6 Tg C y<sup>-1</sup> due to non-burning forest conversion.

Forest conversion to agriculture, including oil palm plantations, frequently involves burning for land preparation (Saharjo and Munoz, 2005). Our model results showed that the total peat carbon at the end simulation after the forest conversion but without burning is about 2,200 Mg C ha<sup>-1</sup>. If the total carbon stock before the conversion is 3,100 Mg C ha<sup>-1</sup> then it is estimated that the carbon loss is 900 Mg C ha<sup>-1</sup> over 100 years of simulation or equivalent with a rate of 9 Mg C ha<sup>-1</sup> y<sup>-1</sup> due to the conversion without burning. The carbon loss from the simulation of the forest conversion with burning to 20 cm depth every 25 years was 1600 Mg C ha<sup>-1</sup> and, hence, over 4 rotations (100 years) the burning practice itself may release about 600 Mg C ha<sup>-1</sup> from peat, equivalent to 150 Mg C ha<sup>-1</sup> for each burning. A much higher carbon loss per unit area of 250 – 320 Mg C ha<sup>-1</sup> was estimated from the 1997 peat fires in the Mega Rice Project, West Kalimantan due to a deeper peat burning of 51 ± 5 cm (Page et al., 2002). Using the reported range in peat burnt area in Indonesia (Table 5), peat burning to 20 cm would release carbon in a range of 0.22 – 1.02 Gt C.

Our simulation results show that land conversion with burning led to 2.3 – 3 m reductions in peat depth, from 5.8 m to 2.8 m in coastal peatlands and 6.1 m to 3.8 m in inland peatlands; equivalent to mean subsidence rates of 3 and 2.3 cm y<sup>-1</sup> for coastal and inland respectively. Measured peat subsidence rates in oil palm were 5.4 ± 1.1 cm y<sup>-1</sup> with the burning practice for land clearing, and in *Acacia* plantations in Sumatra were about 5 ± 2.2 cm y<sup>-1</sup> without burning activities (Hooijer et al., 2012). This value, however, is a total subsidence rate, comprising

oxidation, compaction and consolidation components, in which oxidation is the dominant component (75% to 90% of total subsidence), but compaction and consolidation dominate the subsidence in the initial few years (Hooijer et al., 2012). Similar research has taken place in peninsular Malaysia, where the average subsidence rate was  $2 \text{ cm y}^{-1}$ , of which 60% was due to peat oxidation and the remaining portion caused by shrinkage (Wösten et al., 1997). In this model, however, the subsidence rates were only generated by the peat oxidation.

#### **4.4. Model uncertainty**

HPMTrop simulation results are comparable to published peat depth-age profile and peat carbon stocks. The simulated long-term apparent carbon accumulation for both inland and coastal peatlands is similar to observed values based on radiocarbon dating. Over somewhat shorter periods, however, there are discrepancies between the observed and simulated carbon accumulation rates. Figure 18 shows that in the period after 7 kBP, the simulated peat accumulation rate for inland peatland scenario is higher than peat accumulation measured from a peat core sampled in Sebangau catchment, which have a smaller slope in their peat age-depth profile after 7 kBP (Figure 18). This may be due to the stabilizing of sea level in Sunda Shelf ( $\pm 5\text{m}$ ), which is not incorporated in HPMTrop.

To accumulate organic matter, the decomposition rates must be lower than vegetation productivity; in peatlands this is affected by water-logging which



creates anoxic conditions, slowing decomposition. In HPMTrop, the degree of peat saturation was driven by water table position in the peat profile. The water table position is a result of hydrological processes occurring in the peat, which are determined by climate conditions, local topography, and peat physical properties. This is modeled in HPM as a site-level water balance. However, due to uncertainty and lack of field data for model development and testing, HPM's water balance equations were not used in HPMTrop, and instead an empirical water table estimation based on the monthly water deficit was implemented. The calculation of the water deficit requires monthly rainfall data and, hence, a monthly rainfall reconstruction throughout the Holocene is required to drive HPMTrop. Due to the absence of such a published rainfall reconstruction, monthly rainfall was generated by combining the pattern of oxygen isotope ( $\delta^{18}\text{O}$ ) values from cave stalagmites sampled in northern Borneo with El-Niño frequencies in the 20<sup>th</sup> century. The measured water table depth used to develop empirical water table model based on the water deficit was recorded from Sebangau catchment, located in the southern of Borneo (Wösten et al., 2010). According to Aldrian and Dwi Susanto (2003), however, rainfall seasonality in northern Borneo is less pronounced than in southern Borneo. Therefore, it might be appropriate to use the  $\delta^{18}\text{O}$  reconstruction from Liang Luar, Flores, Indonesia (Griffiths et al., 2009) to represent long term rainfall in the Sebangau area. A more robust rainfall reconstruction throughout the Holocene, incorporating both frequency and

intensity of ENSO and long-term variations in total annual rainfall, as well as rainfall seasonality, would improve HPMTrop water table simulations.

Since HPMTrop did not vary NPP rates between coastal and inland peatland simulations, as there were no data on which to base this, so more rapid accumulation in the coastal peatlands had to arise from slower decomposition in the coastal peatlands. This was accomplished by two differences – (i) a shallower water table, and (ii) a shorter anoxia scale length in the coastal peatlands. In HPMTrop, anoxia scale length,  $c_4$  (Table 1), was used as one parameter in equation 5 to represent an exponential decline in peat decomposition rate below the water table. It is used as a simple representation of several processes that could influence oxygen penetration below the water table – e.g., high frequency water table variability (i.e., sub-monthly), inputs of oxygenated rainwater, general diffusion, plant-mediated transport. Based on an in-situ experiment of peat drying-rewetting, lowering the water table generates oxygen penetration into the peat pores and thus the dissolved oxygen may still be detected below, but close to, the water table (Estop-Aragónés et al., 2012). It is also shown in HPMTrop sensitivity analysis that changing the pattern of water table seasonality affects both carbon stocks and peat depth at the end simulation. In the scenario for simulating peat accumulation in coastal and inland peatlands, the anoxia scale length values are 0.18 and 0.27 m, respectively. Those values were obtained based on sensitivity tuning by comparing the simulated peat age-depth profiles with the measured profiles reported by

Dommain et al. (2011). I found only one set of multi-year water table data (inland peatland), so the shallower water table for coastal peatlands was also set by sensitivity tuning.

Sea level changes after the last glaciation are also an important factor of peat accumulation in Southeast Asia (Dommain et al., 2011). An increase of sea level likely changes the hydrology of low-lying and flat land areas, which could increase the water table and create favorable conditions for peat formation and accumulation. HPMTrop, however, does not take into account the effect of sea level for estimating the water table.

In this first version of HPMTrop, the only PFT included was trees, which were partitioned into three components for litter inputs, i.e., leaf, wood, and root. Parameters for those components, both productivity and decomposition rates, required in this model were obtained from a limited number of published field studies (see Hergoualc'h and Verchot, 2011). There is a knowledge gap related to that, especially with the wood and root parameters. The only literature for productivity and decomposition rate for wood and roots are from a Micronesian peatland (Chimner and Ewel, 2005); it is unknown how well this represents conditions in other tropical peatlands, and in particular, PSFs in Southeast Asia as simulated in this study. Besides trees, however, other vegetation types are found in tropical PSF, such as herbs, sedges, aroids, pandanus, ferns and epiphytes (Anderson, 1963; Wust and Bustin, 2004). A better PFT parameterization, including other PFTs, should be considered for the next study.

HPMTrop simulation results indicated that a large amount of carbon would be lost from tropical peat swamp forests converted to agriculture, due to draining, reduced litter inputs, and burning. Nevertheless, this amount of carbon release was generated only by peat oxidation due to the peat decomposition and fires. Any other carbon forms that could be released from peat, such as methane and fluvial dissolved organic carbon, were not modeled in HPMTrop. A recent study in a disturbed Kalimantan peatland showed that total fluvial organic carbon, comprising dissolved organic carbon and particulate organic carbon, flowing out of a drained, disturbed peat swamp forest ranged between 88 to 100 g C m<sup>-2</sup> y<sup>-1</sup> (0.88 to 1.0 Mg C ha<sup>-1</sup> y<sup>-1</sup>), and potentially increased the peat carbon lost by about 20% (Moore et al., 2013). Including both methane emission and fluvial organic carbon are important next steps in model improvement for studying the carbon dynamics in tropical peatlands.

## V. CONCLUSIONS

HPMTrop is the first process-based model to simulate long-term carbon accumulation dynamics in tropical peat ecosystems. It is based on a peat model that had been successfully tested for northern peatlands. Some modification and simplifications were performed so that the model could be used for the tropical ecosystems. Using a simple carbon balance as the difference between tree productivity and decomposition rates, and including the effects of a seasonally and interannually varying water table on decomposition rates, HPMTrop simulates annual peat cohort mass and thickness, and total peat profile carbon stocks and peat depth. At the end of simulation, the simulated peat profile can be 'cored' and compared with the peat cores sampled from the field. The simulated long-term carbon accumulation rates for coastal and inland peatlands were 0.26 and 0.63 Mg C ha<sup>-1</sup> y<sup>-1</sup>, respectively. These rates are within the range of measured rates, 0.12 to 0.77 Mg C ha<sup>-1</sup> y<sup>-1</sup>, based on the peat radiocarbon dating of tropical peats (Yu et al., 2010; Dommain et al., 2011).

Peat swamp forests contain very large carbon stocks, and this carbon is mostly stored as surface peat. At the end of HPMTtrop simulations reported here, carbon stocks for coastal and inland scenarios are 3,150 Mg C ha<sup>-1</sup> and 3,270 Mg C ha<sup>-1</sup>, respectively. These values are at the high end of carbon stocks measured in PSF of Tanjung Puting NP and Berbak NP, Indonesia, which ranged

from 1,000 – 3,000 Mg C ha<sup>-1</sup>. Using our data and previously published carbon density reveals that Indonesian PSFs store an immense carbon stock, ranging from 11 – 18 Pg C; these values exclude Papua.

One of the big challenges of PSF in Indonesia is high rates of deforestation, which is predominantly conversion to industrial plantation (Koh et al., 2011; Miettinen et al., 2012) and also associated with lowering water tables and fire prone conditions. Over a simulation of a 100-year conversion, carbon loss caused by the forest conversion to oil palm plantation with the periodic burning was about 1,100 and 1,500 Mg C ha<sup>-1</sup> for inland and coastal peatlands, respectively; this is equivalent to 6,000- and 3,000-years of peat accumulation for inland and coastal peatlands, respectively. In the coastal peatland scenario, furthermore, carbon in amount of 150 Mg C ha<sup>-1</sup> could be potentially released to atmosphere due to peat fires and produce a total carbon emission of about 0.22 – 1.02 Gt C. Overall, we produced three types of emission factors due to forest conversion to oil palm plantation: 15 Mg C ha<sup>-1</sup> y<sup>-1</sup> for conversion with burning, 9 Mg C ha<sup>-1</sup> y<sup>-1</sup> for the conversion without fires, and 150 Mg C ha<sup>-1</sup> for the carbon losses due to peat burning. In a REDD+ mechanism (e.g., Murdiyarso et al. 2010), these emission factors are very important for estimating the total carbon emission impact of land cover change occurring in peatlands.

By developing a model for simulating the carbon dynamics in tropical PSFs, we found that there are some knowledge gaps and further research is needed to fill those gaps. Long-term observation of tree productivity in PSF is a crucial

research for studying the carbon balance in this ecosystem. What is the impact of rainfall seasonality, which is common in tropical regions and may affect water table variability, on the PSF tree? Studies about wood and root decomposition processes in tropical PSF are also important, as I found only one published research paper reporting wood/root decomposition rates, and that study only measured for one year (Chimner and Ewel, 2004). Tropical peatland hydrology is another area needing more study, since few publications discuss peat hydraulic characteristics, including water retention and hydraulic conductivity (Dommain et al., 2010; Rais, 2011).

While the HPMTrop results are generally consistent with measured data, some improvements are needed to improve the model representation of processes occurring in tropical peat ecosystem.

- Better parameterization of plant functional types, including additional PFTs besides trees such as pandanus, sedge and shrubs.
- Modeling the impact of sea level rise after the last glacial maximum on the PSF hydrology and water table.
- More robust long-term climate reconstruction.
- Better understanding of how to represent the anoxia scale length effect.
- Improved, process-based hydrological modeling for estimating long-term monthly water table.

Table 1. List of parameters used in HPMTrop

| Parameter  | Value  | Units                                  | Reference  |
|--|--------|--|--|
| NPP  |        |  |  |
| Leaves   | 0.079  | kg m <sup>-2</sup> month <sup>-1</sup> | Hergoualc'h and Verchot, 2011  |
| Wood   | 0.057  | kg m <sup>-2</sup> month <sup>-1</sup> | Chimner and Ewel, 2005   |
| Roots  | 0.025  | kg m <sup>-2</sup> month <sup>-1</sup> | Hergoualc'h and Verchot, 2011  |
| k <sub>0</sub> (initial litter decomposition rate, Eq. 10) |        |  |  |
| Leaves   | 0.1055 | month <sup>-1</sup>                    | Chimner and Ewel, 2005; Brady 1997; Shimamura and Momose, 2005; Yule and Gomez, 2008 |
| Wood   | 0.0224 | month <sup>-1</sup>                    | Chimner and Ewel, 2005   |
| Roots  | 0.0685 | month <sup>-1</sup>                    | Chimner and Ewel, 2005   |
| Anoxia scale length, c <sub>4</sub> in Eq. 9               |        |  |  |
| Coastal  | 0.18   | m                                      |  |
| Inland   | 0.27   | m                                      |  |
| root depth (max) 0.5 m                                     |        |  |  |
| Peat water content (Eq. 5, 6)                              |        |  |  |
| W <sub>min</sub>   | 0.03   | m <sup>3</sup> m <sup>-3</sup>         | Frolking et al., 2010  |
| c <sub>1</sub>   | 0.5    |  | Frolking et al., 2010  |
| c <sub>2</sub>   | 20     | kg m <sup>-3</sup>                     | Frolking et al., 2010  |
| Saturation factor for the decomposition rate (Eq. 7, 8, 9) |        |  |  |
| W <sub>opt</sub>   | 0.45   |  | Frolking et al., 2010  |
| W <sub>sat</sub>   | 1      |  | Frolking et al., 2010  |
| f <sub>max</sub>   | 1      |  | Frolking et al., 2010  |
| f <sub>sat</sub>   | 0.3    |  | Frolking et al., 2010  |
| f <sub>min</sub>   | 0.001  |  | Frolking et al., 2010  |
| Bulk density (Eq. 12)                                      |        |  |  |
| c <sub>5</sub>   | 0.2    |  | Frolking et al., 2010  |
| c <sub>6</sub>   | 0.1    |  | Frolking et al., 2010  |
| ρ <sub>min</sub>   | 90     | kg m <sup>-3</sup>                     | Warren et al., 2012  |
| Δρ   | 40     | kg m <sup>-3</sup>                     | Warren et al., 2012  |



Table 2. ENSO probabilities used for different intervals in Holocene simulations.

| Rainfall class | Probability         |                   |                  |
|----------------|---------------------|-------------------|------------------|
|                | Before 6000 year BP | 6000 – 3000 yr BP | 3000 – 0 year BP |
| El Niño        | 5                   | 15                | 30               |
| Normal         | 75                  | 65                | 50               |
| La Niña        | 20                  | 20                | 20               |

Table 3. Sensitivity analysis for the coastal peatland scenario. Peat carbon mass remaining for each tree component, total peat carbon, peat depth, total NPP through the 5000 year simulation, and the ratio of peat mass at the end simulation to total NPP were chosen as the model responses. Base run values are the model output simulated using the default parameters shown in Table 1. Parameters were adjusted  $\pm 25\%$ .

| No | Parameter                | Value | peat carbon (MgC/ha) |        |        |           | Depth (m) | NPP total | C/NPP |
|----|--------------------------|-------|----------------------|--------|--------|-----------|-----------|-----------|-------|
|    |                          |       | leaves               | wood   | roots  | C (total) |           |           |       |
| 1  | base run                 |       | 479.6                | 1807.2 | 920.5  | 3207.3    | 6.0       | 47863.6   | 6.7   |
| 2  | Leaves                   | 0.099 | 667.1                | 1998.5 | 976.2  | 3641.8    | 6.8       | 53745.2   | 6.8   |
| 3  |                          | 0.059 | 310.9                | 1578.0 | 848.3  | 2737.2    | 5.1       | 41987.1   | 6.5   |
| 4  | Wood                     | 0.071 | 635.1                | 2925.8 | 1085.9 | 4646.8    | 8.7       | 52097.3   | 8.9   |
| 5  |                          | 0.043 | 327.0                | 937.4  | 725.5  | 1989.8    | 3.7       | 43632.5   | 4.6   |
| 6  | Roots                    | 0.031 | 507.2                | 1899.1 | 1215.6 | 3621.9    | 6.7       | 49720.2   | 7.3   |
| 7  |                          | 0.019 | 455.5                | 1717.3 | 650.0  | 2822.8    | 5.2       | 46007.9   | 6.1   |
| 8  | total                    | 0.246 | 915.6                | 3317.8 | 1486.6 | 5720.0    | 10.7      | 59830.5   | 9.6   |
| 9  |                          | 0.147 | 191.8                | 735.6  | 444.0  | 1371.4    | 2.5       | 35897.7   | 3.8   |
| 10 | Leaves                   | 0.132 | 325.9                | 1621.9 | 859.7  | 2807.5    | 5.2       | 47864.4   | 5.9   |
| 11 |                          | 0.079 | 769.9                | 2044.8 | 993.5  | 3808.2    | 7.1       | 47871.1   | 8.0   |
| 12 | Wood                     | 0.028 | 393.0                | 1204.0 | 806.6  | 2403.7    | 4.4       | 47860.8   | 5.0   |
| 13 |                          | 0.017 | 610.2                | 2921.9 | 1084.8 | 4616.9    | 8.6       | 47861.1   | 9.6   |
| 14 | Roots                    | 0.086 | 457.3                | 1730.8 | 720.4  | 2908.4    | 5.4       | 47867.4   | 6.1   |
| 15 |                          | 0.051 | 487.9                | 1842.1 | 1200.6 | 3530.7    | 6.6       | 47864.9   | 7.4   |
| 16 | total                    | 0.246 | 244.2                | 992.0  | 570.2  | 1806.5    | 3.3       | 47864.5   | 3.8   |
| 17 |                          | 0.147 | 976.0                | 3273.6 | 1474.5 | 5724.0    | 10.8      | 47866.0   | 12.0  |
| 18 | anoxia scale length      | 0.23  | 340.1                | 1299.4 | 550.6  | 2190.1    | 4.1       | 47865.5   | 4.6   |
| 19 |                          | 0.14  | 681.1                | 2489.1 | 1421.6 | 4591.8    | 8.6       | 47866.0   | 9.6   |
| 20 | $\rho_{min}$             | 112.5 | 313.4                | 1206.5 | 689.3  | 2209.3    | 3.4       | 47863.0   | 4.6   |
| 21 |                          | 67.5  | 748.9                | 2711.9 | 1207.9 | 4668.7    | 11.1      | 47869.4   | 9.8   |
| 22 | $\Delta p$               | 50    | 447.2                | 1693.8 | 875.1  | 3016.1    | 5.4       | 47866.2   | 6.3   |
| 23 |                          | 30    | 504.3                | 1894.9 | 953.4  | 3352.6    | 6.5       | 47864.7   | 7.0   |
| 24 | c5                       | 0.25  | 489.1                | 1841.5 | 925.9  | 3256.5    | 6.1       | 47865.5   | 6.8   |
| 25 |                          | 0.15  | 468.4                | 1769.2 | 914.7  | 3152.2    | 5.8       | 47862.4   | 6.6   |
| 26 | c6                       | 0.125 | 466.3                | 1763.4 | 906.0  | 3135.6    | 5.8       | 47862.8   | 6.6   |
| 27 |                          | 0.075 | 503.9                | 1888.6 | 949.4  | 3341.9    | 6.3       | 47863.2   | 7.0   |
| 33 | Precipitation multiplier | 1.25  | 571.7                | 2125.2 | 1031.2 | 3728.0    | 6.9       | 47830.8   | 7.8   |
| 34 |                          | 0.75  | 307.1                | 1180.4 | 659.9  | 2147.5    | 4.0       | 47948.8   | 4.5   |
| 35 | WT multiplier            | 1.25  | 417.2                | 1586.9 | 804.6  | 2808.7    | 5.2       | 47868.6   | 5.9   |
| 36 |                          | 0.75  | 550.9                | 2054.8 | 1018.9 | 3624.7    | 6.8       | 47849.2   | 7.6   |

Table 4. Summary of measured carbon density in this study and previously published literature.

| Location                   | N   | C density (kg C m <sup>-3</sup> ) |      | Sources                |
|----------------------------|-----|-----------------------------------|------|------------------------|
|                            |     | mean                              | SD   |                        |
| Berbak, Sumatra            | 75  | 53.2                              | 13.4 | This study             |
| Tanjung Puting, Kalimantan | 140 | 50.6                              | 13.2 | This study             |
| Sentarum, Kalimantan       | 433 | 65.9                              | 20.8 | Warren et. al. (2012)  |
| Sebangau, Kalimantan       | 96  | 65.1                              | 23.3 | Warren et. al. (2012)  |
| Central Kalimantan         | 31  | 64.5                              | 14.0 | Shimada et. al. (2001) |
| Central Kalimantan         | 67  | 71.5                              | 17.3 | Shimada et. al. (2001) |
| Central Kalimantan         | 15  | 55.8                              | 8.7  | Shimada et. al. (2001) |
| Central Kalimantan         | 32  | 53.6                              | 12.5 | Shimada et. al. (2001) |
| Central Kalimantan         | 57  | 72.9                              | 16.2 | Shimada et. al. (2001) |
| Riau & West Kalimantan     | 29  | 48.7                              | 6.3  | Shimada et. al. (2001) |
| Total                      | 975 | 62.3                              | 14.6 |                        |

Table 5. Reported area and depth of peat burning, and simulated total carbon loss caused by the fires in Indonesia estimated using coastal peatlands scenario.

|   |           |                                 |
|---|-----------|---------------------------------|
| Area of peat burnt (ha)                                       | 1,450,000 |                                 |
|   | 2,441,000 | (Page et al., 2002)             |
|   | 6,804,688 |                                 |
|   | 1,909,200 | (Heil et al., 2006)             |
|   | 2,300,500 |                                 |
|   | 1,331,367 | (Ballhorn et al., 2009)         |
| Thickness of peat burnt (cm)                                  | 51 ± 5    | (Page et al., 2002)             |
|   | 33 ± 18   | (Heil et al., 2006)             |
|   | 20        | (Hergoualc'h and Verchot, 2011) |
| Carbon stock at end of simulation (Mg C ha <sup>-1</sup> )    |           |                                 |
| No LC <sup>1</sup>  | 3,100     | This study                      |
| LC only <sup>2</sup>  | 2,200     | This study                      |
| LC + fire (20 cm) <sup>3</sup>                                | 1,600     | This study                      |
| Carbon loss (Mg C ha <sup>-1</sup> )                          |           |                                 |
| LC only <sup>4</sup>  | -900      | This study                      |
| LC + fire (20 cm) <sup>5</sup>                                | -1500     | This study                      |
| Carbon loss due to fire (Mg C ha <sup>-1</sup> ) <sup>6</sup> | -150      | This study                      |
| Total carbon loss (Gt C) <sup>7</sup>                         |           |                                 |
| Lower estimate  | -0.22     | This study                      |
| Upper estimate  | -1.02     | This study                      |

<sup>1</sup> simulation without land cover change.

<sup>2</sup> land cover change simulation – 100 years of drainage, but without peat burning.

<sup>3</sup> land cover change and peat burning simulation with 20 cm of peat burnt every 25 years.

<sup>4</sup> calculated as carbon stock of LC only (2) minus no LC (1).

<sup>5</sup> calculated as carbon stock of LC+fire (3) minus no LC (1).

<sup>6</sup> calculated as carbon loss of LC+fire (5) – LC only (4) divided by the number of fire occurrences—four in this study.

<sup>7</sup> product of carbon loss due to fire (6) and minimum and maximum areas of peat burnt.

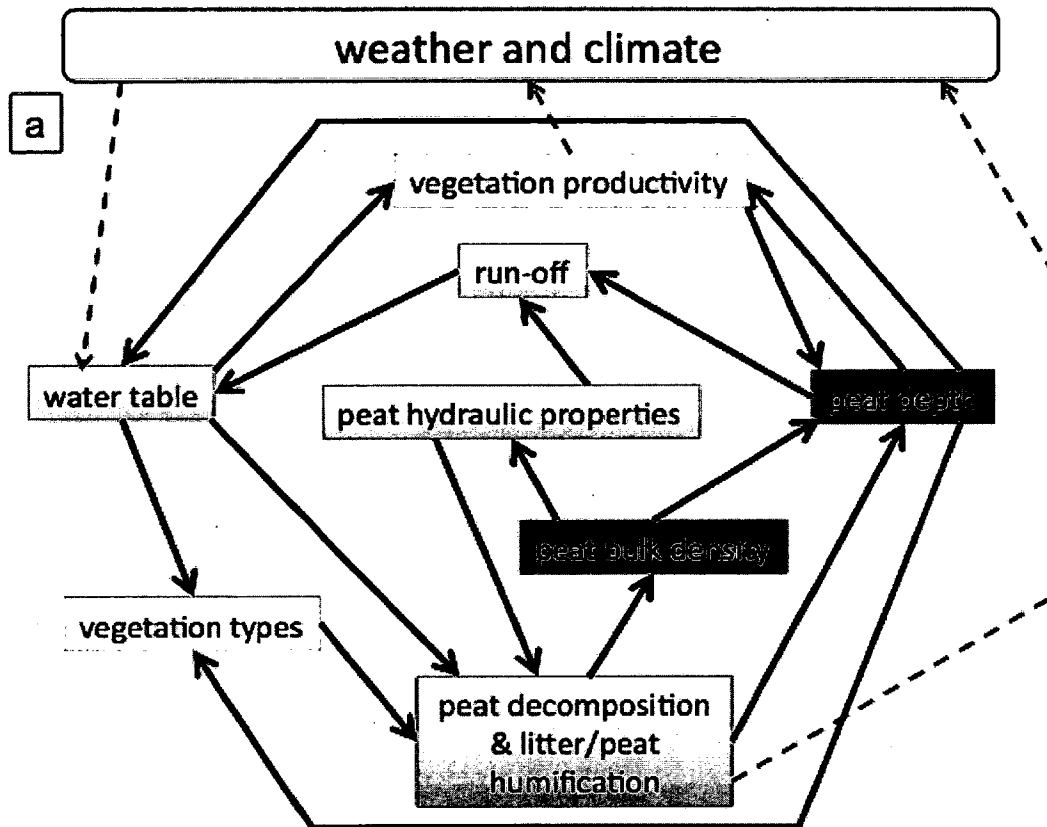


Figure 1. A schematic of some of the links among variables and processes in HPM.

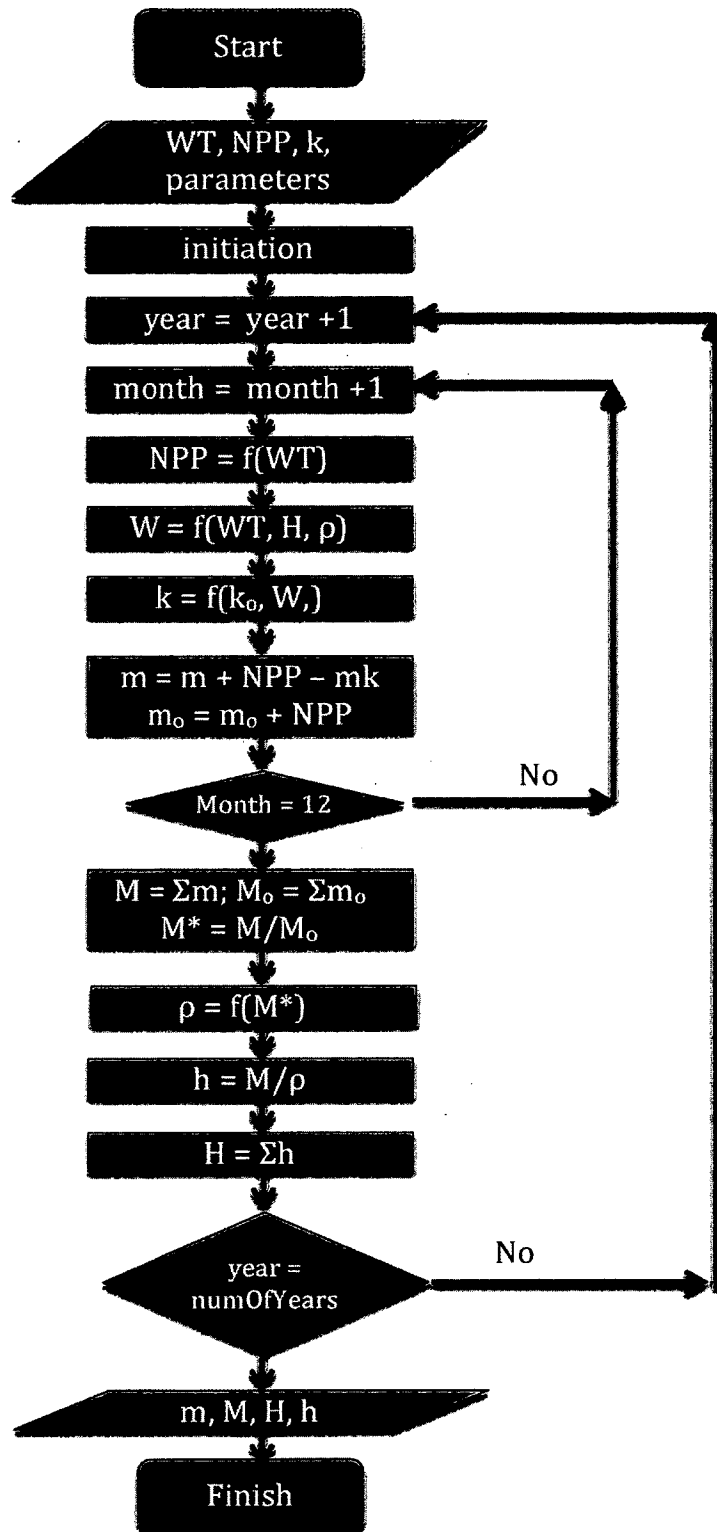


Figure 2. Flowchart of HPMTrop calculations.

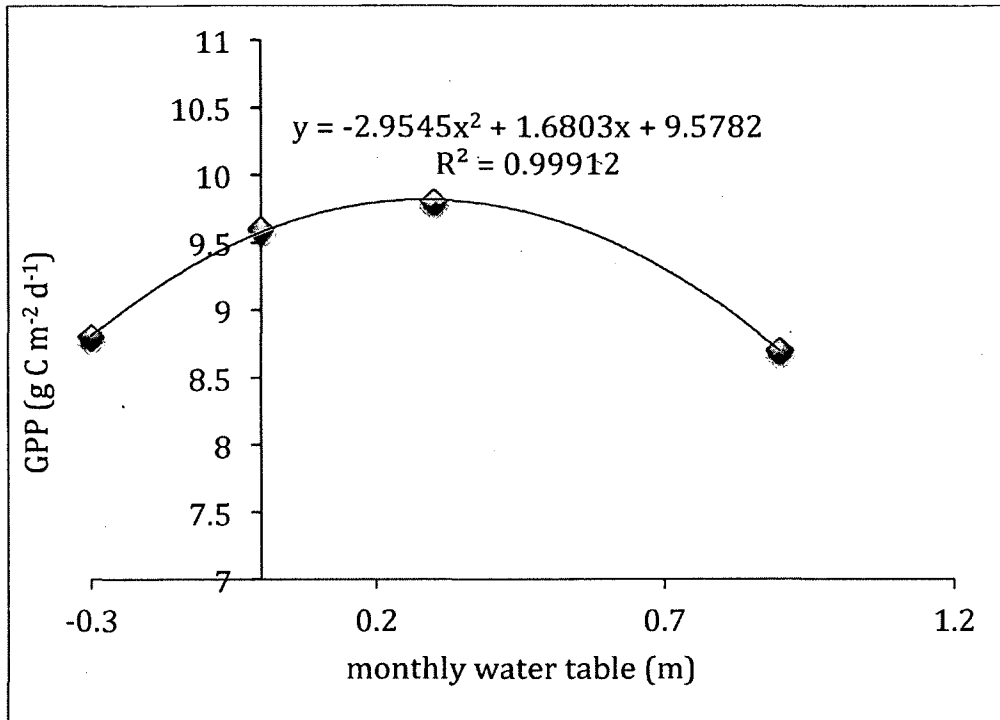


Figure 4. Quadratic relationship between measured monthly water table and gross primary production (GPP) in Sebangau, Kalimantan (modified from Hirano et. al 2012). Positive values in monthly water table (X-axis) shows the position of water table is below the peat surface.

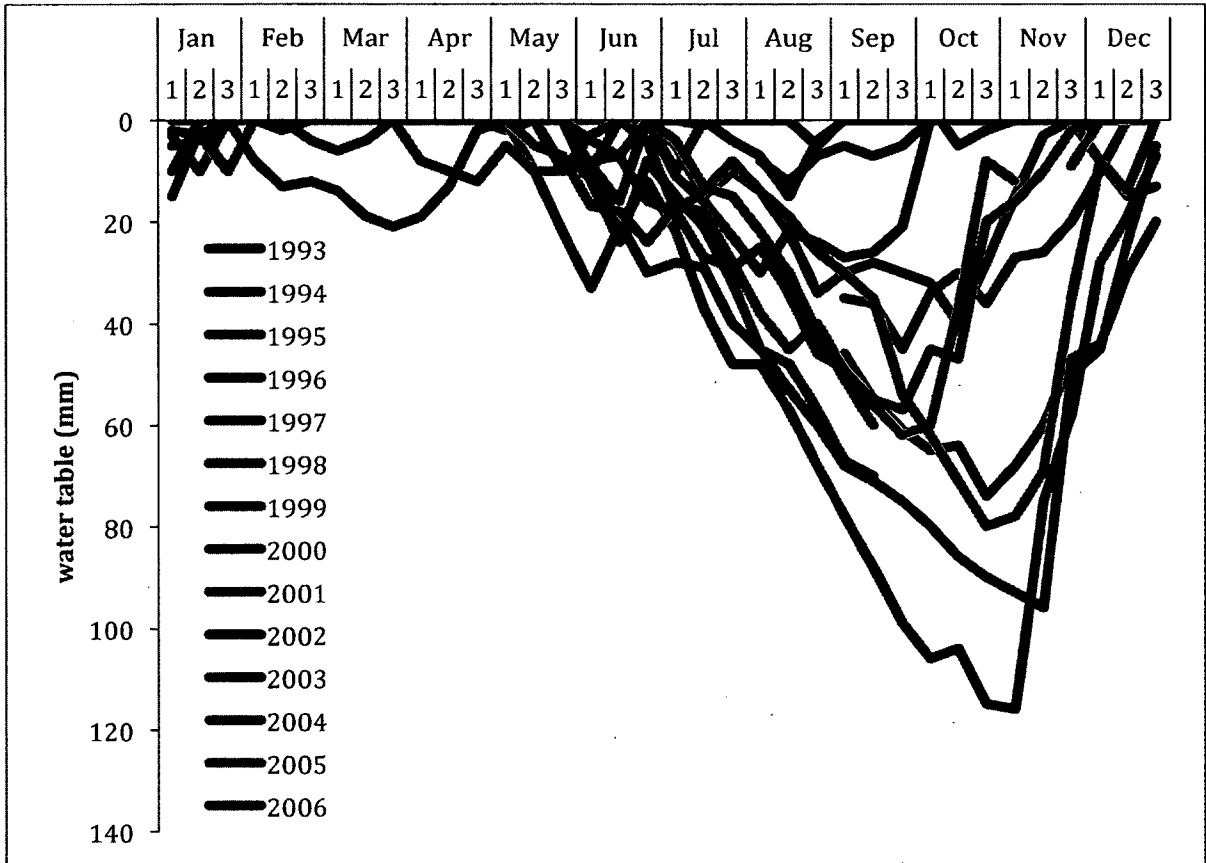


Figure 4. Measured peat water table in Sebangau peat swamp forests, Kalimantan Indonesia from 1993-2006 (modified from Wösten et. al., 2010)



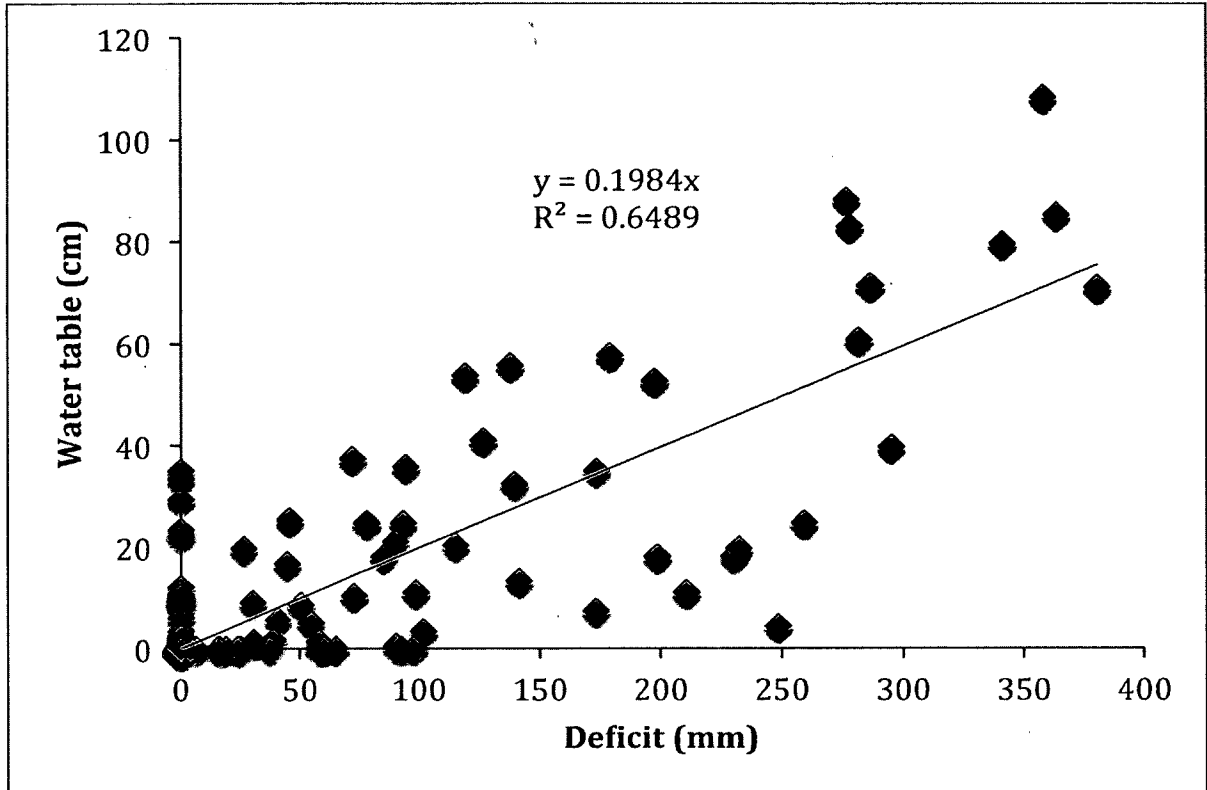


Figure 5. Scatterplot of estimated monthly water deficit (Equation 15) and measured monthly mean water table (see Figure 3); line is linear fit.

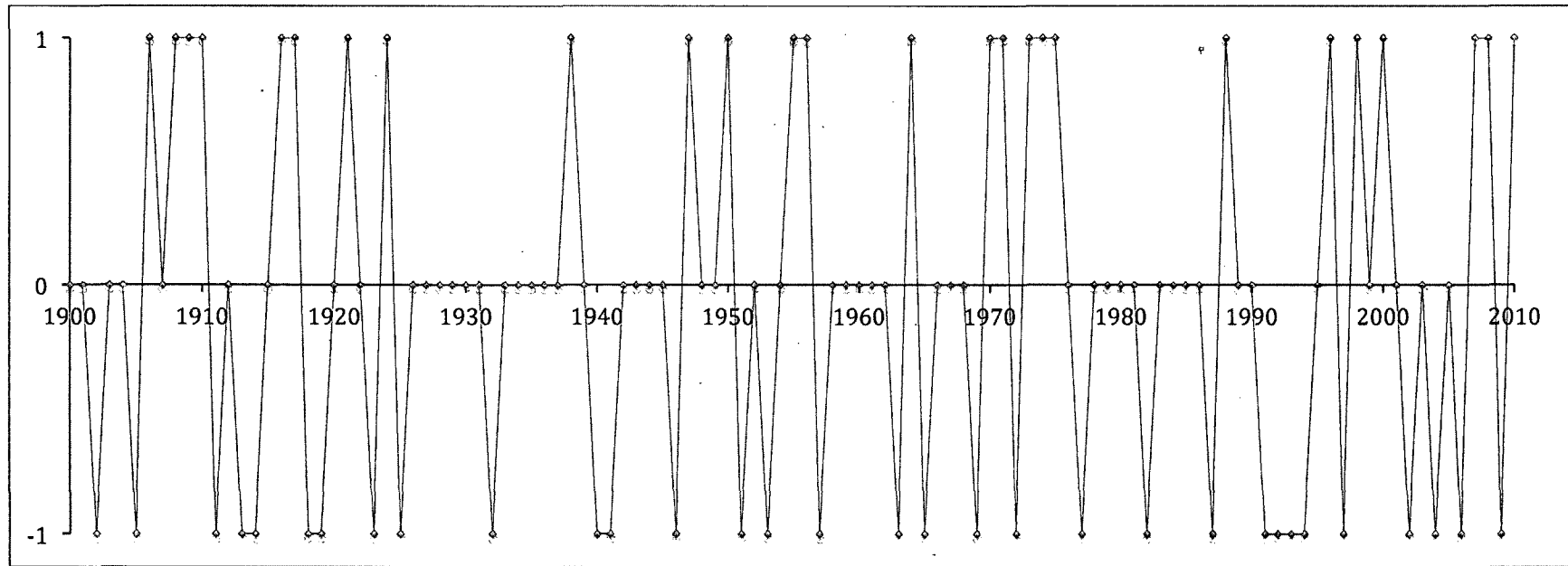


Figure 6. Annual rainfall classification based on the Southern Oscillation index from 1900-2010 (after McKeon et. al., 2004). The Y-axis shows the rainfall classes: 1. La Niña, 2. Normal, 3. El Niño.

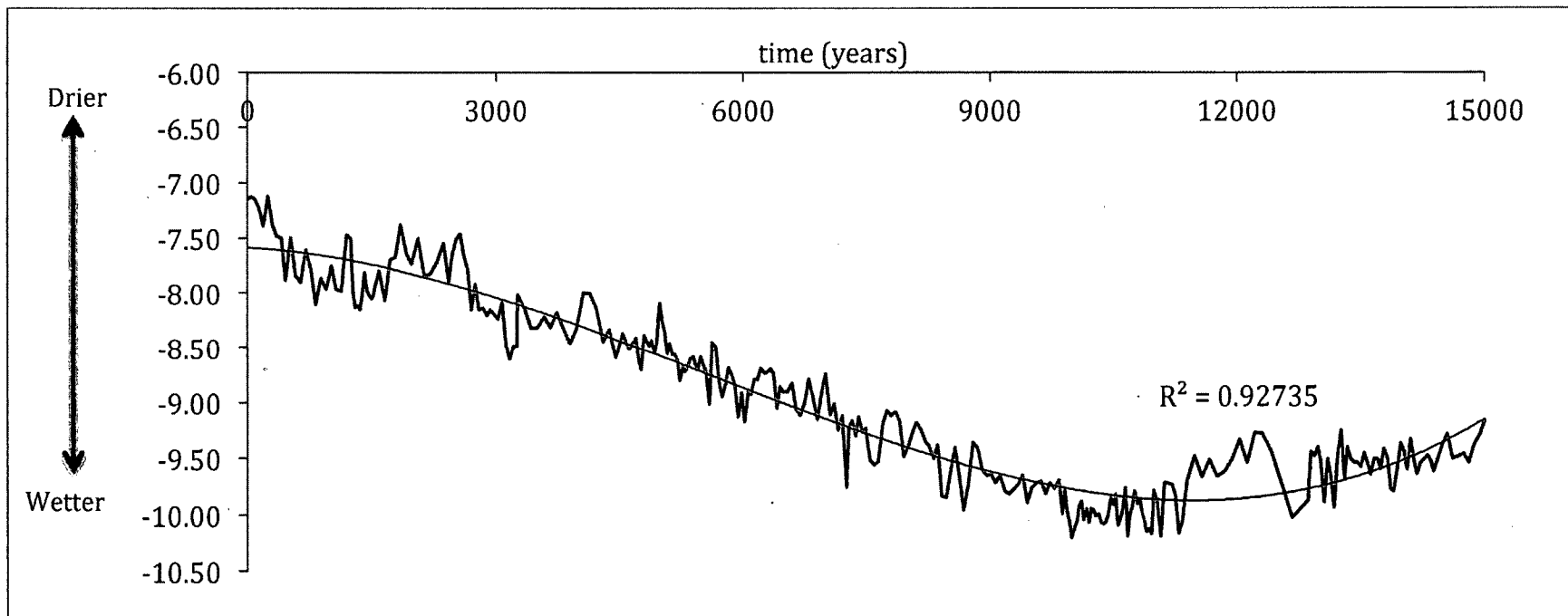


Figure 7. The stalagmite  $\delta^{18}\text{O}$  record sampled from Gunung Buda, northern Borneo since late Pleistocene (modified from Partin et al., 2007). More negative values can be interpreted as wetter conditions. Note that time on x-axis is time since start of record, so 0 = 15,000 years BP and 15,000 is present day. Line is polynomial fit (Equation 16).

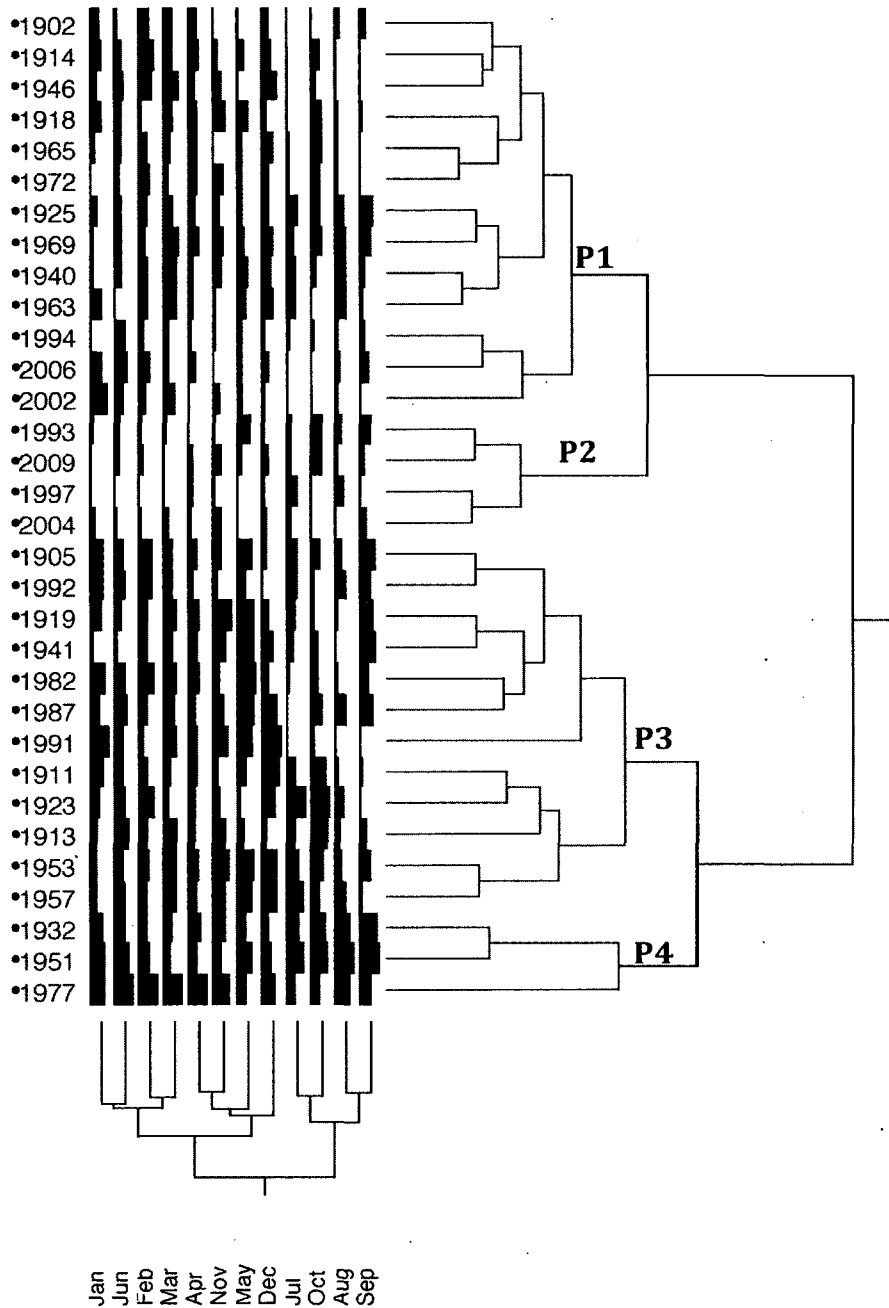


Figure 8. The dendrogram of the two-way cluster analysis using the monthly rainfall data classified as the El Niño years. Four clusters of years were extracted from this analysis (P1, P2, P3, and P4). The X-axis and Y-axis represent month and year, respectively, with the rainfall depth shown for each month.

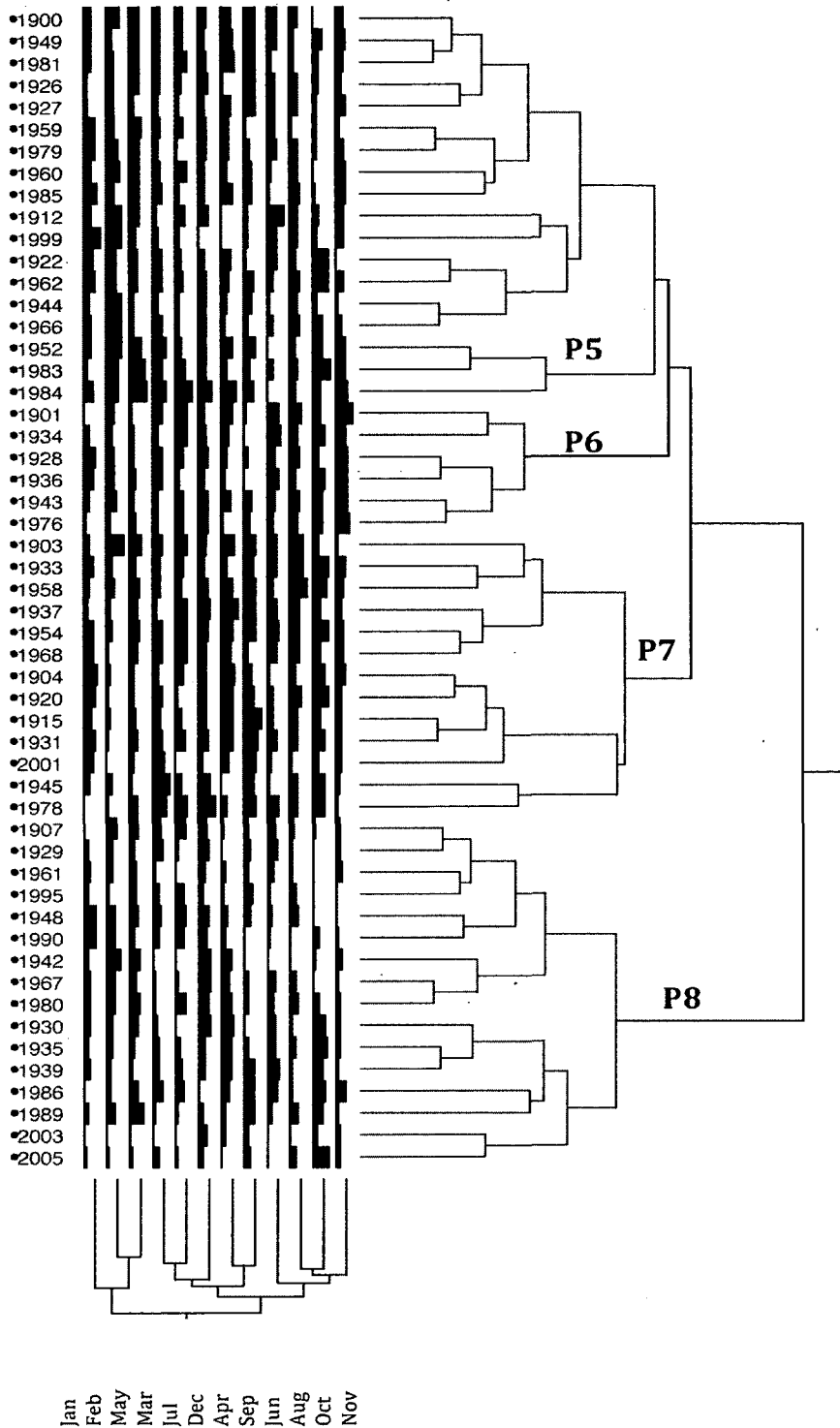


Figure 9. Same as Figure 7 with the rainfall data from normal years. Clusters are P5-P8.

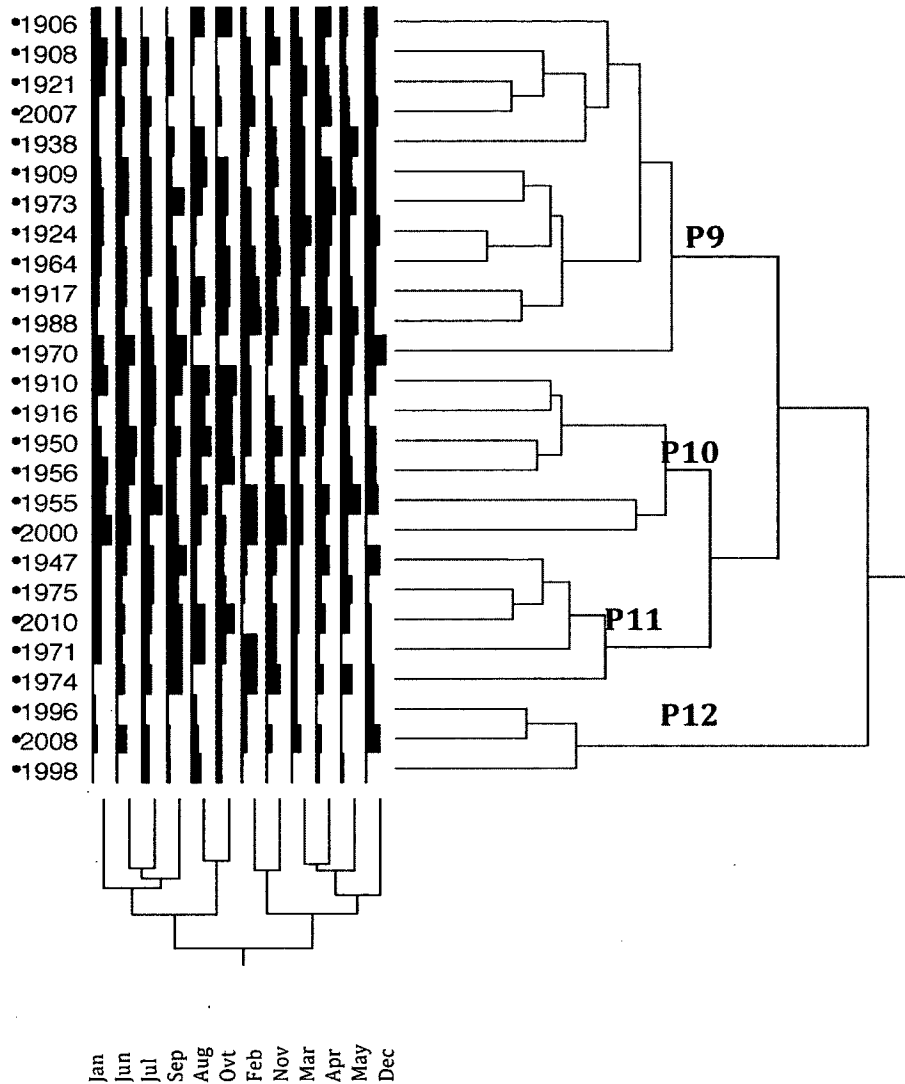


Figure 10. Same as Figure 7 with the rainfall data from La Niña years. Clusters are P9-P12.

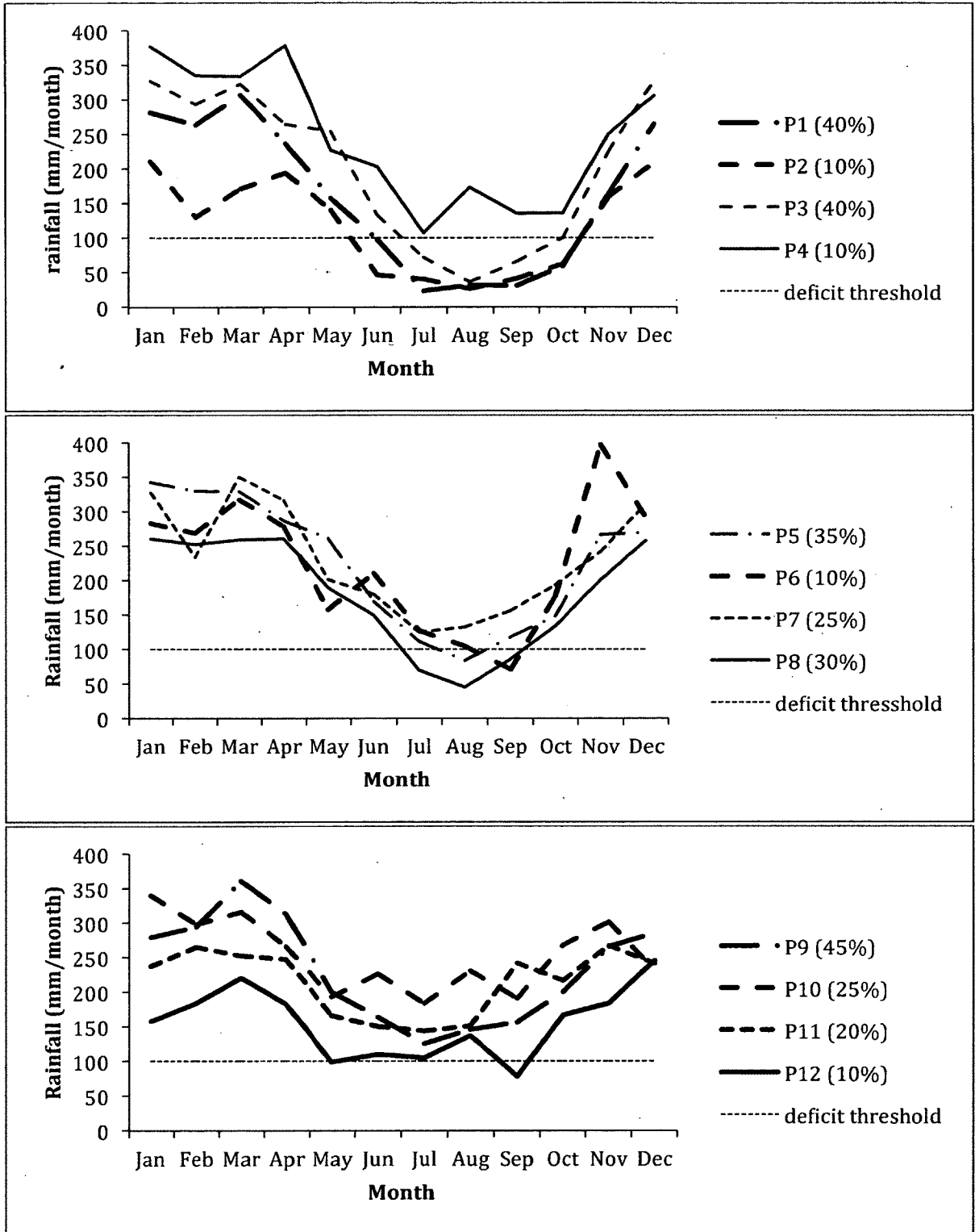


Figure 11. Mean monthly rainfall depth of each group derived by the cluster analysis (see Figures 7-9) for El Niño (top), normal (middle), and La Niña (bottom). Values in the legends represent the probability for every rainfall group within the broad El Niño, normal, and La Niña classes.

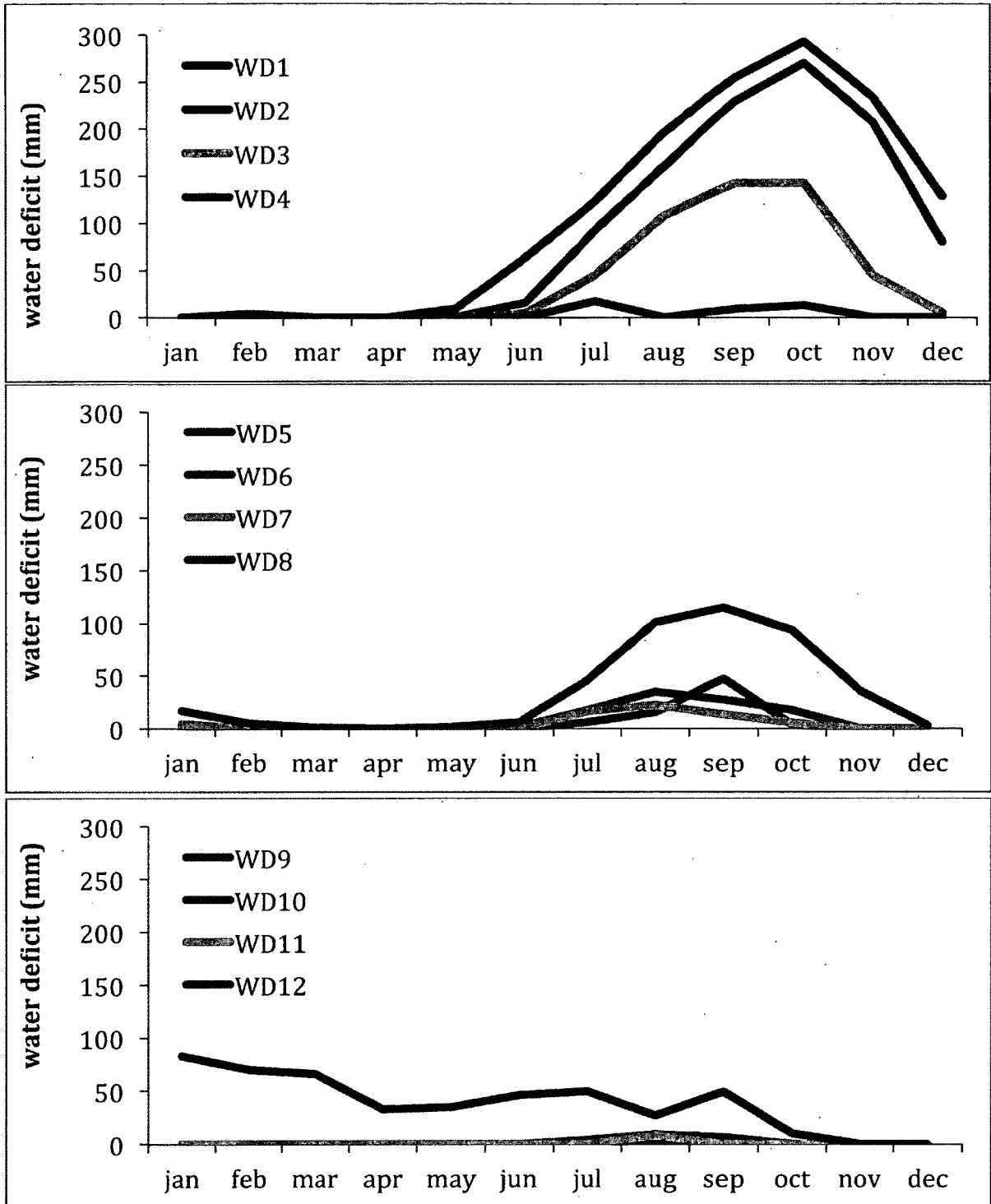


Figure 12. Mean monthly water deficit of each rainfall group (P1-P12, see Figure 10) for: El Niño (top), normal (middle), and La Niña (bottom).



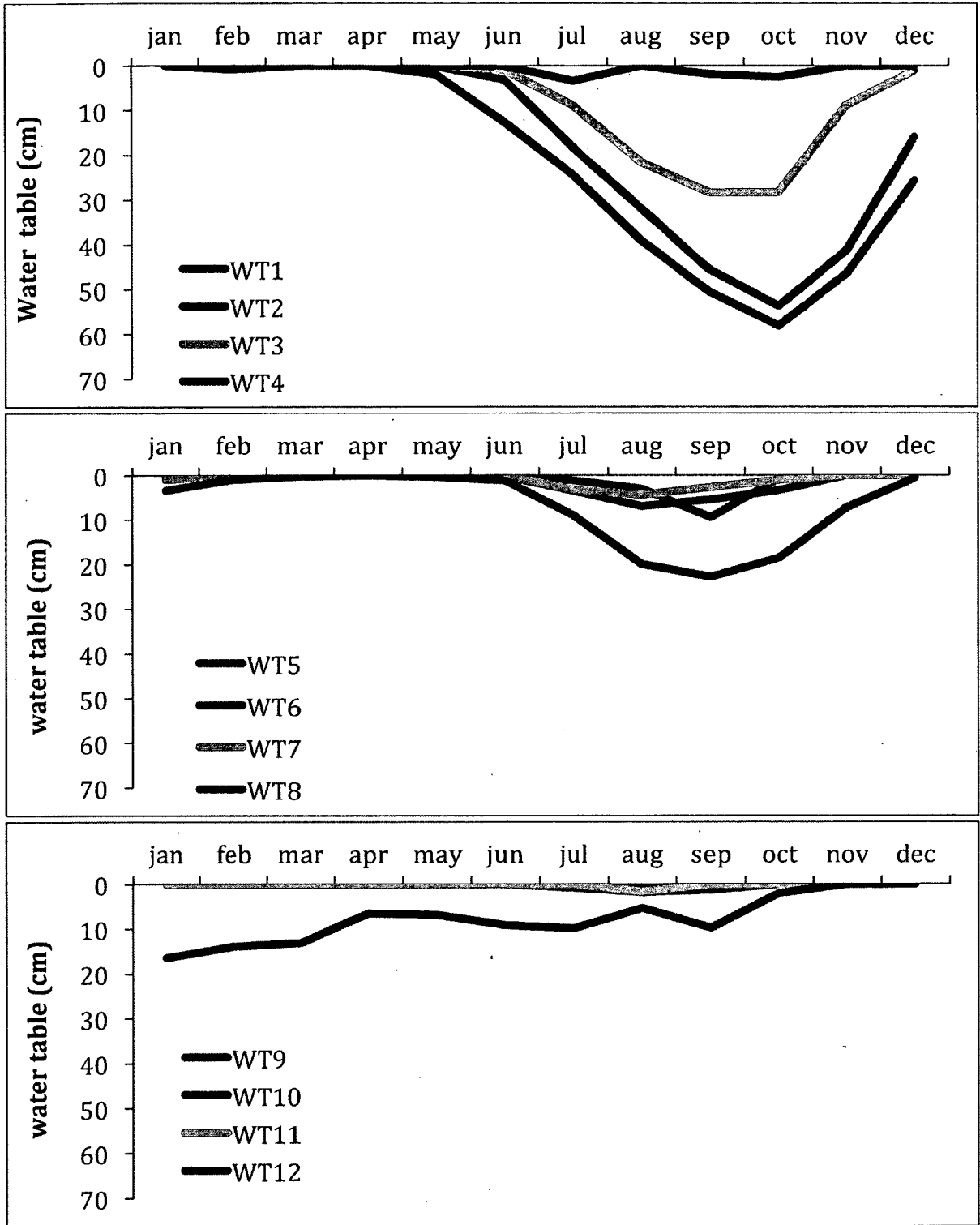


Figure 13. Mean monthly water table of each water deficit group (WD1-WD12; see Figures 10-11) for: El Niño (top), normal (middle), and La Niña (bottom).

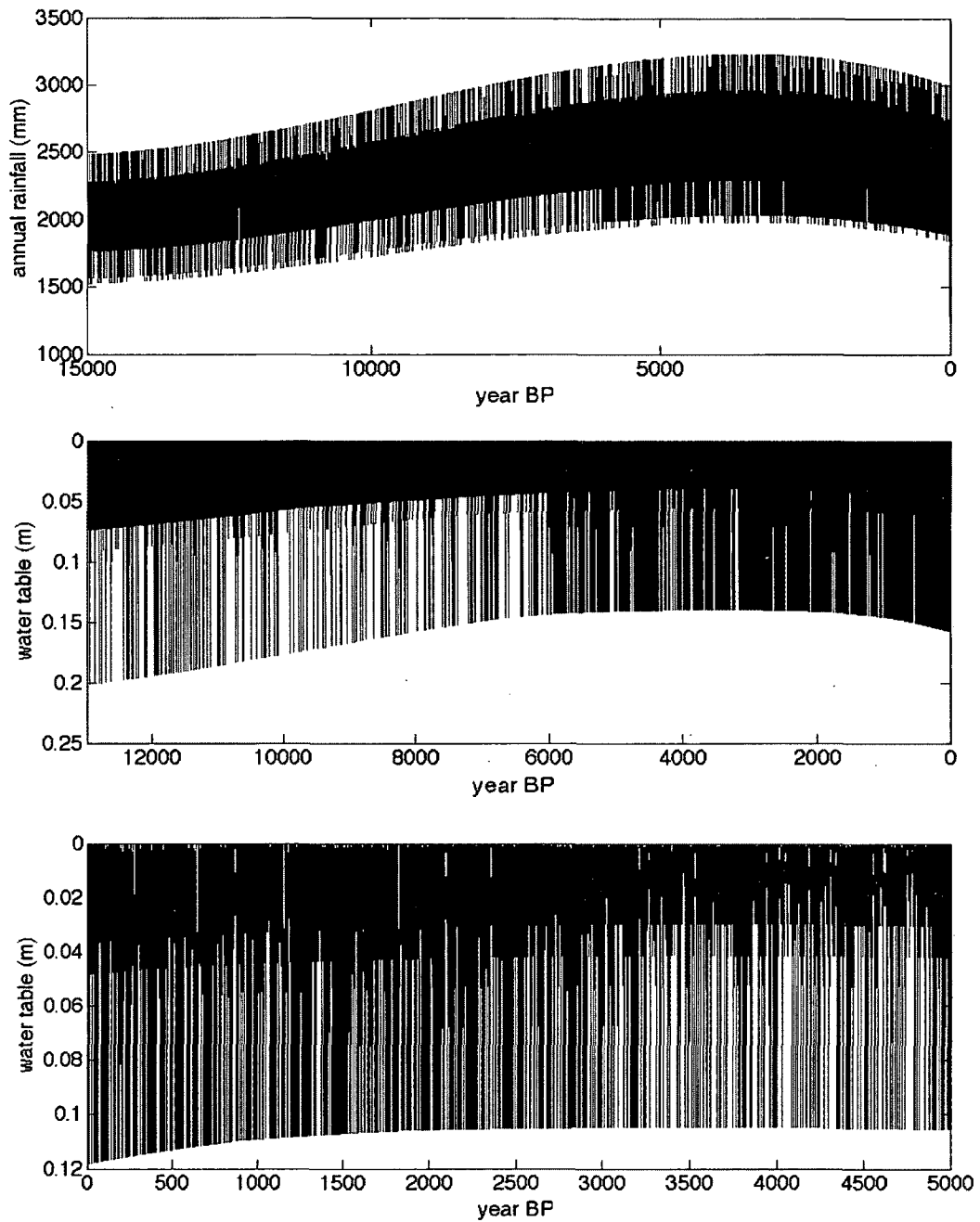


Figure 14. (top) Estimated annual rainfall over 15,000 years. Estimated mean annual water table for inland (middle) and coastal peatland (bottom) calculated as a distance from peat surface to the water level. The black line represents the 25-year moving average. Note that monthly water table is much more variable, and goes much deeper than the annual values (see Figure 10).

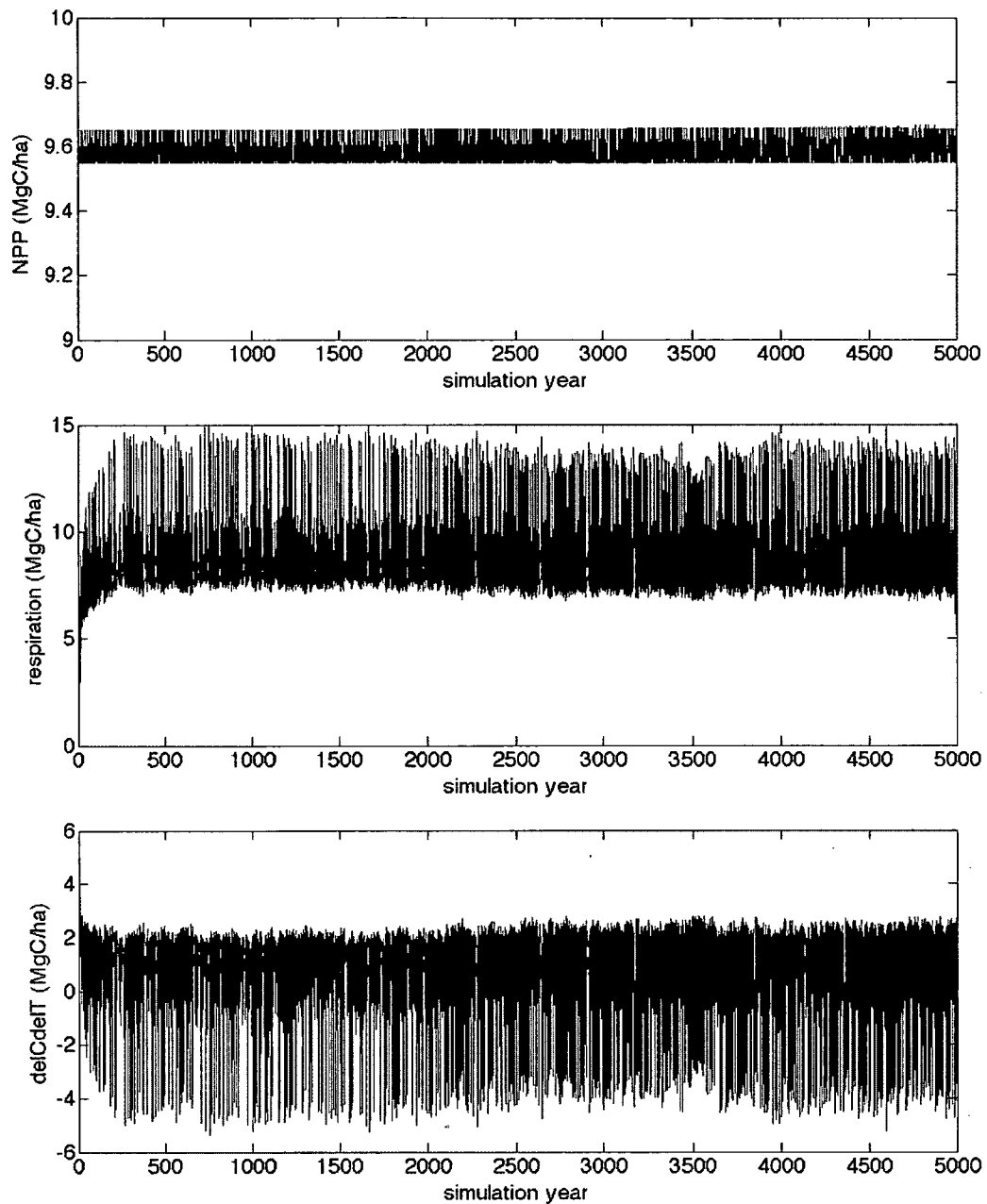


Figure 15. (*top*) Simulated annual NPP calculated as the total of litter fall, wood productivity and root mortality, and as a function of water table. (*middle*) Simulated annual decomposition rate. (*bottom*) Simulated rate of change peat mass remaining; a positive value corresponds to net carbon gain in the peat, a negative value to net carbon loss. The black line represents the 25-year moving average. This simulation was generated for coastal peatlands.

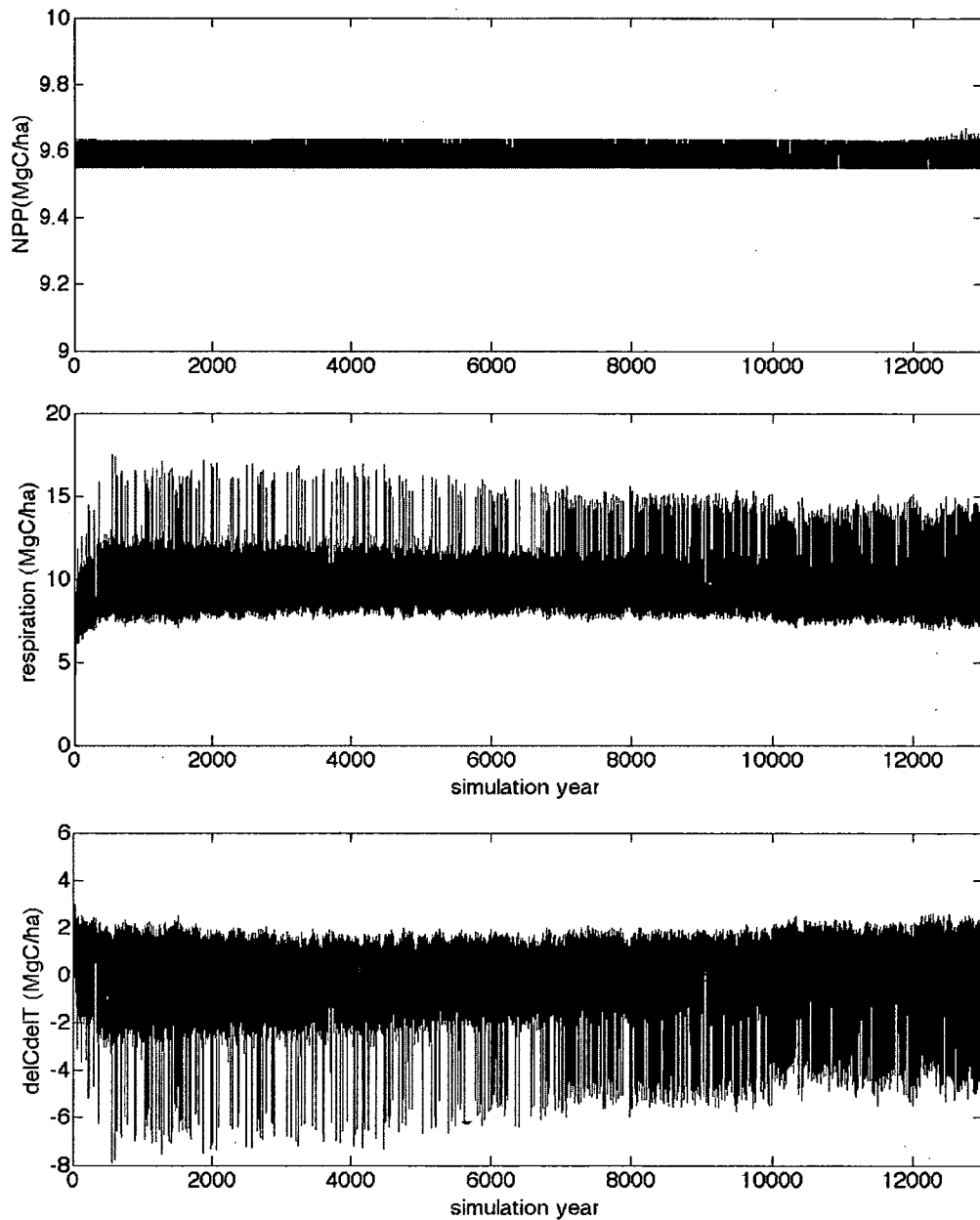


Figure 16. (*top*) Simulated annual NPP calculated as the total of litter fall, wood productivity and root mortality, and as a function of water table. (*middle*) Simulated annual decomposition rate. (*bottom*) Simulated rate of change peat mass remaining; a positive value corresponds to net carbon gain in the peat, a negative value to net carbon loss. The black line represents the 25-year moving average. This simulation was generated for inland peatlands.

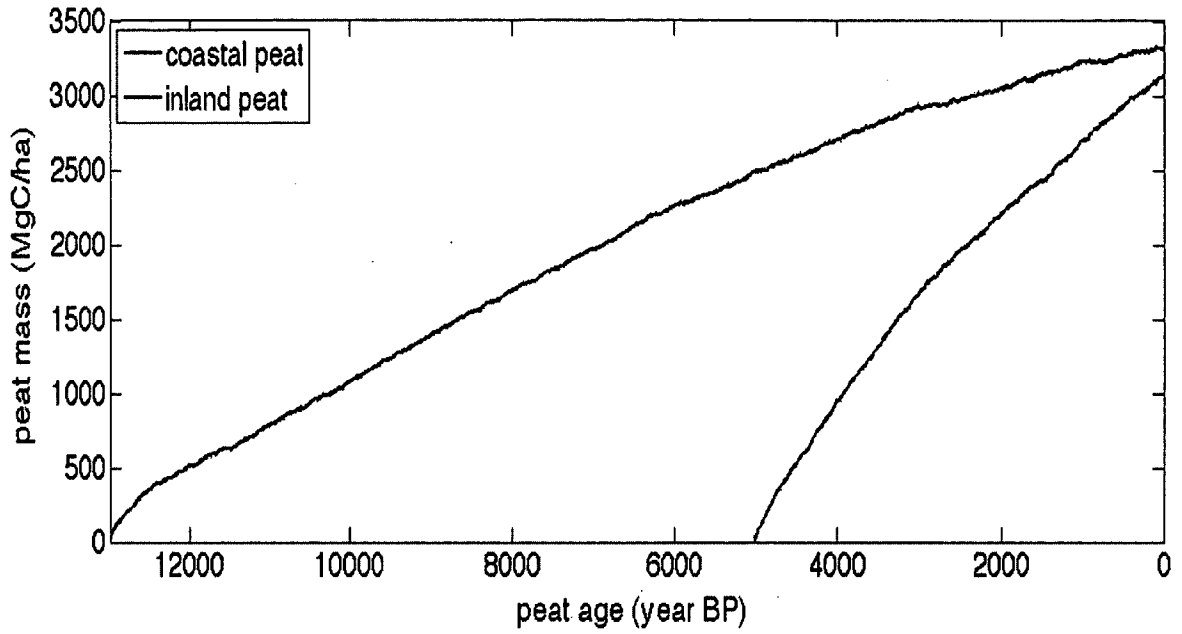


Figure 17. Time series of simulated accumulation of peat mass for coastal (blue) and inland (red) peatlands.

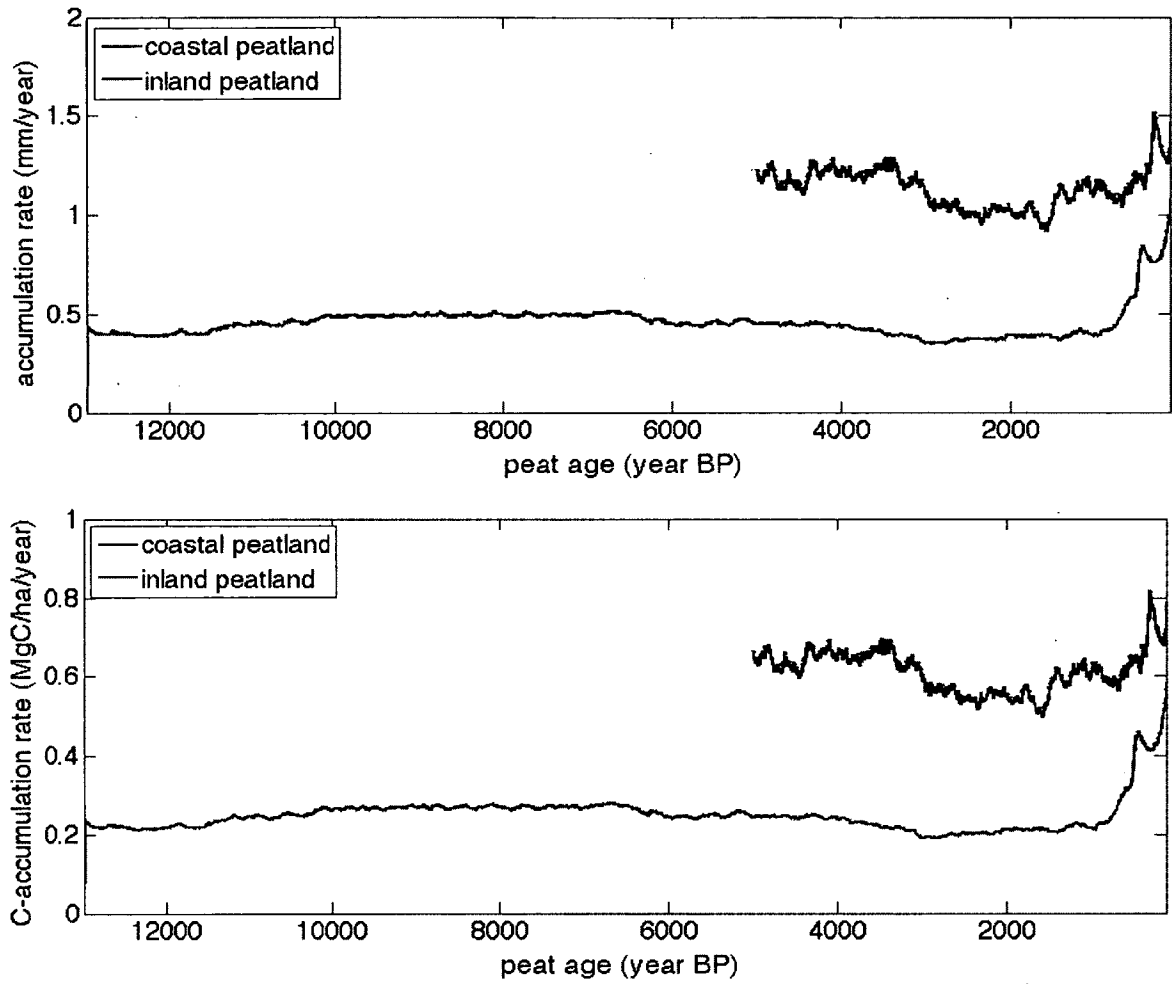


Figure 18. The simulated apparent peat accumulation rate ( $\text{mm y}^{-1}$ ) (top) and carbon accumulation rate (bottom) for coastal and inland peatlands.

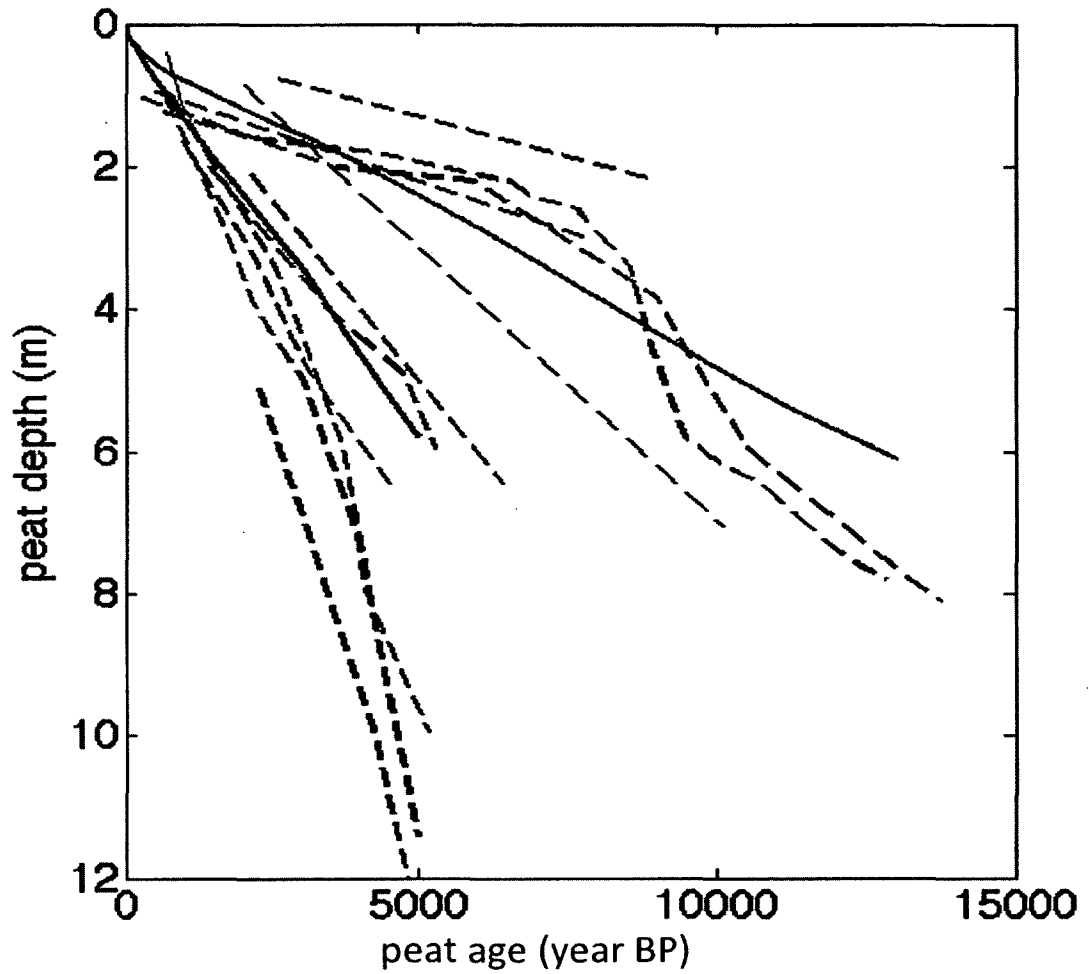


Figure 19. Relationship of peat age to depth at the end of the simulations for the coastal (black) and inland (green) peatlands, overlaid with measured age-depth profiles of coastal (blue) and inland (red) peatlands from Southeast Asia. Measured peat depth-age profiles were obtained from Dommain et al. (2011).

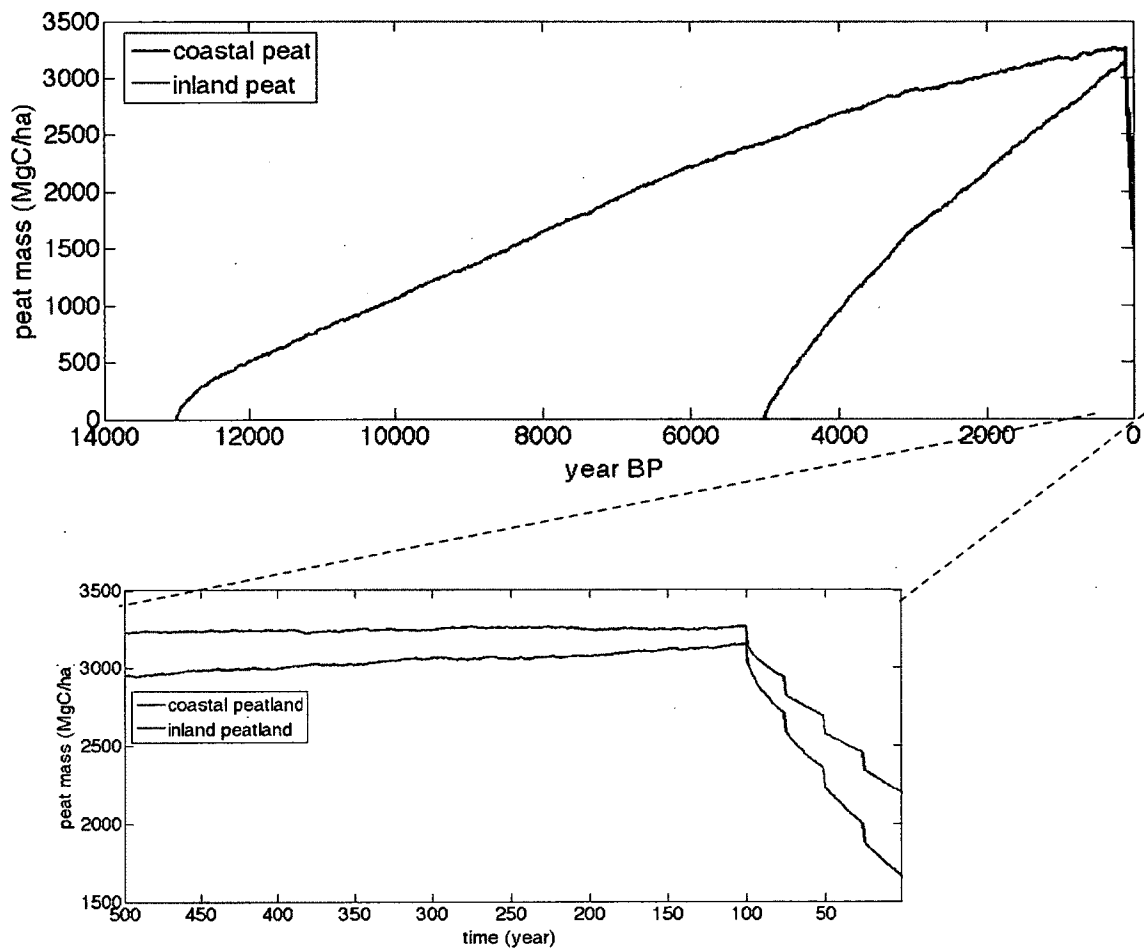


Figure 20. Simulated peat mass accumulation for coastal peatlands over 5,000 years and inland peatland over 13,000 years, with conversion to oil palm and periodic burning in the last 100 years of the simulation.



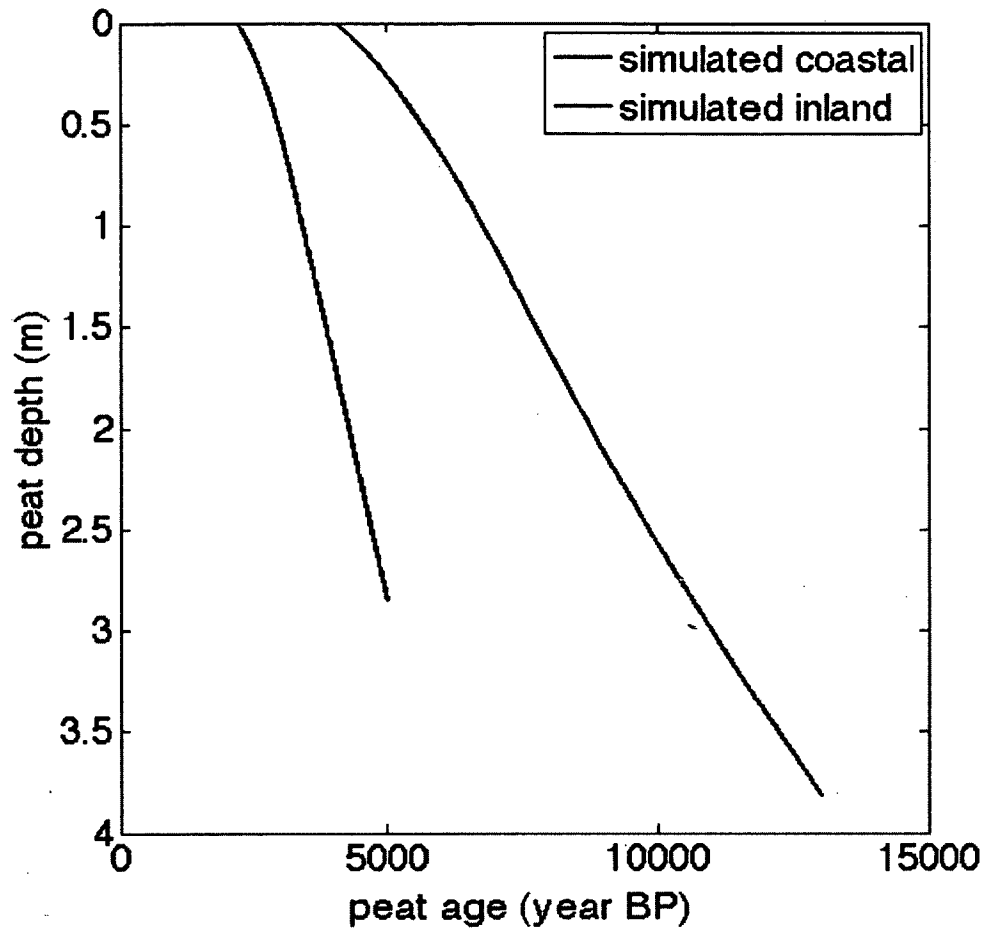


Figure 21. Simulated age-depth relationship for coastal and inland peatlands with the forest conversion to oil palm plantation scenario.

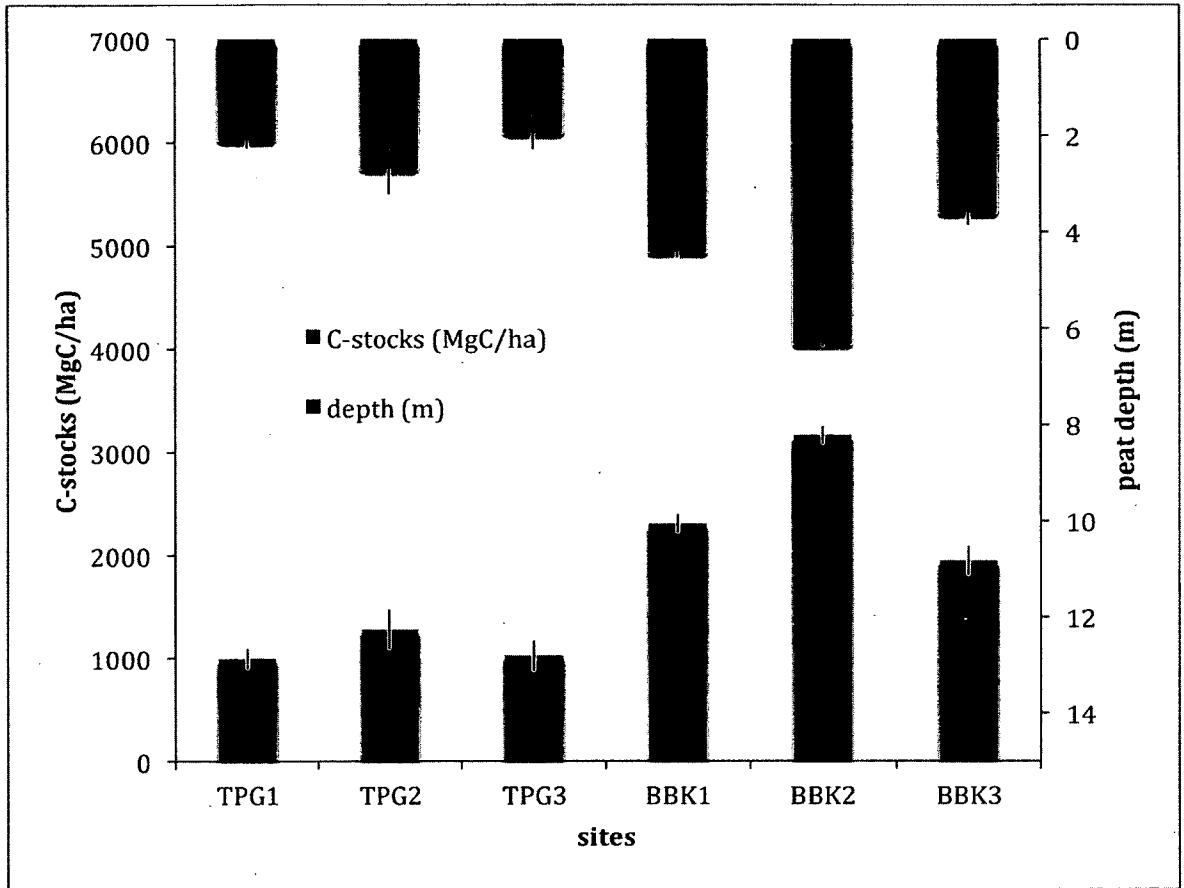


Figure 22. Measured depth of peat profiles (red bars) and stored carbon per unit area (blue bars) for sites in Tanjung Puting National Park, Kalimantan, Indonesia (TPG1-TGP3) and Berbak National Park, Sumatra, Indonesia (BBK1-BBK3). The bars and error lines represent the average and standard error from six plots sampled within each site.

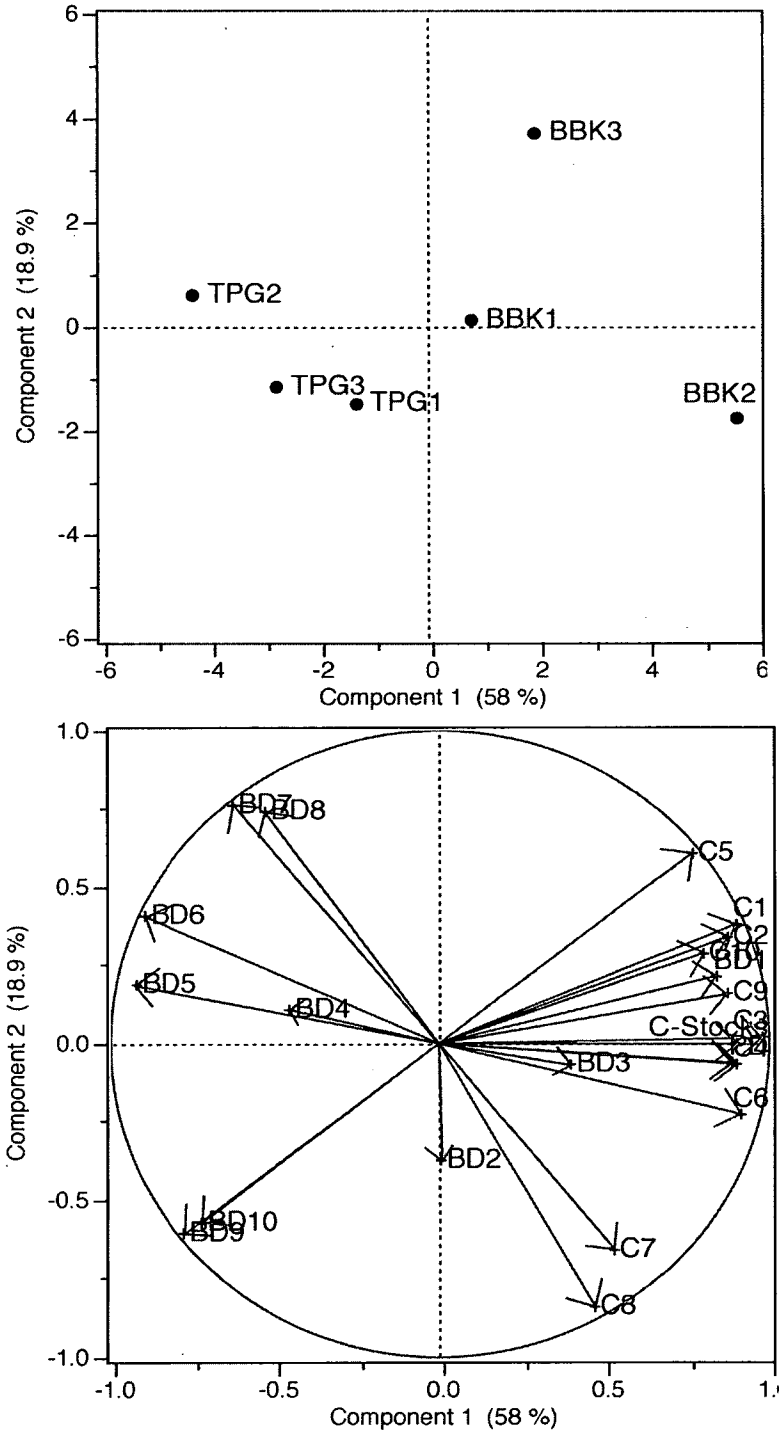


Figure 23. (top) Plot of the principal component scores of the first two components in different sites. (bottom) Plot of the individual loading score generated by bulk density (BD,  $\rho$  in the text), carbon content (C) along the peat profiles, peat depth (PD) and C-stocks. Numbers following the bulk density and carbon content represents the standardized depth, 1: 0 – 0.1 m, 2: 0.1 – 0.2 m, 3: 0.2 – 0.3 m, 4: 0.3 – 0.4 m, 5: 0.4 – 0.5 m, 6: 0.5 – 0.6 m, 7: 0.6 – 0.7 m, 8: 0.7 – 0.8 m, 9: 0.8 – 0.9 m, 10: 0.9 – 1.0 m.

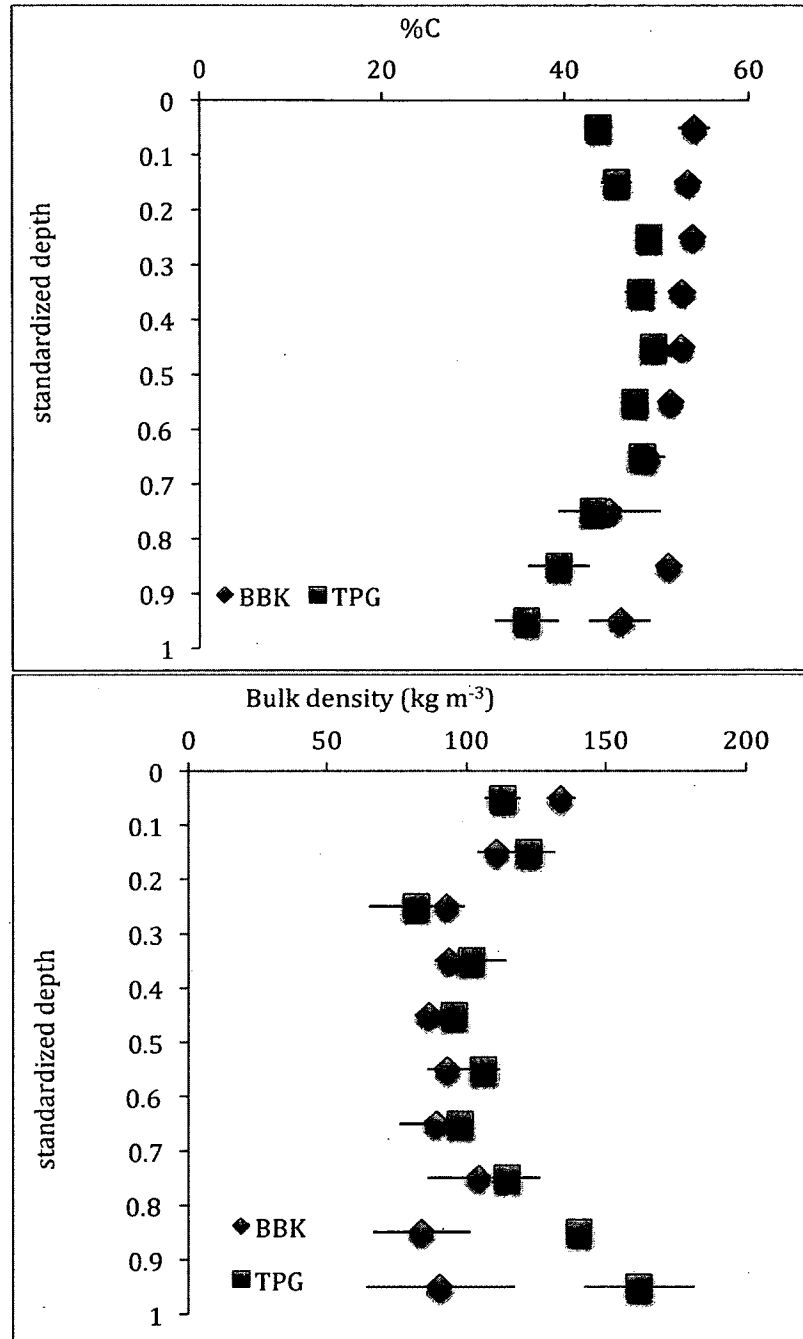


Figure 24. Bulk density (top), and carbon concentration (bottom) along the peat profile (standardized depth) sampled from three sites in Tanjung Putting National Park (TPG, red) and three sites in Berbak National Park (BBK, blue), Indonesia. The standardized depth in a profile was calculated as the ratio between sampling depths and the maximum depth of that profile.

## LIST OF REFERENCES

- Aldrian, E., Dwi Susanto, R., 2003. Identification of three dominant rainfall regions within Indonesia and their relationship to sea surface temperature. *International Journal of Climatology* 23, 1435–1452.
- Amthor, J., 2000. The McCree–de Wit–Penning de Vries–Thornley Respiration Paradigms: 30 Years Later. *Annals of Botany* 86, 1–20.
- Anderson, J., 1963. The flora of the peat swamp forests of Sarawak and Brunei, including a catalogue of all recorded species of flowering plants, ferns and fern allies. *Gardens Bulletin, Singapore* 20, 131–228.
- Anshari, G., Kershaw, A.P., van der Kaars, S., 2001. A Late Pleistocene and Holocene pollen and charcoal record from peat swamp forest, Lake Sentarum Wildlife Reserve, West Kalimantan, Indonesia. *Palaeogeography, Palaeoclimatology, Palaeoecology* 171, 213–228.
- Anshari, G., Kershaw, A.P., Van Der Kaars, S., Jacobsen, G., 2004. Environmental change and peatland forest dynamics in the Lake Sentarum area, West Kalimantan, Indonesia. *Journal of Quaternary Science* 19, 637–655.
- Anshari, G.Z., Afifudin, M., Nuriman, M., Gusmayanti, E., Arianie, L., Susana, R., Nusantara, R.W., Sugardjito, J., Rafiastanto, a., 2010. Drainage and land use impacts on changes in selected peat properties and peat degradation in West Kalimantan Province, Indonesia. *Biogeosciences* 7, 3403–3419.
- Aragão, L.E.O.C., Malhi, Y., Roman-Cuesta, R.M., Saatchi, S., Anderson, L.O., Shimabukuro, Y.E., 2007. Spatial patterns and fire response of recent Amazonian droughts. *Geophysical Research Letters* 34, L07701.
- Ballhorn, U., Siegert, F., Mason, M., Limin, S., 2009. Derivation of burn scar depths and estimation of carbon emissions with LIDAR in Indonesian peatlands. *Proceedings of the National Academy of Sciences of the United States of America* 106, 21213–8.
- Beilman, D.W., Vitt, D.H., Bhatti, J.S., Forest, S., 2008. Peat carbon stocks in the southern Mackenzie River Basin: uncertainties revealed in a high-resolution case study. *Global Change Biology* 14, 1221–1232.

- Chimner, R.A., Ewel, K.C., 2004. Differences in carbon fluxes between forested and cultivated micronesia tropical peatlands. *Wetlands Ecology and Management* 12, 419–427.
- Chimner, R.A., Ewel, K.C., 2005. A Tropical Freshwater Wetland: II. Production, Decomposition, and Peat Formation. *Wetlands Ecology and Management* 13, 671–684.
- Cobb, K.M., Westphal, N., Sayani, H.R., Watson, J.T., Di Lorenzo, E., Cheng, H., Edwards, R.L., Charles, C.D., 2013. Highly variable El Niño-Southern Oscillation throughout the Holocene. *Science (New York, N.Y.)* 339, 67–70.
- Conroy, J.L., Overpeck, J.T., Cole, J.E., Shanahan, T.M., Steinitz-Kannan, M., 2008. Holocene changes in eastern tropical Pacific climate inferred from a Galápagos lake sediment record. *Quaternary Science Reviews* 27, 1166–1180.
- Couwenberg, J., Dommain, R., Joosten, H., 2009. Greenhouse gas fluxes from tropical peatlands in south-east Asia. *Global Change Biology* 16, 1715–1732.
- DeLucia, E.H., Drake, J.E., Thomas, R.B., Gonzalez-Meler, M., 2007. Forest carbon use efficiency: is respiration a constant fraction of gross primary production? *Global Change Biology* 13, 1157–1167.
- Dommain, R., Couwenberg, J., Joosten, H., 2010. Hydrological self-regulation of domed peatlands in south-east Asia and consequences for conservation and restoration. *Mires and Peat*, Article 6, 1–17.
- Dommain, R., Couwenberg, J., Joosten, H., 2011. Development and carbon sequestration of tropical peat domes in south-east Asia: links to post-glacial sea-level changes and Holocene climate variability. *Quaternary Science Reviews* 30, 999–1010.
- Estop-Aragonés, C., Knorr, K.-H., Blodau, C., 2012. Controls on in situ oxygen and dissolved inorganic carbon dynamics in peats of a temperate fen. *Journal of Geophysical Research* 117, G02002.
- Frolking, S., Milliman, T., Palace, M., Wisser, D., Lammers, R., Fahnestock, M., 2011. Tropical forest backscatter anomaly evident in SeaWinds scatterometer morning overpass data during 2005 drought in Amazonia. *Remote Sensing of Environment* 115, 897–907.

- Frolking, S., Roulet, N.T., Moore, T.R., Richard, P.J.H., Lavoie, M., Muller, S.D., 2001. Modeling Northern Peatland Decomposition and Peat Accumulation. *Ecosystems* 4, 479–498.
- Frolking, S., Roulet, N.T., Tuittila, E., Bubier, J.L., Quillet, a., Talbot, J., Richard, P.J.H., 2010. A new model of Holocene peatland net primary production, decomposition, water balance, and peat accumulation. *Earth System Dynamics* 1, 1–21.
- Frolking, S., Talbot, J., Jones, M.C., Treat, C.C., Kauffman, J.B., Eeva-Stiina, T., Roulet, N., 2011. Peatlands in the Earth ' s 21 st century climate system. *Environmental Reviews* 19, 371–396.
- Giardina, C.P., Ryan, M.G., Binkley, D., Fowners, J.H., 2003. Primary production and carbon allocation in relation to nutrient supply in a tropical experimental forest. *Global Change Biology* 9, 1438–1450.
- Gorham, E., 1991. Northern peatlands: Role in the carbon cycle and probable responses to climate change. *Ecological Applications* 1, 182–195.
- Griffiths, M., Drysdale, R., Gagan, M., Zhao, J.–., Ayliffe, L., Hellstorm, J., Hantoro, W., Frisia, S., Feng, Y.–., Cartwright, I., St. Pierre, E., Fischer, M., Suwargadi, B., 2009. Increasing Australian–Indonesian monsoon rainfall linked to early Holocene sea-level rise. *Nature Geoscience* 2, 4–7.
- Hanebuth, T., Stategger, K., Grootes, P.M., 2000. Rapid Flooding of the Sunda Shelf : A Late-Glacial Sea-Level Record. *Science* 288, 1033–1035.
- Heil, A., Langmann, B., Aldrian, E., 2006. Indonesian peat and vegetation fire emissions: Study on factors influencing large-scale smoke haze pollution using a regional atmospheric chemistry model. *Mitigation and Adaptation Strategies for Global Change* 12, 113–133.
- Heinemeyer, A., Croft, S., Garnett, M., Gloor, E., Holden, J., Lomas, M., Ineson, P., 2010. The MILLENNIA peat cohort model: predicting past, present and future soil carbon budgets and fluxes under changing climates in peatlands. *Climate Research* 45, 207–226.
- Hergoualc'h, K., Verchot, L. V., 2011. Stocks and fluxes of carbon associated with land use change in Southeast Asian tropical peatlands: A review. *Global Biogeochemical Cycles* 25, doi:10.1029/2009GB003718.
- Hilbert, D.W., Roulet, N., Moore, T., 2000. Modelling and analysis of peatlands as dynamical system. *Journal of Ecology* 88, 230–242.

- Hirano, T., Segah, H., Kusin, K., Limin, S., Takahashi, H., Osaki, M., 2012. Effects of disturbances on the carbon balance of tropical peat swamp forests. *Global Change Biology* 18, 3410–3422.
- Hooijer, A., Page, S., Canadell, J.G., Silvius, M., Kwadijk, J., Wösten, H., Jauhiainen, J., 2010. Current and future CO<sub>2</sub> emissions from drained peatlands in Southeast Asia. *Biogeosciences* 7, 1505–1514.
- Hooijer, A., Page, S., Jauhiainen, J., Lee, W.A., Lu, X.X., Idris, A., Anshari, G., 2012. Subsidence and carbon loss in drained tropical peatlands. *Biogeosciences* 9, 1053–1071.
- Hutrya, L.R., Munger, J.W., Nobre, C.A., Saleska, S.R., Vieira, S.A., Wofsy, S.C., 2005. Climatic variability and vegetation vulnerability in Amazônia. *Geophysical Research Letters* 32, L24712.
- Jaenicke, J., Rieley, J., Mott, C., Kimman, P., Siegert, F., 2008. Determination of the amount of carbon stored in Indonesian peatlands. *Geoderma* 147, 151–158.
- Kauffman, J.B., Donato, D.C., 2012. Protocols for the measurement, monitoring and reporting of structure, biomass and carbon stocks in mangrove forests. CIFOR, Bogor, Indonesia.
- Kleinen, T., Brovkin, V., von Bloh, W., Archer, D., Munhoven, G., 2010. Holocene carbon cycle dynamics. *Geophysical Research Letters* 37, L02705.
- Kleinen, T., Brovkin, V., Schuldt, R.J., 2012. A dynamic model of wetland extent and peat accumulation: results for the Holocene. *Biogeosciences* 9, 235–248.
- Koh, L.P., Miettinen, J., Liew, S.C., Ghazoul, J., 2011. Remotely sensed evidence of tropical peatland conversion to oil palm. *Proceedings of the National Academy of Sciences of the United States of America* 108, 5127–32.
- Lähteenoja, O., Page, S., 2011. High diversity of tropical peatland ecosystem types in the Pastaza-Marañón basin, Peruvian Amazonia. *Journal of Geophysical Research* 116, G02025.
- Lähteenoja, O., Ruokolainen, K., Schulman, L., Oinonen, M., 2009. Amazonian peatlands: an ignored C sink and potential source. *Global Change Biology* 15, 2311–2320.



- Malhi, Y., Aragao, L.E.O.C., Galbraith, D., Huntingford, C., Fisher, R., Zelazowski, P., Sitch, S., McSweeney, C., Meirb, P., 2009. Exploring the likelihood and mechanism of a climate-change-induced dieback of the Amazon rainforest. *Proceedings of the National Academy of Sciences of the United States of America* 106, 20610–20615.
- Malmer, N., Holm, E., 1984. Variation in the C/N-quotient of peat in relation to decomposition rate and age determination with <sup>210</sup>Pb. *Oikos* 43, 171–182.
- Matsuura, K., Willmott, C.J., 2009. Terrestrial Precipitation: 1900-2008 Gridded Monthly Time Series. Center for Climatic Research, Department of Geography, University of Delaware, Newark, DE.
- Melling, L., Hatano, R., Goh, K.J., 2005. Soil CO<sub>2</sub> flux from three ecosystems in tropical peatland of Sarawak, Malaysia. *Tellus B* 57, 1–11.
- Miettinen, J., Hooijer, A., Shi, C., Tollenaar, D., Vernimmen, R., Liew, S.C., Malins, C., Page, S.E., 2012. Extent of industrial plantations on Southeast Asian peatlands in 2010 with analysis of historical expansion and future projections. *GCB Bioenergy* doi: 10.1111/j.1757–1707.2012.01172.x.
- Miettinen, J., Liew, S.C., 2010a. Status of Peatland Degradation and Development in Sumatra and Kalimantan. *Ambio* 39, 394–401.
- Miettinen, J., Liew, S.C., 2010b. Degradation and development of peatlands in Peninsular Malaysia and in the islands of Sumatra and Borneo since 1990. *Land Degradation & Development* 21, 285–296.
- Miettinen, J., Shi, C., Liew, S.C., 2011. Deforestation rates in insular Southeast Asia between 2000 and 2010. *Global Change Biology* 17, 2261–2270.
- Miettinen, J., Shi, C., Liew, S.C., 2012. Two decades of destruction in Southeast Asia's peat swamp forests. *Frontiers in Ecology and the Environment* 10, 124–128.
- Moore, S., Evans, C.D., Page, S.E., Garnett, M.H., Jones, T.G., Freeman, C., Hooijer, A., Wiltshire, A.J., Limin, S.H., Gauci, V., 2013. Deep instability of deforested tropical peatlands revealed by fluvial organic carbon fluxes. *Nature* 493, 660–3.
- Murdiyarso, D., Hergoualc'h, K., Verchot, L. V, 2010. Opportunities for reducing greenhouse gas emissions in tropical peatlands. *Proceedings of the National Academy of Sciences of the United States of America* 107, 19655–19660.

- Neuzil, S.G., 1997. Onset and Rate of Peat and Carbon Accumulation in Four Domed Ombrogenous Peat Deposits, Indonesia, in: Rieley, J.O., Page, S. (Eds.), *Biodiversity and Sustainability of Tropical Peatlands - Proceedings of the International Symposium on Tropical Peatlands*. Samara Publishing Limited, Cardigan, Palangkaraya, Indonesia, pp. 55–72.
- Page, S., Wüst, R., Banks, C., 2010. Past and present carbon accumulation and loss in Southeast Asian peatlands. *PAGES NEWS* 18, 25–27.
- Page, S.E., Rieley, J.O., Banks, C.J., 2011. Global and regional importance of the tropical peatland carbon pool. *Global Change Biology* 17, 798–818.
- Page, S.E., Rieley, J.O., Shotyk, W., Weiss, D., 1999. Interdependence of peat and vegetation in a tropical peat swamp forest. *Philosophical transactions of the Royal Society of London. Series B, Biological sciences* 354, 1885–9187.
- Page, S.E., Siegert, F., Rieley, J.O., Boehm, H. V., Jayak, A., Limink, S., 2002. The amount of carbon released from peat and forest fires in Indonesia during 1997. *Nature* 1999, 61–65.
- Page, S.E., Wüst, R. a. J., Weiss, D., Rieley, J.O., Shotyk, W., Limin, S.H., 2004. A record of Late Pleistocene and Holocene carbon accumulation and climate change from an equatorial peat bog (Kalimantan, Indonesia): implications for past, present and future carbon dynamics. *Journal of Quaternary Science* 19, 625–635.
- Partin, J.W., Cobb, K.M., Adkins, J.F., Clark, B., Fernandez, D.P., 2007. Millennial-scale trends in west Pacific warm pool hydrology since the Last Glacial Maximum. *Nature* 449, 452–455.
- Phillips, V.D., 1998. Peat swamp ecology and sustainable development in Borneo. *Biodiversity and Conservation* 7, 651–671.
- Rais, D.S., 2011. Peatland hydrology and its role in tropical peatland sustainability, in: *Proceedings National Symposium on Ecohydrology*. Jakarta, pp. 114–140.
- Rieley, J.O., Wust, R., Jauhiainen, J., Page, S.E., Wösten, H., Hooijer, A., Siegert, F., Limin, S.H., Vasander, H., Stahlhut, M., 2008. Tropical peatlands: carbon stores, carbon gas emissions and contribution to climate change processes, in: Strack, M. (Ed.), *Peatlands and Climate Change*. International Peat Society, Jyväskylä, Finland, pp. 148–181.

- Rosenthal, Y., 2003. The amplitude and phasing of climate change during the last deglaciation in the Sulu Sea, western equatorial Pacific. *Geophysical Research Letters* 30, 1428.
- Saharjo, B.H., Munoz, C.P., 2005. Controlled burning in peat lands owned by small farmers: a case study in land preparation. *Wetlands Ecology and Management* 13, 105–110.
- Sandweiss, D.H., Maasch, K.A., Burger, R.L., Richardson, J.B.I., Rollins, H.B., Clement, A., 2001. Variation in Holocene El Niño frequencies: Climate records and cultural consequences in ancient Peru. *Geological Society of America* 29, 603–606.
- Sathiamurthy, E., Voris, H., 2006. Maps of Holocene Sea Level Transgression and Submerged Lakes on the Sunda Shelf. *The Natural History of Chulalongkorn University* 1–44.
- Shimada, S., Takahashi, H., Haraguchi, A., Kaneko, M., 2001. The carbon content characteristics of tropical peats in Central Kalimantan, Indonesia: Estimating their spatial variability in density. *Biogeochemistry* 53, 249–267.
- Shimamura, T., Momose, K., 2005. Organic matter dynamics control plant species coexistence in a tropical peat swamp forest. *Proceedings of Biological sciences / The Royal Society* 272, 1503–1510.
- Smith, D.E., Harrison, S., Firth, C.R., Jordan, J.T., 2011. The early Holocene sea level rise. *Quaternary Science Reviews* 30, 1846–1860.
- St-Hilaire, F., Wu, J., Roulet, N.T., Froking, S., Lafleur, P.M., Humphreys, E.R., Arora, V., 2010. McGill wetland model: evaluation of a peatland carbon simulator developed for global assessments. *Biogeosciences* 7, 3517–3530.
- Steinke, S., Kienast, M., Hanebuth, T., 2003. On the significance of sea-level variations and shelf paleo-morphology in governing sedimentation in the southern South China Sea during the last deglaciation. *Marine Geology* 201, 179–206.
- Wang, Y., Cheng, H., Edwards, R.L., He, Y., Kong, X., An, Z., Wu, J., Kelly, M.J., Dykoski, C. a, Li, X., 2005. The Holocene Asian monsoon: links to solar changes and North Atlantic climate. *Science* 308, 854–857.
- Wania, R., Ross, I., Prentice, I.C., 2009a. Integrating peatlands and permafrost into a dynamic global vegetation model: 2. Evaluation and sensitivity of vegetation and carbon cycle processes. *Global Biogeochemical Cycles* 23, GB3015.

- Wania, R., Ross, I., Prentice, I.C., 2009b. Integrating peatlands and permafrost into a dynamic global vegetation model: 1. Evaluation and sensitivity of physical land surface processes. *Global Biogeochemical Cycles* 23, GB3014.
- Warren, M.W., Kauffman, J.B., Murdiyarso, D., Anshari, G., Hergoualc, K., Kurnianto, S., Purbopuspito, J., Gusmayanti, E., Afifudin, M., Rahajoe, J., Alhamd, L., Limin, S., Iswandi, A., 2012. A cost-efficient method to assess carbon stocks in tropical peat soil. *Biogeosciences* 9, 4477–4485.
- Wösten, H., Ritzema, H., Rieley, J.O., 2010. Assessment of Risks and Vulnerabilities of Tropical Peatland Carbon Pools : Mitigation and Restoration Strategies CARBOPEAT Technical Reports. Technical Report 3, EU CARBOPEAT Project, Carbon-Climate-Human Interactions in Tropical Peatlands: Vulnerabiliti. University of Leicester, United Kingdom.
- Wösten, J., Clymans, E., Page, S., Rieley, J., Limin, S., 2008. Peat–water interrelationships in a tropical peatland ecosystem in Southeast Asia. *Catena* 73, 212–224.
- Wösten, J., Ismail, A., van Wijk, A., 1997. Peat subsidence and its practical implications: a case study in Malaysia. *Geoderma* 78, 25–36.
- Wu, Y., Blodau, C., 2013. PEATBOG : a biogeochemical model for analyzing coupled carbon and nitrogen dynamics in northern peatlands. *Geoscientific Model Development Discussions* 6, 1599–1688.
- Wust, R.A., Bustin, R., 2004. Late Pleistocene and Holocene development of the interior peat-accumulating basin of tropical Tasek Bera , Peninsular Malaysia. *Palaeogeography, Palaeoclimatology, Palaeoecology* 211, 241–270.
- Yu, Z., Beilman, D., Froking, S., MacDonald, G., Roulet, N., Camill, P., Charman, D., 2011. Peatlands and Their Role in the Global Carbon Cycle. *Eos* 92, 97–108.
- Yu, Z., Loisel, J., Brosseau, D.P., Beilman, D.W., Hunt, S.J., 2010. Global peatland dynamics since the Last Glacial Maximum. *Geophysical Research Letters* 37, L13402.
- Yule, C.M., Gomez, L.N., 2008. Leaf litter decomposition in a tropical peat swamp forest in Peninsular Malaysia. *Wetlands Ecology and Management* 17, 231–241.

## APPENDIX

## Appendix 1. HPM Trop model code

### Matlab code for the main routine

```
% ~~~~~  
%  
% INITIALIZE THINGS AND BUILD FIRST COHORT  
%  
% ~~~~~  
  
% load in HPM parameters & initialize  
% check parameter file, but typical mass units are kg/m^2 dry mass & m water  
%   depth (ET,PPT, Runoff, ...)  
  
%% load parameters and make the arrays  
hpm_paramsT1_2;  
  
params=load('hpmT1_param_vals');  
  
nveg = params.num_veg;  
  
num_years = params.sim_len;  
  
timestep = 1; % [y] BE CAREFUL ABOUT CHANGING THIS FROM ONE (1)!!!  
istep = num_years / timestep;  
  
%base_ppt = params.ann_ppt; % annual ppt (m/y) from Roulet PAM  
  
% ***** moss fraction *****  
% (S. Frolking)  
% variables for binning moss fraction of peat *****  
nbins = 250; % for binning cohorts in output  
maxheight = 13; % total potential height (meters)  
delx = maxheight/nbins; % total possible ht (meters)  $\sqrt{\Sigma}$  # of bins  
  
mossfrac = zeros(istep,1); % cohort mass fraction that is moss  
bin_moss_frac = -0.9999 * ones(nbins,istep); % bin mass fraction that is moss  
cohortheight = zeros(istep,1); % height of top of cohort above bottom of peat  
% *****  
  
% preallocate arrays to speed up simulations  
  
% small m arrays are masses as annual cohort by veg types  
m = zeros(istep,nveg); % remaining mass in cohort (layer) i and veg type
```

```

m_0 = zeros(istep,nveg); % total input mass in cohort i and veg type
m_0_age = zeros(istep,nveg); % total input mass in cohort i and veg type
m_star = zeros(istep,nveg); % = m / m_0

% capital M vectors are masses as annual cohort accumulated across the veg
types
M = zeros(istep,1); % = sum m across veg. types in cohort/layer i
M_0 = zeros(istep,1); % = sum m_0 across veg. types in cohort/layer i
M_0_age = zeros(istep,1); % = sum m_0 across veg. types in cohort/layer i
M_star = zeros(istep,1); % = M / M_0 in cohort/layer i
M_overlying = zeros(istep,1); % = sum M_total in profile above cohort/layer i
del_M_tot = zeros(istep,1); % annual change in total peat mass

% these are temporary arrays
mstemp = zeros(istep,nveg);
ms0temp = zeros(istep,nveg);
ms0agetemp = zeros(istep,nveg);
mstartemp = zeros(istep,nveg);
ktemp = zeros(istep,nveg);
agebiastemp = zeros(istep,nveg);
agebiastemparr = zeros(istep,nveg);

% vectors down the profile
depth = zeros(istep,1); % cohort (layer) depth in meters
thick = zeros(istep,1); % cohort (layer) thickness in meters
zbottom = zeros(istep,1); % depth (m) from top of peat to bottom of cohort
porosity = zeros(istep,1); % cohort (layer) porosity (m3/m3)
prev_thick = zeros(istep,1); % cohort (layer) thickness in meters (from previous
time step)
dens = zeros(istep,1); % cohort (layer) bulk density in kg/m3
time = zeros(istep,1); % keeps track of time in years
age_bias = zeros(istep,1); % for keeping track of age bias
tmp_depth = zeros(500,1); % temporary truncated array

% these are temporary arrays
depth2 = depth;
dens1 = dens;
dens_old = dens;
dens_old2 = dens_old;
dens_evolve = zeros(istep,4);

% arrays by cohort and veg type
k = zeros(istep,nveg); % mass loss rate (1/y)

```

```

% vectors down the profile
k_mean = zeros(istep,1);      % mass-weighted mean decomposition factor by
    cohort
anoxiafact = zeros(istep,1);  % anoxia profile, function of water table depth
    (anything else?)

% array of root mass input (kg/m2/layer) by veg type
rootin = zeros(istep,nveg);
rootin2 = zeros(istep,nveg); % temporary array

% arrays by time and veg type
annNPP = zeros(istep,nveg);
biomass = zeros(istep,nveg); %biomass layer for each veg type (J.Talbot)
tot_npp = zeros(istep,1);
annRESP = zeros(istep,1); % annual mass loss (carbon units = biomass/2)
%annRespLitter = zeros(istep,1);
%annRespPeat = zeros(istep,1);
annROOTIN = zeros(istep,1);
annROOTNPP = zeros(istep,1);
annAGMASSIN = zeros(istep,1);
annZ_total = zeros(istep,1);
del_peat_height = zeros(istep,1);
annM_total = zeros(istep,1);
% NPPVEC = zeros(nveg);
del_C_del_t = zeros(istep,1);
del_C_del_t2 = zeros(istep,1);
j5 = zeros(istep,1);

% vectors and arrays for debugging, etc.
junk1 = zeros(istep,3);
junk2 = zeros(istep,3);
temporary = zeros(istep,1);
cohortM = zeros(istep,10);

% vectors by time
annPPT = zeros(istep,1);
annWTD = zeros(istep,1);

peat_water = zeros(istep,1);
total_water = zeros(istep,1);
lagWTD = zeros(istep,1);
annTRANS = zeros(istep,1); % relative hydraulic transmissivity (0-1)
WATER = zeros(istep,7); % array for output that contains annual water balance
    terms

```



```

annTHETA = zeros(istep,1);
annWTD_VAR = zeros(istep,1);
annWFPS = zeros(istep,20);
% prev_annWFPS = zeros(istep,1);
del_peatwater = zeros(istep,1);
net_water_in = zeros(istep,1);
annTEMP_FACT = ones(istep,1);
counter_array = zeros(istep*10,2);
reconstrWTD = zeros(istep,1);

%monthWFPS = ones(istep,12);
monthWTD = zeros(12);

% vectors and arrays for the math
onevec = ones(istep,1);
epsvec = eps*ones(istep,1);
zerovec = zeros(istep,1);
onearr = ones(istep,nveg);
epsarr = eps*ones(istep,nveg);
topvec = zeros(1,nveg);
topval = 0;

% initialize new variables for tracking the cohort
ncolMM = floor(num_years/1000)-1;
MM = zeros(istep,ncolMM); % mass of 10 adjacent cohorts that are at surface
each 1000 years

MD = zeros(istep, ncolMM); % height of mid-cohort of these 10 from bottom of
peat
%% initialize surface cohort with aboveground litter inputs from all plant types

time(1) = timestep / 2 ;
thick(1) = 0.05; % placeholder value for first year NPP calculation

%NPP = hpm_nppT1_2(params);
NPP = params.NPP_trees;
% NPP = hpm_npp_4(annWTD(itime), thick, params);

% Biomass initialization (J. Talbot)

m(1,:) = NPP .* params.ag_frac_npp_trees;
m_0 = m;
m_0_age = m * (params.sim_len - 0.5);

```

```

m_star = m ./ (epsarr + m_0);
age_bias(1) = 1;

M = sum(m,2);

M_0 = M;

M_0 = M * (params.sim_len - 0.5);
M_star = M ./ (epsvec + M_0);

cohortM(1,:) = [sum(M) 0 0 0 0 0 0 0 0];

M_overlying(1) = 0;
prev_M_tot = 0;

annNPP(1,:) = NPP;
% NPP(1,1) = params.npp(1) * 2; % * (1 + 0.5 *sin(2*3.14159*itime/500));
% NPP(1,2) = params.npp(2) * 2; % * (1 + 0.5 *sin(2*3.14159*itime/500));
% NPP(1,3) = 0.; % params.npp(3) * 2 * (0. + itime/num_years); % * (1 + 0.5
% *sin(2*3.14159*itime/500));
% NPP(1,4) = 0.; % params.npp(4) * 2 * (0. + itime/num_years); % * (1 + 0.5
% *sin(2*3.14159*itime/500));
annWTD(1) = params.wtd_0;
annWTD_VAR(1) = annWTD(1)/3;
% AG_FRAC_NPP(1,:) = params.ag_frac_npp(:);
% FAST_POOL_FRAC(1,:) = params.fast_pool_frac(:);
annTEMP_FACT(1) = 1.0;

% calculate layer density, thickness, and depth

% ???????
% peat density function not well developed (30 jan 07)
% link hydraulic conductivity/transmissivity/runoff to peat density?
% ???????

dens = hpm_densT1(M_star, M_overlying, params, onevec);
% dens = params.min_bulk_dens * onevec + params.del_bulk_dens .* (onevec -
% 0.5*(onevec + erf((m_star - c1*onevec)/c2/sqrt(2))));

% thick(1) = M_total(1) / (eps + dens(1));
thick(1) = M(1) / (eps + dens(1));
zbottom(1) = thick(1);
prev_thick(1) = thick(1);
depth = cumsum(thick) - onevec * thick(1)/2;

```

```

annZ_total(1) = thick(1);
annM_total(1) = M(1);
% last_Z_total = 0;

litter_m = 0;
litter_m0 = 0;
tic;

dynamic_watbal_time_start = 0;

flag1 = 0; % set to 1 when simulation of dynamic water balance begins
flag2 = 0; % set to 1 when simulation of dynamic water balance begins

% REC_annppt = hpm_precipT1(istep, params); %reconstructed annual
    precipitation
meanWTD = annWTD(1);

%% calculating which year for middle period will end/time period

%
% for 8000 simulation year: 0-2000;2000-5000;5000-8000

sizeWT = size(WT,1);
endOfYearMid = num_years-sizeWT;
endOfPeriodI = max(0,endOfYearMid-3000);

WTprob = zeros(1,12);

%% ~~~~~
%
% LOOP THROUGH YEARS OF SIMULATION
%
% ~~~~~
fire = 1;
x=1;
corrTime = 15000 - num_years;
for itime = 2:timestep:num_years
    corrTime = corrTime+1;
    time(itime) = (itime - 0.5) * timestep;

    if (mod(itime,500*timestep) == 0) % tracks/writes out clock time per 1000 y of
        simulation
            toc;

```

```

    tic;
    timex = (itime - 0.5) * timestep
end

if (itime < 2.5)
    delpeat = annZ_total(itime-1);
else
    delpeat = annZ_total(itime-1) - annZ_total(itime-2);
end

% delpeat = annZ_total(itime-1) - last_Z_total;
% last_Z_total = annZ_total(itime-1);

%% CALCULATE ANNUAL MASS COHORT IN MONTHLY TIME STEPS

% net water increase = precipitation + runon - (evapotranspiration + runoff)

% MOVED TO PARAMS -> start_depth = 0.25; % peat depth [m] when
dynamic water balance starts

%===== Not simulating water balance =====%

flagWTsim = 0; % 0 not simulating the water table; 1: lowering the water table

%the data of mothly water table depth
%should be moved to hpm_param
%month_wtd_wfps5 = [0 0 0 0 0.1 0.3 0.4 0.6 0.9 1 0.4 0.2];

%{
month_wtd_wfps5 = [0 0 0 0 0 0.1 0.3 0.4 0.6 0.7 0.4 0.2];
month_wtd_wfps4 = [0 0 0 0 0 0 0.2 0.3 0.4 0.5 0.3 0];
month_wtd_wfps3 = [0 0 0 0 0 0 0.15 0.25 0.3 0.2 0.15 0];
month_wtd_wfps2 = [0 0 0 0 0 0 0.1 0.2 0.2 0 0 0];
month_wtd_wfps1 = [0 0 0 0 0 0 0 0 0 0 0 0];
%}
% don't use dynamic water table in HPMT
initflag = 1;
% for simulating the Water table; change the flagWTsim to 0 or 1
if (flagWTsim < 1)
    %annWTD(itime) = params.wtd_0;
    lagWTD(itime) = params.wtd_0;
else
    if (itime < 40000)

```

```

annWTD(itime) = params.wtd_0;
lagWTD(itime) = params.wtd_0;

else
    annWTD(itime) = 0.2;
    lagWTD(itime) = 0.2;
end
end
annWTD(itime) = 0;
annNPP(itime,:) = 0;
annRespLitter = 0;
annRespPeat = 0;
annROOTIN(itime) = 0;

prob = rand(1);
prob2 = rand(1);

% period2 = params.start_year+params.trans_length1; %ex p2 = 3000+1000
%period3 = period2+params.trans_length2; %ex p3 = 4000+1000
%period4 = period3+params.trans_length3; %p4 = 5000+1000
scenarioLU = params.scenario_LU;
for i=1:1:12 %monthly time step
    if(params.ID ==0) %id=0: coastal; id=1: inland
        monWTD = 0.75*params.monthly_WT(corrTime,i);
    else
        monWTD = params.monthly_WT(corrTime,i);
        % impact of the lowering sea level to WT after 6000 yearBP
        if(monWTD>0)
            a = 0.25;
            b = 2500;
            monWTD = monWTD + a * max(0,(itime-6000)/b);
        end
    end
    zstar = params.wfps_c1 * onevec + (params.wfps_c2 -
    params.wfps_c1)*((dens - params.min_bulk_dens)...
    ./((dens - params.min_bulk_dens + params.wfps_c3)));
    zwtd = depth - monWTD; % determines distance each cohort is from WT
    (value is positive if cohort is below WT, i.e., submerged)
    zwtd = max(zerovec, -zwtd); % determines distance above WT, set to zero
    if at or below WT
    monthWFPS = params.wfps_c1 + (1 - params.wfps_c1) * exp(-zwtd./zstar);
    % see notes and file 'anoxia & bulk dens & WFPS % profile.xls')
    %% calculating litter properties

```

```

if(scenarioLU==1)
  if(itime<=num_years-100)
    ag_frac_npp = params.ag_frac_npp_trees;
    bg_frac_npp = params.bg_frac_npp_trees;
    monthNPP = hpm_nppT1_2(params,monWTD,0);
  else
    ag_frac_npp = params.ag_frac_npp_OP;
    bg_frac_npp = params.bg_frac_npp_OP;
    monthNPP = hpm_nppT1_2(params,monWTD,1);
  end
else
  ag_frac_npp = params.ag_frac_npp_trees;
  bg_frac_npp = params.bg_frac_npp_trees;
  monthNPP = hpm_nppT1_2(params,monWTD,0);
end

%monthNPP = hpm_nppT1_2(monWTD,1, thick, params); %calculating
monthly NPP
litter_in = monthNPP.*ag_frac_npp;
litter_m = litter_m + litter_in;
litter_m0 = litter_m0 + litter_in;
litter_mstar = litter_m./(eps + litter_m0);
k_litter = params.k_0 .* litter_mstar;
decompLitter = litter_m.*k_litter;
litter_m = litter_m-decompLitter;
annRespLitter = annRespLitter + sum(decompLitter);

%% calculating peat properties
rootin = hpm_rootinT1_2(depth, thick, params,bg_frac_npp, monthNPP,
monWTD, annZ_total(itime-1), onevec); % root input
%calculating decomposition factor
if(scenarioLU ==1)
  if(itime<=num_years-100)
    decompfact = hpm_decompT1(depth, monWTD, monthWFPS, params,
onevec, epsvec);
  else
    decompfact = hpm_decompT1_2_LC(depth, monWTD, monthWFPS,
params, onevec, epsvec);
  end
else
  decompfact = hpm_decompT1(depth, monWTD, monthWFPS, params,
onevec, epsvec);
end

```

```

% sensitivity test

k = ((decompfact .* annTEMP_FACT) * params.k_0) .* m_star; %calculate
turnover rate based on decomp factor
decompPeat = m.*k;
m = m + rootin - decompPeat; %cohort mass remaining after decomposition
process and root addition
m_0 = m_0 + rootin; %total mass
annRespPeat = annRespPeat + sum(sum(decompPeat,2));

annWTD(itime) = annWTD(itime) + monWTD/12;
% annWFPS(itime) = annWFPS(itime) + monthWFPS(itime)/12;
if(itime > num_years - 20)
    annWFPS(:,num_years-itime+1) = annWFPS(:,num_years-itime+1) +
    monthWFPS/12;
end
annNPP(itime,:) = annNPP(itime,:) + monthNPP; %annual NPP for each
PFT
annROOTIN(itime) = annROOTIN(itime) + sum(sum(rootin,2));

end
annRESP(itime) = 0.5*(annRespLitter + annRespPeat); %0,5 is a factor for
converting biomass to C
tot_npp(itime) = sum(annNPP(itime,:)); %total annual NPP for all PFT
annAGMASSIN(itime) = sum(annNPP(itime,:) .* ag_frac_npp);
meanWTD = meanWTD + annWTD(itime)/num_years;

del_C_del_t(itime) = (annAGMASSIN(itime)+annROOTIN(itime))/2-
annRESP(itime); %in C unit

mstemp = [topvec; m]; % add zeros to top row
ms0temp = [topvec; m_0];
ms0agetemp = [topvec; m_0_age];
mstartemp = [topvec; m_star];
agebiastemp = [topval; age_bias];

mstemp(end,:) = []; % remove final row (of zeros) to maintain array size
ms0temp(end,:) = [];
ms0agetemp(end,:) = [];
mstartemp(end,:) = [];
agebiastemp(end) = [];

```

```

agebiastemparr = repmat(agebiastemp,1,nveg);

%adding litter to the top of peat profile
mstemp(1,:) = litter_m;
ms0temp(1,:) = litter_m0;
m = mstemp;
m_0 = ms0temp;
%remove the litter
litter_m = 0;
litter_m0 = 0;

%arranging the roots component
rootin2 = [topvec; rootin];
rootin2(end,:) = [];
rootin = rootin2;

%Land cover change with fire
%run only once for the first time in forest conversion
%assume tha peat with depth 0.2m from surface would be burnt
m_star = m./(epsarr + m_0);

if(itime == 25*x+num_years-100)
    fire = 1;
    x=x+1;
end
if(scenarioLU==1 & fire==1)
    if(itime<=num_years-100)
        M = sum(m,2);
    else
        depth = max(0,depth-0.2);
        %thick = [0; diff(depth)];
        loc = find(depth>0,1);
        m(1:loc,:)=0;
        M = sum(m,2);
        fire = 0;
        %M_star = M/(epsvec + M_0);
    end
else
    M = sum(m,2);
end
% calculate new peat depth n thickness

```



```

M_tot = sum(M);
del_M_tot(itime) = M_tot - prev_M_tot;
prev_M_tot = M_tot;

M_0 = sum(m_0,2);
M_star = M./(epsvec + M_0);
M_overlying = cumsum(M) - M;

dens = hpm_densT1(M_star, M_overlying, params, onevec);

porosity = onevec - dens/params.OM_dens;

prev_thick = thick;
thick = M ./ (epsvec+dens);
zbottom = cumsum(thick);
depth = cumsum(thick) - thick/2;

total_porosity = sum(thick .* porosity);

annZ_total(itime) = depth(itime)+thick(itime)/2;
%annZ_total(itime) = depth(itime);
del_peat_height(itime) = annZ_total(itime) - annZ_total(itime -1);
annM_total(itime) = sum(M);

% annWFPS = 0.8 * onevec; %equation from hpmT1(HPM10)
WATER(itime,:) = [0 annPPT(itime) 0 0 0 annWTD(itime) delpeat*100];
junk1(itime,:) = [0 0 0];

for j = 1:1:10

    if (itime >= j*1000 + 10)

        MM(itime,j) = sum(M((itime-j*1000 - 9):(itime - j*1000)));
        distToBottom = cumsum(thick((itime - j*1000 - 5):end));
        MD(itime,j) = distToBottom(end);

    end
end

%% ***** root fraction *****
% calculate root fraction of peat in 'nbins' vertical bins over 'maxheight' meters
% from base
% (can be greater than total peat height; missing value is

```

```

% -0.9999) (S. Frolking)

woodfrac = (m(:,3)) ./ (M + eps);
cohortheight = flipud(cumsum(flipud(thick)));

x1 = 0.;
for ix = 1:1:nbins

    if (x1 > max(cohortheight))
        break;
    end
    x2 = ix * delx;
    tf_bin = (cohortheight > x1) & (cohortheight <= x2);
    tf_bin_sum = sum(tf_bin);
    if(tf_bin_sum>0)
        bin_moss_frac(ix,itime) = sum(woodfrac .* M .* tf_bin) / (sum(M .* tf_bin)
+ eps);
    end

    x1 = x2;
end
end % loop through years

%~~~~~
%
% CALCULATE SOME FINAL METRICS AND WRITE OUT & PLOT RESULTS
%
%~~~~~

age = time;
M_TOTAL = sum(M);
M_TOTAL2 = sum(del_C_del_t); %in C unit
Z_TOTAL = depth(end);

k_mean = sum(m .* k,2) ./ (M + epsvec);

% reconstWTD(:,1) = (m(:,5) * params.WTD_opt(5) + m(:,6) *
params.WTD_opt(6) + m(:,7) * params.WTD_opt(7)...
% + m(:,8) * params.WTD_opt(8) + m(:,9) * params.WTD_opt(9))...
% ./ (m(:,5) + m(:,6) + m(:,7) + m(:,8) + m(:,9) + eps);

WTprob = WTprob./sum(WTprob,2);
log10junk = 2.14287*onevec - 0.042857 * dens;

```

```

hydrconjunk = exp(log(10) * log10junk);
junk3 = thick .* hydrconjunk;
denom = sum(junk3);

%{
for ijunk = 1:1:itime
%   hyd_trans_profile(ijunk) = 0.5 * (1 + sum(junk3(ijunk:end))) / denom); %
    hydraulic transmissivity profile
    hyd_trans_profile(ijunk) = params.Roff_c3 + (1-params.Roff_c3) *
    sum(junk3(ijunk:end)) / denom; % hydraulic transmissivity profile
end
%}
wfps_c1a = 0.03;
wfps_c2a = 0.5;
wfps_c3a = 20;
zstar = wfps_c1 * onevec +(wfps_c2a - wfps_c1a)*((dens -
    params.min_bulk_dens)./(dens - (params.min_bulk_dens - wfps_c3a)));
sp_yld_profile = onevec - zstar + zstar .* ((onevec - zstar) / 0.01) .* exp(-
    max(0.5,depth)./zstar) .* (onevec - exp(0.01*(onevec./zstar)));
sp_yld_profile = max(zerovec,sp_yld_profile); % specific yield profile

M_array = M * ones(1,num_veg);
eps_array = eps * ones(1,num_veg);
mfrac = m ./ (M_array+epsarr);
remain_mass_tot = sum(m);
npp_tot = sum(annNPP);

% annNPPmoss(:,1) = annNPP(:,5) + annNPP(:,6) + annNPP(:,7) + annNPP(:,8)
    + annNPP(:,9);
% annNPPvasc = sum(annNPP,2) - annNPPmoss;

%% smooting variables
window = 100;
mask = ones(1,window)/window;
annWTD_smooth = conv(annWTD,mask,'same');

%% ~~~~~
% WRITE SUMMARY RESULTS TO SCREEN
% ~~~~~

disp(sprintf('total age (y): %d    total mass (MgC/ha): %d    total depth (m):
    %d',num_years, M_TOTAL*10/2, Z_TOTAL));
disp(sprintf('total dC/dt (Mg C/ha): %d ',M_TOTAL2*10));

```

```

disp(sprintf(' mass remaining leaves: %2.2f \n mass remaining woods: %2.2f \n
mass remaining roots: %2.2f \n mass remaining AG_OP: %2.2f \n mass
remainingBG OP: %2.2f',remain_mass_tot*10/2));
disp(sprintf('NPPleaves: %10.2f \n NPPwoods: %10.2f \n NPProots: %10.2f \n
NPPAG_OP: %10.2f \n NPPBG_OP: %10.2f',npp_tot));
disp(sprintf('average of mean water table: %10.4f', meanWTD));
%number of WT from different set scenario
disp(sprintf(' #WT: %f', WTprob));
%~~~~~
~~~~~
% WRITE OUT OUTPUT FILES: core profile, carbon time series, water time
series, params, workspace
%~~~~~
~~~~~

% *****
% conservation of mass tests
% *****

% j3 = annAGMASSIN + annROOTIN - annRESP*2 - del_M_tot;
% j4 = tot_npp - annAGMASSIN - annROOTIN + j5;
% results_5 = [time del_peatwater net_water_in (del_peatwater-net_water_in) j4
tot_npp annAGMASSIN annROOTIN annRESP*2 del_M_tot j3];

% fname5 = [params.outname, '_o_conservation_test.txt'];
% fid5 = fopen(fname5,'w');

% fprintf(fid5,'HPM6 output - conservation tests - units: water - m depth;
NPP/mass - kg/m2/y \n');
% fprintf(fid5,' sim_yr del_peatwater net_water_in del-net_water tot-AG-BG
tot_NPP AG_NPP BG_NPP tot_RESP del_peat net_of_last_4 \n');
% fprintf(fid5,'%7.1f %10.6f %10.6f %11.7f %9.5f %9.5f %9.5f %9.5f %9.5f
%9.5f %9.5f \n', results_5');
% status = fclose(fid5);

% *****
% final core profile
% *****

EndOfSim = [num_years M_TOTAL*10/2, Z_TOTAL meanWTD
remain_mass_tot*10/2 npp_tot];
fname_end = [params.outname, '_EoS.txt'];
file_EoS = fopen(fname_end,'w');
fprintf(file_EoS,'result at the end of simulation\n')

```

```

fprintf(file_EoS,'numOfYear M_total PD WTD m_leaf m_wood m_roots npp_L
npp_W npp_R\n');
fprintf(file_EoS,'%7.0f %8.4f %8.4f %8.4f %10.7f %8.3f %10.7f %10.7f
%10.7f %10.7f %10.7f %10.7f %10.7f %10.7f \n',EndOfSim);
fclose(file_EoS);

results_1 = [time depth M M_0 k_mean dens m mfrac];
fname1 = [params.outname, '_core.txt'];
fid1 = fopen(fname1,'w'); % profile (core) of final state
fprintf(fid1,'HPM9 output - core of final state - units: depth & thickness: m, mass:
kg/m2 or kg/m3, time: y; decomp: 1/y; WFPS: m3/m3 \n');
fprintf(fid1,' cohort_age coh_depth coh_mass coh_m0 coh_k_mean
coh_bulk_dens m_leaves m_woods m_roots m_AG_OP m_BG_OP
m_frac_leaves m_frac_woods m_frac_roots m_frac_AG_OP
m_frac_BG_OP \n');
fprintf(fid1,'%7.1f %8.4f %8.4f %8.4f %10.7f %8.3f %10.7f %10.7f %10.7f
%10.7f %10.7f %10.7f %10.7f %10.7f %10.7f %10.7f \n', results_1);
status = fclose(fid1);

% results_6 = [time depth M m mfrac];

% fname6 = [params.outname, '_o_core_by_PFT.txt'];
% fid6 = fopen(fname6,'w'); % profile (core) of final state by PFT

% fprintf(fid6,'HPM6 output - core by PFT of final state - units: depth & thickness:
m, mass: kg/m2 or kg/m3, time: y; decomp: 1/y; WFPS: m3/m3 \n');
% fprintf(fid6,' cohort_age_(y) cohort_depth_(m) cohort_mass_(kg/m2) m_grass
m_minhrb m_minsdg m_decshb m_brnmoss m_holsphag m_lawnsphag
m_humsphag m_feath m_ombhrb m_ombsdg m_ombshb mfrac_grass
mfrac_minhrb mfrac_minsdg mfrac_decshb mfrac_brnmoss mfrac_holsphag
mfrac_lawnsphag mfrac_humsphag mfrac_feath mfrac_ombhrb
mfrac_ombsdg mfrac_ombshb \n');
% fprintf(fid6,'%7.1f %8.4f %8.4f %10.7f %10.7f %10.7f %10.7f %10.7f
%10.7f %10.7f %10.7f %10.7f %10.7f %10.7f %10.7f %10.7f %10.7f
%10.7f %10.7f %10.7f %10.7f %10.7f %10.7f %10.7f %10.7f %10.7f
%10.7f \n', results_6);
% status = fclose(fid6);

% *****
% carbon time series
% *****

results_2 = [time annNPP annROOTIN WATER(:,7)];

```

```

fname2 = [params.outname, '_carbon.txt'];
fid2 = fopen(fname2,'w'); % time series of carbon dynamics

fprintf(fid2,'HPM8 output - time series of carbon dynamics - units:
depth/thickness: m; NPP: kg/m2/y; time: y \n');
fprintf(fid2,' time npp_leaves npp_woods npp_roots npp_AG_OP npp_BG_OP
root_input delPeatHt_(cm) \n');
fprintf(fid2,'%7.1f %9.5f %9.5f %9.5f %9.5f %9.5f %9.5f %9.5f \n', results_2');
status = fclose(fid2);

result_5 = [time annRESP del_C_del_t depth annZ_total annM_total annWTD
thick];
fname_5 = [params.outname, '_depth.txt'];
fid5 = fopen(fname_5,'w');
fprintf(fid5, 'time resp delCdelT peat_depth peat_height peat_mass WTD
thickness\n');
fprintf(fid5,'%7.1f %9.5f %9.5f %9.5f %9.5f %9.5f %9.5f %9.5f \n',result_5');
fclose(fid5);

% *****
% water time series
% *****

results_3 = [time WATER(:,1:6) del_peat_height*100];

fname3 = [params.outname, '_water.txt'];
fid3 = fopen(fname3,'w'); % time series of water dynamics

fprintf(fid3,'HPM6 output - time series of water dynamics - units: depth/thickness:
m or m/y; time: y \n');
fprintf(fid3,' time AnnDelWat(cm) annPPT annET annRUNOFF annRUNON
annWTD AnnDelPtHt(cm) \n');
fprintf(fid3,'%7.1f %9.5f %9.5f %9.5f %9.5f %9.5f %9.5f %9.5f \n', results_3');
status = fclose(fid3);

% fname6 = [params.outname, '_MM.txt']
% fid6 = fopen(fname6,'w');
% fprintf(fid6,'mass of the surface cohort \n')
% fprintf(fid6,'%9.5f %9.5f %9.5f %9.5f %9.5f %9.5f %9.5f %9.5f %9.5f %9.5f
\n',MM');
% fclose(fid6);
%
% fname7 = [params.outname, '_MD.txt']
% fid7 = fopen(fname7,'w');

```

```

% fprintf(fid7,'mass of the surface cohort \n')
% fprintf(fid7,'%9.5f %9.5f %9.5f %9.5f %9.5f %9.5f %9.5f %9.5f %9.5f %9.5f
  \n',MD');
% fclose(fid7);
% *****
% run parameters
% *****

fname4 = [params.outname, '_params.txt'];
fid4 = fopen(fname4,'w'); % parameters

fprintf(fid4,'HPM8 output - parameters - units: depth/thickness: m, mass: kg/m2 or
  kg/m3, time: y; decomp: 1/y \n');
% fprintf(fid4,params);
fprintf(fid4,'output file name      %8s \n',params.outname);
fprintf(fid4,'simulation length [y]   %g \n',params.sim_len);
fprintf(fid4,'initialization WTD [m]   %6.3f \n',params.wtd_0);
%{
%fprintf(fid4,'ann_ppt [m/y]           %6.2f \n',params.ann_ppt);
%fprintf(fid4,'1-sine,3-ramp,5-ramps,9-MB %6.2f \n',params.ppt_flag);
%fprintf(fid4,'sine/ramp amp [m/y]     %6.2f \n',params.ppt_amp1);
%fprintf(fid4,'ppt noise amp [m/y]     %6.2f \n',params.ppt_amp2);
%fprintf(fid4,'ppt_noise_persist       %6.3f \n',params.ppt_rand_persist);

fprintf(fid4,'initialization PD [m]    %6.3f \n',params.start_depth);
fprintf(fid4,'ET_0 [m/y]                %6.2f \n',params.ET_0);
fprintf(fid4,'Roff_c1                  %6.2f \n',params.Roff_c1);
fprintf(fid4,'Roff_c2                  %6.2f \n',params.Roff_c2);
fprintf(fid4,'Roff_c2a                  %6.2f \n',params.Roff_c2a);
fprintf(fid4,'Roff_c3                  %6.2f \n',params.Roff_c3);
fprintf(fid4,'Roff_c4                  %6.2f \n',params.Roff_c4);
fprintf(fid4,'runon_c1                  %6.2f \n',params.runon_c1);
fprintf(fid4,'runon_c2                  %6.2f \n',params.runon_c2);
fprintf(fid4,'runon_c3                  %6.2f \n',params.runon_c3);

fprintf(fid4,'ET_wtd_1                %6.2f \n',params.ET_wtd_1);
fprintf(fid4,'ET_wtd_2                %6.2f \n',params.ET_wtd_2);
fprintf(fid4,'ET_wtd_3                %6.2f \n',params.ET_wtd_3);
fprintf(fid4,'ET_param                  %6.2f \n',params.ET_param);
fprintf(fid4,'lag years for vascular WTD %6.2f \n',params.lag_years);

fprintf(fid4,'WTD_opt                  %6.2f %6.2f %6.2f %6.2f %6.2f %6.2f %6.2f %6.2f
  %6.2f %6.2f %6.2f %6.2f %6.2f \n', params.WTD_opt');

```

```

fprintf(fid4,'WTD_range_shallow %6.2f %6.2f %6.2f %6.2f %6.2f %6.2f %6.2f
%6.2f %6.2f %6.2f %6.2f %6.2f %6.2f \n', params.WTD_range(1,:));
fprintf(fid4,'WTD_range deep %6.2f %6.2f %6.2f %6.2f %6.2f %6.2f %6.2f
%6.2f %6.2f %6.2f %6.2f %6.2f %6.2f \n', params.WTD_range(2,:));
fprintf(fid4,'PD_opt %6.2f %6.2f %6.2f %6.2f %6.2f %6.2f %6.2f %6.2f
%6.2f %6.2f %6.2f %6.2f %6.2f \n', params.PD_opt);
fprintf(fid4,'PD_opt shallow %6.2f %6.2f %6.2f %6.2f %6.2f %6.2f %6.2f %6.2f
%6.2f %6.2f %6.2f %6.2f %6.2f \n', params.PD_range(1,:));
fprintf(fid4,'PD_opt deep %6.2f %6.2f %6.2f %6.2f %6.2f %6.2f %6.2f %6.2f
%6.2f %6.2f %6.2f %6.2f %6.2f \n', params.PD_range(2,:));
%}
fprintf(fid4,'rootin_c3 %6.2f \n',params.rootin_c3);
fprintf(fid4,'rootin_c4 %6.2f \n',params.rootin_c4);
fprintf(fid4,'rootin_c5 %6.2f \n',params.rootin_c5);
fprintf(fid4,'rootin_alpha %6.2f \n',params.rootin_alpha);
fprintf(fid4,'d80 %6.2f \n',params.rootin_d80);
fprintf(fid4,'wfps_c1 %6.2f \n',params.wfps_c1);
fprintf(fid4,'wfps_c2 %6.2f \n',params.wfps_c2);
fprintf(fid4,'wfps_c3 %6.2f \n',params.wfps_c3);
fprintf(fid4,'wfps_opt %6.2f \n',params.wfps_opt);
fprintf(fid4,'wfps_sat_rate %6.2f \n',params.wfps_sat_rate);
fprintf(fid4,'wfps_min_rate %8.4f \n',params.wfps_min_rate);
fprintf(fid4,'wfps_curve %6.2f \n',params.wfps_curve);
fprintf(fid4,'dens_c1 %6.2f \n',params.dens_c1);
fprintf(fid4,'dens_c2 %6.2f \n',params.dens_c2);
fprintf(fid4,'min_bulk_dens [kg/m3] %6.2f \n',params.min_bulk_dens);
fprintf(fid4,'del_bulk_dens [kg/m3] %6.2f \n',params.del_bulk_dens);
fprintf(fid4,'OM_bulk_dens [kg/m3] %6.2f \n',params.OM_dens);
fprintf(fid4,'anoxic_scale_length [m] %6.2f \n \n',params.anoxia_scale_length);
fprintf(fid4,'num_veg %6.2f \n',params.num_veg);
fprintf(fid4,'max_total_NPP[kg/m2/y] %6.2f \n',sum(NPP_rel));
fprintf(fid4,' grs minh mins mnshr wtms hols lawn hums
fthr ombs ombh ombshr trees\n');
fprintf(fid4,'NPP_relative %6.2f %6.2f %6.2f %6.2f %6.2f %6.2f %6.2f %6.2f
%6.2f %6.2f %6.2f %6.2f %6.2f \n', params.NPP);
fprintf(fid4,'ag_frac_npp %6.2f %6.2f %6.2f %6.2f %6.2f %6.2f %6.2f %6.2f
%6.2f %6.2f %6.2f %6.2f %6.2f \n', params.ag_frac_npp_trees');
fprintf(fid4,'bg_frac_npp %6.2f %6.2f %6.2f %6.2f %6.2f %6.2f %6.2f %6.2f
%6.2f %6.2f %6.2f %6.2f %6.2f \n', params.bg_frac_npp_trees');
fprintf(fid4,'ag_frac_npp_OP %6.2f %6.2f %6.2f %6.2f %6.2f %6.2f %6.2f %6.2f
%6.2f %6.2f %6.2f %6.2f %6.2f \n', params.ag_frac_npp_OP');
fprintf(fid4,'bg_frac_npp_OP %6.2f %6.2f %6.2f %6.2f %6.2f %6.2f %6.2f %6.2f
%6.2f %6.2f %6.2f %6.2f %6.2f \n', params.bg_frac_npp_OP');

```



```

fprintf(fid4,'decomp k_0      %6.2f %6.2f %6.2f %6.2f %6.2f %6.2f %6.2f %6.2f %6.2f
      %6.2f %6.2f %6.2f %6.2f %6.2f %6.2f \n', params.k_0);
fprintf(fid4,\n total age (y): %d  total mass (kg C/m2): %d  total depth (m):
      %d',num_years, M_TOTAL/2, Z_TOTAL);
%fprintf(fid4,\n total dC/dt (kg C/m2): %d ',M_TOTAL2);

status = fclose(fid4);

% *****
% run workspace variable arrays as '.mat' file
% *****

workspace_filename = [params.outname, '_ws'];
save(workspace_filename);

%% ~~~~~
% PLOT FIGURES AND SAVE SOME TO FILES
% ~~~~~

% *****
% FIGURE 1 - 4 (was 5) panel final profiles
% *****

% plot or not

plot_flag = 1;

if (plot_flag > 0)

figure(1)
% SF: removed plot of WTD and reconstructed water table depth (Aug. 2011)
% subplot(1,5,1)
% semilogx(k_mean,depth,thick,depth,'LineWidth',3)
% plot(flipud(annWTD),depth,reconstWTD,depth,'lineWidth',3)
% set(gca,'YDir','reverse')
% hold on
% plot(zerovec,depth,'k','LineWidth',1)
% hold off
% set(gca,'YDir','reverse')
% legend('\fontsize{14}WTD','\fontsize{14}reconstr.','Location','SouthEast')
% ylabel('\fontsize{14}depth [m]')
% xlabel('\fontsize{14}WTD (positive down) [m]')
%plot(m_fast, depth)
%set(gca,'YDir','reverse')

```

```

    %ylabel('depth [m]')
    %title('cohort fast-decomp mass');
    % h1a=gca;
    % set(h1a,'FontSize',14)

subplot(1,4,1)
plot(m, depth,'LineWidth',2)
set(gca,'YDir','reverse')
%ylabel('\fontsize{14}depth [m]')
xlabel('\fontsize{14}cohort mass [kg/m2]')
%title('\fontsize{14}cohort mass');
h1b=gca;
set(h1b,'FontSize',14)

subplot(1,4,2)
plot(m_star, depth,M_star,depth,'LineWidth',2)
set(gca,'YDir','reverse')
% ylabel('depth [m]')
title('\fontsize{14}cohort m-star values');
%      grs  minh  wtms  mins  dshr  hols  lawn  hums  fthr  ombs  ombh  evrs
%      trees
legend('\fontsize{10}leaves', '\fontsize{10}woods', '\fontsize{10}roots',...
       '\fontsize{10}AG_OP', '\fontsize{10}BG_OP', '\fontsize{10}total', 'Location', 'Sout
       hEast')
h1c=gca;
set(h1c,'FontSize',14)

subplot(1,4,3)
plot(dens, depth,'LineWidth',3)
set(gca,'YDir','reverse')
% ylabel('depth [m]')
xlabel('\fontsize{14}bulk dens [kg/m3]');
%title('\fontsize{14}cohort m-star values');
h1d=gca;
set(h1d,'FontSize',14)

subplot(1,4,4)
plot(sp_yld_profile,depth, age/num_years,depth,'LineWidth',3)
set(gca,'YDir','reverse')
title('\fontsize{14}final profile');
%xlabel('\fontsize{14}rel. trans. ');
legend('\fontsize{14}sp.yield', '\fontsize{14}age', 'Location', 'South')
h1e=gca;

```

```

set(h1e,'FontSize',14)

end

%% *****
% FIGURE 2 - 3 panel summary time series
% SF: turned off, added WTD to plot 6, panle 2
% *****

% plot or not

plot_flag = 1;

if (plot_flag > 0)

figure(2)
subplot(3,1,1)
plot(time,annZ_total,age,-depth,'LineWidth',1)
%xlim([dynamic_watbal_time_start+10 num_years+500]);
hold on
plot(time,zerovec,'k','LineWidth',1)
hold off
legend('\fontsize{14}time-height','\fontsize{14}age-depth','Location','East')
ylabel('\fontsize{14}height or depth [m]')
xlabel('\fontsize{14}cohort or preatland age [y]')
% title('\fontsize{14}age-depthprofile #1');
h2a=gca;
set(h2a,'FontSize',14)

subplot(3,1,2)
plot(time,annM_total,'LineWidth',1)
%xlim([dynamic_watbal_time_start+10 num_years+500]);
legend('\fontsize{14}time-mass','Location','East')
ylabel('\fontsize{14}total peat mass [kg/m2]')
xlabel('\fontsize{14}preatland age [y]')
% title('\fontsize{14}age-depthprofile #1');
h2b=gca;
set(h2b,'FontSize',14)

subplot(3,1,3)
plot(time,annPPT,time,-annWTD,'LineWidth',1)
%xlim([dynamic_watbal_time_start+10 num_years+500]);
hold on
plot(time,zerovec,'k','LineWidth',1)

```

```

hold off
% set(gca,'YDir','reverse')
legend('\fontsize{14}ann precip', '\fontsize{14}WTD', 'Location', 'East')
ylabel('\fontsize{14}ann ppt or WTD [m]')
xlabel('\fontsize{14}peatland age [y]')
h2c=gca;
set(h2c,'FontSize',14)
% title('\fontsize{14}age-depth profile #2');

end

%% *****
% FIGURE 3 - 2 panel annual water flows
% *****

% plot or not

plot_flag = 0;

if (plot_flag > 0)

figure(3)
subplot(2,1,1)
plot(annWTD,'LineWidth',3)
%xlim([dynamic_watbal_time_start+10 num_years+500]);
hold on
plot(time,zerovec,'k','LineWidth',1)
hold off
set(gca,'YDir','reverse')
xlabel('\fontsize{14}time [y]')
ylabel('\fontsize{14}WTD [m]')
h3a=gca;
set(h3a,'FontSize',14)

subplot(2,1,2)
plot(WATER,'LineWidth',3)
xlim([dynamic_watbal_time_start+10 num_years+500]);
legend('\fontsize{14}dH2O_{cm}', '\fontsize{14}ppt', '\fontsize{14}ET', '\fontsize{14}
R_{off}', '\fontsize{14}R_{on}', '\fontsize{14}WT', '\fontsize{14}dH_{cm}')
legend('orientation','Horizontal','Location','North')
xlabel('\fontsize{14}time [y]')
ylabel('\fontsize{14}depth [m]')
h3b=gca;
set(h3b,'FontSize',14)

```

```

end

%% *****
% FIGURE 4 - 2 panel annual C flows
% *****

% plot or not

plot_flag = 1;

if (plot_flag > 0)

figure(4)
%subplot(2,1,1)
plot(time, tot_npp/2, time, annRESP, time, del_C_del_t,'LineWidth',3)
%xlim([dynamic_watbal_time_start+10 num_years+500]);
hold on
plot(time,zerovec,'k','LineWidth',1)
hold off
legend('\fontsize{14}total NPP', '\fontsize{14}ann resp', '\fontsize{14}ann dC/dt')
legend('orientation','Horizontal','Location','South')
xlabel('\fontsize{14}time [y]')
ylabel('\fontsize{14}kgC/m2/y')
h4a=gca;
set(h4a,'FontSize',14)

end

%% *****
% FIGURE 5 - 3 panel final core profile by PFT
% *****

% plot or not

plot_flag = 1;

if (plot_flag > 0)

figure(5)
subplot(1,3,1)
plot(M,time,'LineWidth',3)
set(gca,'YDir','reverse')
ylim([50 num_years+50]);

```

```

ylabel('\fontsize{20}cohort age [y]')
xlabel('\fontsize{20}cohort total mass [kg/m2]')
xlim([0 0.5])
h5a=gca;
set(h5a,'FontSize',20)

subplot(1,3,2)
area(m)
view(90, 90)
legend('\fontsize{14}leaves', '\fontsize{14}woods', '\fontsize{14}roots',...
'Location', 'SouthEast')
%xlabel('\fontsize{14}cohort age [y]')
ylabel('\fontsize{20}cohort mass [kg/m2]')
ylim([0 0.25])
xlim([50 num_years+50]);
h5a=gca;
set(h5a,'FontSize',20)

h5c = gcf;
fig5name = [params.outname, '_pft_profile'];
saveas(h5c, fig5name, 'jpg');

end

%% *****
% FIGURE 6 - 2 panel C time series
% *****

% plot or not

plot_flag = 1;

if (plot_flag > 0)

figure(6)
subplot(2,1,1)
plot(time,annZ_total, time, annM_total/100, age,-depth,'LineWidth',3)
xlim([dynamic_watbal_time_start+10 num_years+500]);
hold on
plot(time,zerovec,'k','LineWidth',1)
hold off
legend('\fontsize{10}time-height', '\fontsize{10}time-mass/100', '\fontsize{10}age-
depth', 'Location', 'East')
ylabel('\fontsize{14}[kg/m2] or [m]')

```

```

xlabel('\fontsize{14}cohort or peatland age [y]')
% title('\fontsize{14}age-depthprofile #1');
h6a=gca;
set(h6a,'FontSize',14)

subplot(2,1,2)
plot(time,tot_npp/2, time,annRESP, time,-annWTD,'LineWidth',1)
% xlim([dynamic_watbal_time_start+10 num_years+500]);
hold on
plot(time,zerovec,'k','LineWidth',1)
hold off
legend('\fontsize{9}tot NPP','\fontsize{9}tot resp','\fontsize{9}WTD')
legend('orientation','Horizontal','Location','North')
xlabel('\fontsize{14}time [y]')
ylabel('\fontsize{14}[kg C/m2/y]')
h6b=gca;
set(h6b,'FontSize',14)

h6c = gcf;
fig6name = [params.outname, '_H_M_NPP_R'];
saveas(h6c, fig6name,'jpg');

end

%% *****
% FIGURE 7 - 2 panel annual water
% *****

% plot or not

plot_flag = 0;

if (plot_flag > 0)

figure(7)
subplot(2,1,1)
plot(WATER(:,2:5),'LineWidth',3)
xlim([dynamic_watbal_time_start+10 num_years+500]);
legend('\fontsize{10}ppt','\fontsize{10}ET','\fontsize{10}R_{off}','\fontsize{10}R_{on}
}')
legend('orientation','Horizontal','Location','North')
xlabel('\fontsize{14}time [y]')
ylabel('\fontsize{14}[m/y]')
h7b=gca;

```

```

set(h7b,'FontSize',14)

subplot(2,1,2)
plot(annWTD,'LineWidth',3)
xlim([dynamic_watbal_time_start+10 num_years+500]);
hold on
plot(time,zerovec,'k','LineWidth',1)
hold off
set(gca,'YDir','reverse')
xlabel('\fontsize{14}time [y]')
ylabel('\fontsize{14}WTD [m]')
h7a=gca;
set(h7a,'FontSize',14)

h7c =(gcf);
fig7name = [params.outname, '_water'];
saveas(h7c, fig7name,'jpg');

end

%% *****
%% FIGURE 8 - 1 (was 2) panel core profiles
%% *****

% plot or not

plot_flag = 1;

if (plot_flag > 0)

    figure(8)
    % SF: removed plot of WTD and reconstructed water table depth (Aug. 2011)
    subplot(1,2,1)
    % semilogx(k_mean,depth,thick,depth,'LineWidth',3)
    plot(annWFPS,depth,'lineWidth',3)
    xlim([0 1.25])
    set(gca,'YDir','reverse')
    % hold on
    % plot(zerovec,depth,'k','LineWidth',1)
    % hold off
    % set(gca,'YDir','reverse')
    % legend('\fontsize{10}WTD','\fontsize{10}reconstr.','Location','SouthEast')
    ylabel('\fontsize{14}depth [m]')
    xlabel('\fontsize{14}WFPS')

```



```

%plot(m_fast, depth)
%set(gca,'YDir','reverse')
%ylabel('depth [m]')
title('Water filled pore space');
h8a=gca;
set(h8a,'FontSize',14)

subplot(1,2,2)
plot(dens/100,depth,      sp_yld_profile,depth,      age/num_years,depth,
      'LineWidth',3)
set(gca,'YDir','reverse')
title('\fontsize{14}final profile');
%xlabel('\fontsize{14}rel. trans. ');

      legend('\fontsize{10}bulkdens/100','\fontsize{10}sp.yield','\fontsize{10}age','L
      ocation','South')
h8b=gca;
set(h8b,'FontSize',14)

h8c = gcf;
fig8name = [params.outname, '_final_profile'];
saveas(h8c, fig8name,'jpg');

end
%% figure 9
% plotting the smoothing of WTD
figure(9)
plot(time,-annWTD_smooth,'LineWidth',1)
%xlim([dynamic_watbal_time_start+10 num_years+500]);
%hold on
%plot(time,zerovec,'k','LineWidth',1)
%hold off
% set(gca,'YDir','reverse')
legend('\fontsize{14}WTD')
ylabel('\fontsize{14}WTD [m]')
xlabel('\fontsize{14}peatland age [y]')
h2c=gca;
set(h2c,'FontSize',14)

%% figure 10: Depth vs Age

figure (10);

```

```

plot (age, depth);

hold on;
plot (params.age_coastal, params.depth_coastal,'k');
plot(params.age_inland1,params.depth_inland1,'r')
hold off;
legend ('simulated','Domain coastal','Domain_inland');
set(gca,'YDir','reverse')
xlabel('peat age')
ylabel('peat depth')

%% ***** root fraction *****
% (S. Frolking)
% *****
% FIGURE 11 - root fraction
% *****

% plot or not

plot_flag = 1;

if (plot_flag > 0)

    [XXX,YYY] = meshgrid(1:1:itime, 1:1:nbins);
    xxx = [1:1:itime];
    yyy = [0,delx,(maxheight-delx)];
    clim = [-0.1 1];

    %tf_sp = bin_moss_frac == -0.9999;
    %bin_moss_frac
    bin_moss_frac.*(bin_moss_frac>=0)+bin_moss_frac.*(bin_moss_frac<0).*N
    aN;

    figure(11)
    % contourf(XXX, YYY, bin_moss_frac,100,'LineStyle','none')
    % xlim([0 itime])
    %imagesc(xxx,flipr(yyy),bin_moss_frac,clim);
    h=imagesc(xxx,yyy,bin_moss_frac,clim);
    colormap([1,1,1];jet);

    %set(h,'alphadata',~isnan(bin_moss_frac))

    hold on;

```

```

plot(xxx,(annZ_total-annWTD_smooth),'linewidth',1.5,'Color',[0 0 0]);

set(gca,'ydir','normal');

title('\fontsize{30}Root fraction of peat');
colorbar('location','eastoutside');
% ylim([0 nbins])
% zlim([0 1])
% colorbar
% caxis([0 1])
xlabel('\fontsize{20}Simulation time [yr]')
ylabel('\fontsize{20}Peat height [m]')
zlabel('\fontsize{20}Root fraction of peat')
h24a=gca;
set(h24a,'FontSize',18)

h24c = gcf;
fig24name = [params.outname, '_rootfrac'];
saveas(h24c, fig24name,'jpg');
end
% *****

```

**Matlab code for inputting all parameters required by HPMTrop including estimating the long-term water table.**

```

% *****
% Output file base name
% *****

outname = 'inland_test';

ID = 1; %id coastal=0; id inland = 1
scenario_LU = 0; % 0: no land cover changes; 1: Land cover changes;

%% different peat types have different simulation year
% coastal peatland(1): 5000 year
% mid(2): 8000 year ==> default value
% inland peatland(3): 13000 year
if(ID==0)
    sim_len = 5000;
else

```

```

sim_len = 13000; % simulation length (annual)
end

%% *****
% VEGETATION NPP; DONT FORGET TO CHANGE THE NPP FOR TREES
AND NONTREES
% *****
% NOTE: in initial version plants don't grow, so litterfall = NPP

num_veg = 5;
%NPP for trees and Oil palm plantation
NPP = [0.0792 0.057 0.025 0.025 0.06]; %NPP leaf, wood, roots of trees,
litterfall, root of Oil palm
%NPP = [0.0792 0.057 0.025 0.0000001 0.00000001]
NPP_trees = NPP .* [1 1 1 0 0];
NPP_OP = NPP .* [0 0 0 1 1];

ag_frac_npp_trees = [1 1 0 0 0];
bg_frac_npp_trees = [0 0 1 0 0];

ag_frac_npp_OP = [0 0 0 1 0];
bg_frac_npp_OP = [0 0 0 0 1];

%% *****
% SITE WATER BALANCE. not be used in HPMTrop
% *****
wtd_0 = 0.05; % initialization period water table depth (m)

%% *****
% DECOMPOSITION (DONT FORGET TO CHANGE THE K VALUES FOR
TREES AND
% NONTREES
% *****

% initial decomposition (mass-loss) rates and anoxia factor
% (make anoxia factor more variable, as in new paper by Blodau?)
% Added values for trees leaves and wood based on ????? (J. Talbot)

%   grs minh mins dshr wtms hols lawn hums fthr ombh ombs evrs trees

%k_exp leaves woods roots non-trees
%k_exp = [0.10552 0.02243 0.0685 0.039]; %0.371 0.0644 0.0685 values from
Chimner&Ewel2005; values from some lit (see file) 0.10552 0.02243 0.0685
0.039

```

```

k_exp = [0.10552 0.02243 0.0685 0.09 0.09];

% k for trees only
%k_exp = k_exp .* [1 1 1 0]

%k for nontrees only
%k_exp = k_exp .* [0 0 0 1];

k_0 = k_exp .* (1 + 3 * k_exp); %see spreadsheet 'simple decomp models.xls';
adjusts k_0 for m/m0 model of decay

wfps_opt = 0.45; % must be <= 0.5; optimum WFPS for decomposition (see
spreadsheet 'simple decomp models.xls')
wfps_max_rate = 1.0; % decomp rate multiplier at WFPS = WFPS_opt.
wfps_sat = 1.0; % WFPS at saturation
wfps_min = 0.1; %minimum of WFPS
wfps_sat_rate = 0.3; % decomp rate multiplier at WFPS = 1.0 (i.e., at annual
mean WTD).
wfps_min_rate = 0.001; % decomp rate multiplier minimum, deep in catotelm.
wfps_curve = (wfps_sat - wfps_opt)^2 / (4 * (wfps_max_rate - wfps_sat_rate)); %
parabola with value of 0.1 at WFPS = 1.0
wfps_wtd = 0.12;

%% *****
% BOG or FEN??
% *****

bog_fen_id = 1; % fen-to-bog = 1, persistent fen = 2

if (bog_fen_id <1.5) % FEN-TO-BOG VALUES % Trees added (J. Talbot

    %coastal 0.18
    %inland 0.27
    if(ID==0)
        anoxia_scale_length = 0.18;
    else
        anoxia_scale_length = 0.27;
    end

    anoxia_scale_length_OP = 0.3;
    % anoxia_scale_length = 0.25; % exponential decline in decomp in catotelm
    from wfps_sat_rate to wfps_min_rate

```

```

%{
runon_c1 = 1.0; % total peat depth (m) where runon declines by ~50%
runon_c2 = 0.5; % controls rate of decline of runon (see 'HPM vegetation
productivity.xls')
runon_c3 = 0.; % magnitude of maximum runon (m/y)
%}
%}
end

```

```

%non trees only
rootin_c3 = 0.5; %base value for northern peatland 0.2; TROP: 0.5 for trees;0.1
for non-trees
%trees only
%rootin_c3 = 0.5;

```

```

rootin_d80 = 0.3;
rootin_alpha = -log(rootin_d80) / (1. - 0.8);
rootin_c4 = 2.0;
rootin_c5 = 0.04;

```

```

%% *****
% BULK DENSITY
% *****

```

```

min_bulk_dens = 90.; % base value 50; kg/m3
del_bulk_dens = 40.; % base value 60; bulk density increase down profile,
kg/m3
dens_c1 = 0.2; % base value 0.2;m_star value at which bulk density rises
halfway from min to max
dens_c2 = 0.1; % base value:0.05; parameter controlling steepness of bulk
density transition (smaller is steeper)
OM_dens = 1300; % density of organic matter [kg/m3]

```

```

%% *****
% WATER BALANCE
% not used in HPMTrop
% *****

```

```

wfps_c1 = 0.03;
wfps_c2 = 0.5;
wfps_c3 = 20;

```

```

% wfps_c2 = 0.7;
% wfps_c3 = 60;

%% rainfall data generator
% based on the the gridded rainfall 20th century in around sebangau area
% for the data see: RF_sebangau.xlsx

% rainfall data based the cluster analysis
% P1-P4 elnino years;P5-P8: normal;P9-P12: lanina
deficit = zeros(1332,1);
P = zeros(5000,12);
Ptemp = zeros(15000,12);
topvec = zeros(1,12);

P1 = [282 264 307 237 158 98 23 32 31 59 164 265];
P2 = [210 130 171 194 140 46 40 27 42 62 159 209];
P3 = [327 294 322 264 255 133 72 36 66 100 225 328];
P4 = [377 335 334 378 227 203 107 173 135 136 250 306];
P5 = [343 330 329 286 261 170 112 84 119 148 267 269];
P6 = [283 269 317 278 157 211 127 104 71 177 397 292];
P7 = [328 234 350 317 201 180 125 132 156 194 242 310];
P8 = [261 252 259 260 190 150 69 45 86 134 201 258];
P9 = [279 294 361 313 200 164 125 146 156 201 266 286];
P10 = [340 298 316 266 193 226 183 231 191 268 302 231];
P11 = [237 265 252 247 166 151 144 151 242 217 268 241];
P12 = [158 184 221 182 99 110 105 137 78 167 184 246];

for i=1:1:15000
    prob = rand(1);
    prob2 = rand(1);
    if(i<=9000)
        if(prob>=.95)
            if(prob2>=0.4)
                P = P1;
            elseif(prob2>=0.5)
                P = P2;
            elseif(prob2>=0.1)
                P = P3;
            else
                P = P4;
            end
        end
    end
end

```

```

elseif(prob>=.75) % 10% LaNina
    if(prob2 >= 0.55)
        P = P9;
    elseif(prob2>=0.3)
        P = P10;
    elseif(prob2>=0.1)
        P = P11;
    else
        P = P12;
    end
else % 90% normal
    if(prob2>=0.65)
        P = P5;
    elseif(prob2>=.55)
        P = P6;
    elseif(prob2>=.30)
        P = P7;
    else
        P = P8;
    end
end
elseif(i>9000 & i<=12000)
    if(prob>=0.85) %10 el Nino
        if(prob2>=0.4)
            P = P1;
        elseif(prob2>=0.5)
            P = P2;
        elseif(prob2>=0.1)
            P = P3;
        else
            P = P4;
        end
    elseif(prob>=.65) % 20% LaNina
        if(prob2 >= 0.55)
            P = P9;
        elseif(prob2>=0.3)
            P = P10;
        elseif(prob2>=0.1)
            P = P11;
        else
            P = P12;
        end
    else %50% normal
        if(prob2>=0.65)

```



```

        P = P5;
    elseif(prob2>=.55)
        P = P6;
    elseif(prob2>=.30)
        P = P7;
    else
        P = P8;
    end
end
end
else
    if(prob>=0.7) %30 el Nino
        if(prob2>=0.4)
            P = P1;
        elseif(prob2>=0.5)
            P = P2;
        elseif(prob2>=0.1)
            P = P3;
        else
            P = P4;
        end
    elseif(prob>=.5) % 20% LaNina
        if(prob2 >= 0.55)
            P = P9;
        elseif(prob2>=0.3)
            P = P10;
        elseif(prob2>=0.1)
            P = P11;
        else
            P = P12;
        end
    else %50% normal
        if(prob2>=0.65)
            P = P5;
        elseif(prob2>=.55)
            P = P6;
        elseif(prob2>=.30)
            P = P7;
        else
            P = P8;
        end
    end
end
end
%corrTime = 15000 - num_years;

```

```

delO = 2.7011e-12*i^3 - 4.4591e-08*i^2 - 4.2942e-05*i - 7.5886;
delOtime(i) = delO;
fP = delO/-9.3;
P = fP*P;
Pfinal(i,:) = P;
%age(i) = 15000-i;

end

for i=1:1:15000
    age(i) = 15000-i;
end

%RFfinal = [Pfinal;RF20];
%PAnnual = sum(Pfinal,2);
monthlyRF = reshape(Pfinal',15000*12,1);
ETPminP = 100 - monthlyRF;

for i=2:1:15000*12
    if(ETPminP(i)>0 | deficit(i-1)>0)

        deficit(i) = max(0,deficit(i-1) + ETPminP(i));
    else
        deficit(i) = 0;

    end
    %year(i) = year(i-1) + 1900;
end
WT = 0.1984.*deficit;

% monthly_WT = zeros(15000,12);
% monthly_WT = monthly_WT + .1;
% for i=1:1:15000
%   monthly_WT(i,:) = [0 0 0 0 0 0 0 0 0 0.4 0.4 0.4];
% end

monthly_WT = 0.01 .* reshape(WT,12,15000)';

monthly_deficit = reshape(deficit,12,15000)';
annual_deficit = mean(monthly_deficit,2);
annual_WT = mean(monthly_WT,2);
annualP = sum(Pfinal,2);

```

```

if(scenario_LU==1)
    monthly_WT = [monthly_WT(1:14899,:); monthly_WT(14900:end,:)+0.6];
end
window = 25;
mask = ones(1,window)/window;
annP_smooth = conv(annualP,mask,'same');
annWT_smooth = conv(annual_WT,mask,'same');
annDef_smooth = conv(annual_deficit,mask,'same');

```

```

figure (20)
plot(age,annualP)
hold on
plot(age,annP_smooth,'k')
hold off
xlabel('year BP')
ylabel('rainfall (mm)')

```

```

figure (21)
plot(age,annual_WT)
hold on
plot(age,annWT_smooth,'k')
hold off
xlabel('year BP')
ylabel('Water table (m)')
set(gca, 'YDir','reverse')

```

```

figure (23)
plot(age,annual_deficit)
hold on
plot(age,annDef_smooth,'k')
hold off
xlabel('year BP')
ylabel('water deficit (mm)')

```

```

%% graph peat depth vs age from Dommain paper
depth_inland1 = [99.5 201 220.5 384.5 436.5 595.5 780.5 809.5]' .* .01;
age_inland1 = [114 3608 5949 9005 9337 10518 13204 13752]';

```

```

depth_coastal = [95 195 295 395 495 715 795 995]' .* .01;
age_coastal = [647 1206 1740 2189 3011 3965 4110 5148]';

```

```

%% SAVING THE PARAMETER VALUES

```

```

save('hpmT1_param_vals','outname','sim_len','num_veg','ag_frac_npp_trees','ag
_frac_npp_OP',...

'bg_frac_npp_trees','bg_frac_npp_OP','rootin_d80','rootin_alpha','rootin_c3','rooti
n_c4','rootin_c5',...
'wfps_opt','wfps_curve','wfps_min','wfps_wtd','wfps_sat','wfps_sat_rate',...

'wfps_min_rate','k_0','anoxia_scale_length','anoxia_scale_length_OP','wtd_0',...
'min_bulk_dens','del_bulk_dens','dens_c1','dens_c2','OM_dens',...
'wfps_c1','wfps_c2','wfps_c3','NPP_trees','NPP_OP',...
'NPP','monthly_WT','depth_inland1',...
'age_inland1','depth_coastal','age_coastal','ID','scenario_LU'); %deteling
maxnpp

```

### **Matlab code for estimating the multiplier factor for the effect on decomposition rate of peat water content**

```

function wfps_fact = hpm_decompT1(depthvec, wtdnow, annwfps, params,
onevct, epsvct)
wfps_fact = (1.0 - ((annwfps - params.wfps_opt).^2)/(4 * params.wfps_curve)) .*
(depthvec < wtdnow)...
+ (depthvec >= wtdnow) .* (params.wfps_min_rate +
(params.wfps_sat_rate - params.wfps_min_rate)...
* exp(-(depthvec - wtdnow) / params.anoxia_scale_length));
return

```

### **Matlab code for calculating root input**

```

function root_in = hpm_rootinT1_2(depthvec, thickvec, params,bg_frac, nppvec,
zwt, peatheight, onevct)

non_sedge_tot_root = bg_frac .* nppvec;

zstar = max(zwt, params.rootin_c3); % maximum root depth for non-sedge
vascular plants

% SF: new routines for root input (August 2011)

% uniform input per layer for non-sedge roots (rather than proportional to layer
thickness)
% uniform input per layer for upper range of sedge roots (depth < 'd80' from
parameters (depth to 80% of root input)

```

```
% input proportional to layer thickness below 'd80', with total of 20% from 'd80'
to 2 meters
```

```
% ***NON-SEDGE ROOTS***
```

```
input_equal_per_layer = 1;
if (input_equal_per_layer > 0.5)
```

```
    number_root_layers = find(depthvec > zstar, 1, 'first')-1;
    % root_frac = 1;
```

```
    if (isempty(number_root_layers))
        number_root_layers = find(thickvec > 0, 1, 'last');
        if (isempty(number_root_layers))
            number_root_layers = 1;
        end
    end
```

```
    % root_frac = depthvec(number_root_layers) / (zstar + eps);
end
```

```
    non_sedge_root_in = onevct / (max(1, number_root_layers));
% non_sedge_root_in = root_frac * (onevct / (number_root_layers));
    tf_root1 = thickvec > 0;
    tf_root2 = depthvec <= zstar;
    tf_root = tf_root1 .* tf_root2;
    if (isempty(tf_root))
        tf_root = 0 * thickvec;
        tf_root(1) = 1;
    end
    non_sedge_root_in = non_sedge_root_in .* tf_root;
    non_sedge_root_in = non_sedge_root_in * min(1, peatheight/zstar); % adjust
total to fraction of root zone that is peat
```

```
else
```

```
% first version (below) uses error function to get a smooth boundary, second has
uniform input to zstar
```

```
% second version lost about 5% of root mass due to discretization(?), hence
divided by sum...
```

```
% non_sedge_root_in = (thickvec/zstar) .* (onevct - 0.5*(onevct +
erf((depthvec - zstar*onevct)/(sqrt(2)*params.rootin_c5))));
```

```
    non_sedge_root_in = (thickvec/zstar) .* (depthvec < zstar);
```

```

    non_sedge_root_in = non_sedge_root_in / (sum((thickvec/zstar) .* (depthvec <
zstar)) + eps); % normalize total to 1.0??
    non_sedge_root_in = non_sedge_root_in * min(1, peatheight/zstar); % adjust
total to fraction of root zone that is peat

%   norm2 = sum((thickvec/zstar) .* (depthvec < zstar)) /
min(1,(peatheight/zstar));
%   non_sedge_root_in = non_sedge_root_in / (norm2 + eps); % normalize
total to 1.0

end

root_in = non_sedge_root_in * non_sedge_tot_root;

%j5a = [ norm1 norm2 ]

return

```

### **Matlab Code for calculating NPP as a function of monthly water table.**

```

function productivity = hpm_nppT1_2(params,WT,scenario)

%% NPP for HPMTrop
% NPP is a function of WT
% see Hirano et al 2012 for the relationship between WT and GPP
% see DeLucia 2007 for the ratio of NPP and GPP (NPP/GPP) in tropical
% forests

nppmin = 0.000001; % min NPP = 1 mg/m2/y for each veg type to prevent
divide by zero errors and to provide 'seed stock'

one_vec = ones(1,params.num_veg);
nppminvec = nppmin * one_vec;

params.PD_range(2,:);

%correction factor of NPP related to WT
factorNPP = -0.3046*WT^2 + 0.1732*WT + 0.9874; %see
SandBoxHPMTropNew.xlsx
if (scenario==0)
    NPP = params.NPP_trees;
else
    NPP = params.NPP_OP;

```

```

end
NPP = NPP*factorNPP;
%NPP
productivity = max(nppminvec, NPP);    % 'kg/m2/y'

return

```

**Matlab code for calculating cohort bulk density as a function of degree of decomposition.**

```

function density = hpm_densT1(mass_star,mass_overlying,params,onevct)

% function calculates peat density at 'depth' in profile
% uses error function to get shape

% mass_star = fraction of original slow pool litter mass remaining
% mass_overlying = total mass of all overlying cohorts
% density = peat bulk density [kg/m3]
% min_bulk_dens = surface (assumed minimum) bulk density [kg/m3]
% del_bulk_dens = increase in bd [kg/m3] from surface to base (assumed
maximum)
% c1 = controls humification (m*) at which bulk density transition occurs [--]
% c2 = controls steepness of bulk density transition [--]

erfactor = erf((mass_star.*params.dens_c1.*onevct)./params.dens_c2./sqrt(2));
density = params.min_bulk_dens * onevct + params.del_bulk_dens .* (onevct -
0.5*(onevct + erfactor));

return

```